Sergey Ushakov

Particulate matter emission characteristics from diesel engines operating on conventional and alternative marine fuels

Doctoral Thesis

Sergey Ushakov

NTNU – Trondheim
Norwegian University of
Science and Technology

NTNU

NTNU – Trondheim
Norwegian University of
Science and Technology

Sergey Ushakov

Particulate matter emission characteristics from diesel engines operating on conventional and alternative marine fuels

Thesis for the degree of philosophiae doctor

Trondheim, December 2012

Norwegian University of Science and Technology
Faculty of Engineering Science and Technology
Department of Marine Technology

NTNU – Trondheim
Norwegian University of
Science and Technology

Abstract

The awareness of adverse health effects associated with diesel aerosol emissions has generated a great public and academic interest in studying various aerosol-producing sources. While automotive industry has achieved significant progress in controlling and reducing particulate matter (PM) emissions, there was only a very limited attention paid to ship transport, i.e. to marine diesel engines (MDE). Nowadays, shipping is one of the biggest contributors of PM emissions to the atmosphere, although is still lacking attention from PM legislators and diesels aerosol researchers. This thesis is focused on measurement and characterization of particulate emissions from diesel engines (both marine and heavy-duty) operating on conventional and alternative marine fuels.

Different PM emission characteristics such as particle size distributions, total and nanoparticle concentrations, PM mass and particle morphology were measured and analysed in current thesis. The observed significant differences in PM results between 2-stroke and 4-stroke marine diesel engines indicate the importance of engine technology, while pronounced contribution of heavy fuel oil's ash fraction (in contrast to MGO) to solid PM reveals the importance of considering the fuel factor. In addition, PM characteristics from marine diesel engines were found to be different from that of heavy-duty engine, but a certain, somewhat surprising, agreement between results for 4-stroke MDE and 4-stroke heavy-duty engine was also observed. Particle morphology analysis confirmed the three main origins (sources) of particulates: fuel, lubrication oil and mechanical wear of moving cylinder parts.

The sole effect of high sulphur level in marine fuels was studies using a sulphur-doping of a reference low-sulphur MGO up to 4% S by mass. The contribution of sulphur to PM mass appeared to be more pronounced than is known from automotive engine studies. The homogeneous nucleation of sulphur and HC compounds was observed only at very low load conditions, while heterogeneous nucleation, i.e. condensation on the surface of existing solid particles, was found to be the dominating mechanism and can be associated with a rather low turbulence level in a primary porous tube diluter and

availability of considerable amount of solid nucleus. As volatile particles are very sensitive to dilution parameters and in order to obtain repeatable and reproducible results, the effects of primary dilution ratio (PDR) and primary dilution air temperature (PDT) were studied. Both these parameters showed no effect on solid carbonaceous particles formed inside the engine cylinders, and at the same time were vital for semivolatile HC and sulphur compounds. Increase in PDR reduces the partial pressure of volatile compounds, and hence their tendency to nucleate; too low PDR should be avoided as water condensation can occur leading to some deceptive results. Increasing PDT results in increased saturation vapour pressure of volatile compounds, which is also suppressing nucleation. Effect of filter media on the results of gravimetric PM analysis was studied and no filter type was found overwhelmingly superior due to various positive and/or negative artifacts associated with each filter type.

The environmental benefits in terms of gaseous, smoke and PM emissions of fish oil (FO) biofuel and GTL synthetic fuel as alternatives to conventional MGO were investigated. A fairly good ignition and combustion properties together with excellent emission characteristics were observed in case of FO, which although requires some additional testing of its rheological and cold temperature properties and oxidation stability. GTL fuel showed reduction in PM mass, smoke and all gaseous emissions except THC, which together with registered particle number concentration showed a visible increase. This can be associated with possible higher incidence of wall-wetting by GTL fuel as its volumetric flow rates were increased to compensate for lower fuel density (lower volumetric energy content). Injection system tuning/modification or shift to common rail injection system can be proposed for reduction of gaseous (especially THC) and PM emissions even further.

Preface

This thesis is submitted to the Norwegian University of Science and Technology (NTNU) for partial fulfilment of the requirements for the degree of philosophiae doctor.

This doctoral work has been carried out at the Department of Marine Technology, NTNU, Trondheim, with supervisor Professor Harald Valland, NTNU and co-supervisor Professor Vilmar Æsøy from Ålesund University College.

Acknowledgements

Finally, special thanks should be addressed to my family and parents for their love and support. Katya, thank you for your patience: the work has taken the most part of my time, especially during last year, and only you were able to remind me about the most important things of my live.

Sergey Ushakov

December 2012, Trondheim, Norway

List of publications

I.   Ushakov S., Valland H., Nielsen J.B., Hennie, E. (2012). Particulate emission characteristics from medium-speed marine diesel engines. *Proceedings of PACIFIC 2012 International Maritime Conference*, 31 January - 02 February 2012, Sydney, Australia.

II.   Ushakov S., Valland H., Nielsen J.B., Hennie, E. (2011). Particle size distributions from heavy-duty diesel engine operated on low-sulfur marine fuel. Accepted for publication in *Fuel Processing Technology*.

III. Ushakov S., Valland H., Nielsen J.B., Hennie, E. (2012). Effect of high sulphur content in marine fuels on particulate matter emission characteristics. Submitted to *Proceedings of IMarEST Part A: Journal of Marine Engineering and Technology*.

IV.   Ushakov S., Valland H., Nielsen J.B., Hennie, E. (2012). Effects of dilution conditions on diesel particle size distribution and filter mass measurements in case of marine fuels. Submitted to *Fuel Processing Technology*.

V.   Ushakov S., Valland H., Æsøy V. (2013). Combustion and emission characteristics of fish oil fuel in a heavy-duty diesel engine. *Energy Conversion and Management, 65, 228-238*.

VI.   Ushakov S., Halvorsen N.G.M., Valland H., Williksen D.H., Æsøy V. (2012). Emission characteristics of a diesel engine operated on marine gas oil and gas-to-liquid Fischer-Tropsch fuel. Accepted for publication in *Transportation research, Part D: Transportation and Environment*.

Contents

List of Figures

List of Tables

Nomenclature

Abbreviations

C	Carbon
CMD	Count Median Diameter
CO	Carbon Monoxide
CO_2	Carbon Dioxide
CPC	Condensation Particle Counter
DI	Direct Injection
DMA	Differential Mobility Analyzer
DMDS	Dimethyl Disulfide
DPF	Diesel Particulate Filter
DR	Dilution Ratio
EC	Elemental Carbon
ELPI	Electrical Low Pressure Impactor
EU	Europe Union
FAME	Fatty Acid Methyl Ester
FO	Fish Oil (fuel)
FSN	Filter Smoke Number
FT	Fischer-Tropsch
GTL	Gas-to-liquid (Fischer-Tropsch fuel)
HC	Hydrocarbons
HD	Heavy Duty (engine)
HFO	Heavy Fuel Oil
ICE	Internal Combustion Engines
ISO	International Organization for Standardization
MDE	Marine Diesel Engine
MGO	Marine Gas Oil
NO_x	Nitrogen Oxides
OC	Organic Carbon
PAH	Polycyclic Aromatic Hydrocarbons

PDR	Primary Dilution Ratio
PDT	Primary Dilution (air) Temperature
PM	Particulate Matter
REGR	Reformed Exhaust Gas Recirculation
S	Sulphur
SCR	Selective Catalytic Reduction
SMPS	Scanning Mobility Particle Sizer
SOF	Soluble Organic Fraction
THC	Total (Unburnt) Hydrocarbons
UNECE	United Nations Economic Commission for Europe
VOF	Volatile Organic Fraction

Symbols

C	Cunningham slip correction factor
d or D_p	diameter of particle
ρ	density

Subscripts

0	unit value (1 g/cm^3)
a	aerodynamic
eff	effective
m	mobility
p	particle

1.   Introduction

By definition, the particle pollution (also called particulate matter or PM) is the term for a mixture of solid particles and liquid droplets found in the air. Essentially, it has irritated people for centuries with the mentioning that date back 13th century or even earlier (Stern et al., 1973; Chambers, 1976). Firstly, the people struggled with the smoke, which became more harmful and widely spread with the intensive urbanization and growth of cities, and in 19th century in Great Britain police was empowered to enforce provisions against smoke (Stern et al., 1973). With the appearance of new technological improvements and with the switch to the oil from coal as a main fuel, the soot emissions decreased (Cooper and Alley, 1986), but in last century a number of automobiles increased dramatically and new pollution problem raised: smog, formed during some particular weather conditions, when motor vehicle emission can form large light scattering particles through photochemical reactions (Haagen-Smith and Wayne, 1976). No doubt that strict regulation to PM level had to be developed and first motor vehicle particulate matter mass (before it was the exhaust gas opacity) emission started to be federally regulated in the USA in 1987, and in Europe Union (EU) the Euro I standard, defining acceptable limits for PM emissions, was introduced and came into power in 1992 and 1994 respectively. Since that every several years the allowed PM emission limits became stricter and stricter, for example, currently active Euro V standard has the allowed PM mass levels, which are almost 98% lower than in firstly introduced Euro I standard. Moreover, Euro V standard also sets the allowed limits for emitted particle number concentration (in particles per kilometre).

The main driving force for limiting particulate mass and number concentrations was the confirmed existence of strong statistical correlation between adverse health effects to humans and exposure to small particles, which was confirmed by recent toxicological and epidemiological studies (e.g. Dockery et al.,1993; Pope et al., 1995; Pope, 2000; Oberdörster, 2000; Forsberg et al., 2005) with fine particles being more clearly linked to the most serious health effects (McKenna et al., 2008), and people having lung disease, the elderly, and children being most at risk. PM can accumulate in human respiratory

system and can cause, for example, cardiac arrhythmias (Watkinson et al., 2000) and emphysema, changes in lung function (Pietropaoli et al., 2004), lung inflammation (Ghio et al., 2001), elevate blood pressure, increases vascular inflammation (Rueckerl et al., 2006), cause lung cancer (Pope et al., 2002), number of other diseases, and may lead to premature death (Pope et al., 2004). Particles with $D_p < 100$ nm, so-called ultrafine, have been identified as a particular concern for human health (Pope and Dockery, 2006; Pope et al., 1995) with some laboratory studies showing that particles which are non-toxic at $D_p \sim 1$ µm can be toxic when $D_p \sim 10$ nm (Donaldson et al., 1996; Seaton et al., 1995; Ban-Weiss et al., 2010). Finally, nanoparticles ($D_p < 50$ nm) is known to penetrate very deep into the human lungs, so have a possibility to enter the circulatory system together with blood cells (Rothen-Rutishauser et al., 2006; Suzuki et al., 2007), and can potentially deposit in vital organs such as brain or heart (Kennedy, 2007). Aerosol particles have also negative environmental impact which normally results in reduced visibility (Doyle and Dorling, 2002), deposition on vegetation and impacts on ecosystems, and damage to paints and building material (McKenna et al., 2008). Carbon particles are also known to affect the earth's radiation balance, hence enhance the global warming (IPCC, 2001). It should be obvious that internal combustion engines (ICE) are one of the major sources of urban PM and that diesel exhaust particles constitute a significant percentage of anthropogenically emitted particles.

At the same time, there are no any direct PM regulations for marine diesel engines. So taking into account that sea shipping contributes almost as much primary PM as road traffic (Eyring et al., 2005) and also the fact that in contrast to PM emissions of industry and transport sectors, which are steadily decreasing, PM emitted by sea shipping are expected to increase, because of expected increase of ship traffic (from 1970 to 2008 the amount of goods transported by sea showed more than threefold increase (Asariotis et al., 2009)), the maritime industry can be concluded a significant contributor to overall PM emissions. Number of investigations (e.g. Cofala et al., 2007; Corbett et al., 2007) showed on average the loss of life expectancy due to particles emitted by sea-going vessels and assessed the possible contribution of shipping particle emission reduction on it. Especially large cities located near to main shipping routes, coastal cities and especially urban areas close to harbour zones experience negative effects of particulate

matter emitted from marine diesel engines (MDE). According to some researchers (e.g. Corbett et al., 2007), approximately 60000 people worldwide die prematurely due to PM from shipping with this number expecting to increase if no preventive measures are taken.

1.1.   Research objectives

This thesis has been motivated by interest in diesel aerosols from marine diesel engines and fuels, which, as discussed above, are becoming one of the biggest contributors to overall PM emissions, but at the same time are lacking attention from aerosol researchers, hence are not yet well investigated. The study was mainly focused on characterization of number size distributions and morphology, overall mass and total number concentrations of particulates emitted by diesel engines operated on typical marine low- and high-sulfur fuels, as well as on potential alternative fuels. The main targets of the thesis can be divided into several groups as follows: 1) study PM emission characteristics from marine diesel engines and fuels (Paper I and II); 2) investigate the sole effect of high sulfur level in marine fuels on particle emissions (Paper III) and how they are affected by various dilution parameters (Paper IV); 3) study gaseous and PM emission reduction potential of fish oil (FO) fuel (Paper V) and gas-to-liquid (GTL) Fischer-Tropsch fuel (Paper VI) as potential alternatives to conventional marine gas oil.

In Paper I particulate matter emissions from both 2-stroke and 4-stroke marine diesel engines are studied and compared to that of 4-stroke heavy-duty engine. Paper II studies effects of engine operating parameters and verify dilution system performance when MGO fuel is used. In Paper III the sole effect of high sulfur level in fuel (simulated using sulfur doping agent) on particle number and mass emission characteristics is investigated, while Paper IV studies how dilution ratio, primary dilution air temperature and other factors can affect PM results if high-sulfur fuel is used. Gaseous and particle emissions from FO biofuel and GTL synthetic fuel, in comparison to conventional MGO, are studied in Paper V and Paper VI respectively.

As seen the entire thesis consists of six original publications. The author was entirely responsible for laboratory measurements reported in Paper II-IV, while measurements for Paper V and Paper VI were performed by author together with Vilmar Æsøy and Nadine G.M. Halvorsen respectively. The complete experimental data analysis and writing of Paper I-IV and VI was done by author. Author was also responsible for major part of data analysis and writing process for Paper V. In addition, author developed spreadsheet for assessment of particle losses during exhaust sample extraction and transport (Appendix A), which was used to correct PM data in Paper II-VI.

2.   Characteristics of diesel exhaust particles

In this section, the basics of the diesel particulate matter composition, structure and formation process are considered.

2.1. Diesel aerosol composition and structure

Diesel exhaust is a complex mixture of organic and inorganic compounds and gas, liquid, and solid phase materials. Some of the aforesaid materials are not well explored and are of more interest nowadays, one of them is particulate matter and by itself it has an untrivial structure (Figure 1) and very complex composition (Figure 2) that includes such major fractions like soot, soluble or volatile organic fraction (SOF or VOF respectively), sulphates, nitrates and ash.
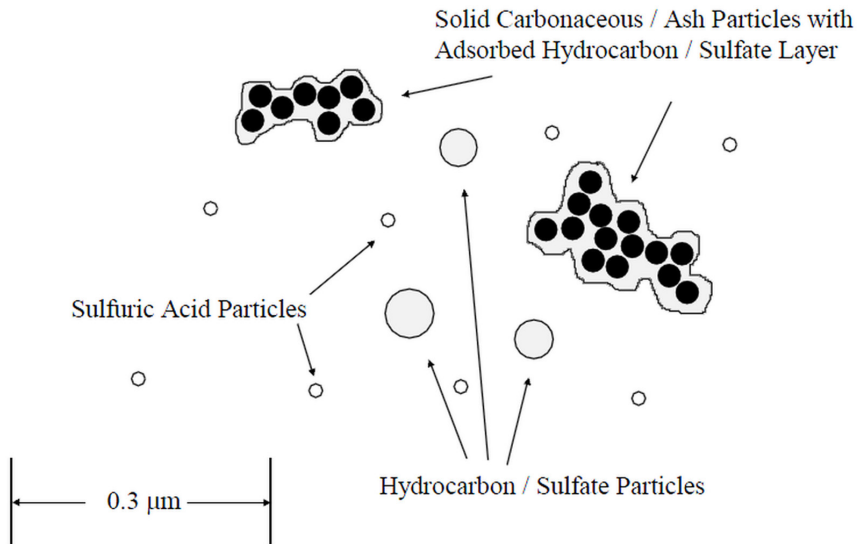
Figure 1:   Typical structure of engine exhaust particles (Kittelson, 1998)
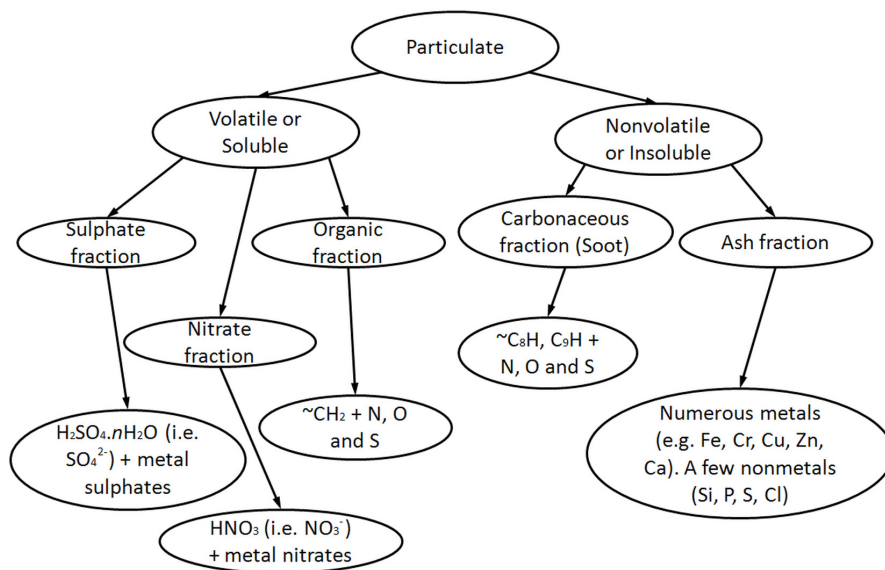
Figure 2:   Conceptual model of PM composition, terminating in five distinct groups or fractions: sulphates, nitrates, organics, carbonaceous and ash (adopted from Eastwood, 2008).

2.1.1. Organic and elemental carbon

Carbonaceous particles are one of the most important components of engine emitted aerosols and usually consist of solid elemental carbon (EC), i.e. 'primary' soot particles, and volatile organic carbon (OC). EC (sometimes is also called black carbon (BC)) derived from incomplete combustion of carbon contained materials and is therefore treated as a direct indicator of urban pollution and traffic intensity (Ryall et all., 2002), while OC can be either released directly into the atmosphere (primary OC) or produced from gas-to-particle conversion of volatile organic compounds (secondary OC) (Pandis et al., 1992; Turpin and Huntzicker, 1995; Lewandowska et al., 2010). The 'primary' soot particles are usually in the range of ~10-60 nm in diameter (but mainly 15-30 nm) and sometimes referred as 'spherules', meaning that they are not exactly spherical, but are very close to spherical shape. Initially the number of 'primary' soot particles is large enough for rapid coagulation and formation of much larger particles (Heywood, 1988; Smith 1981), which are often called 'agglomerates' or 'aggregates' (Figure 3).
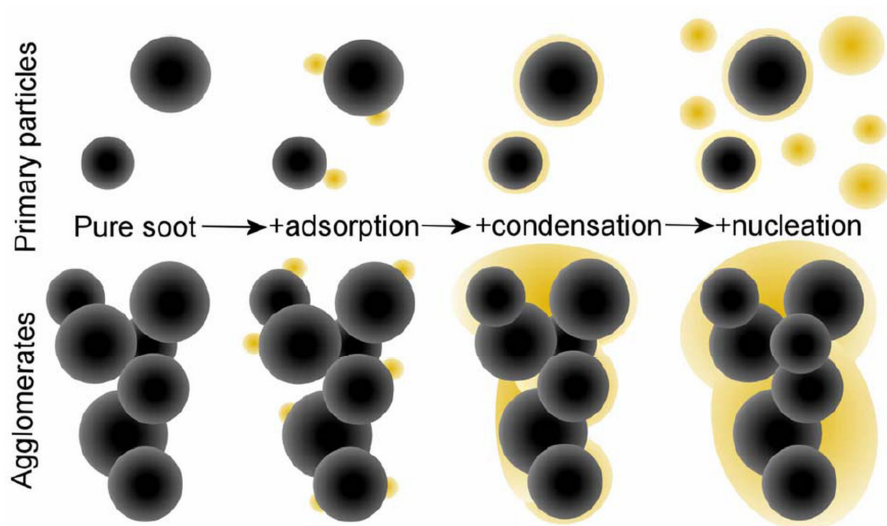
Figure 3:   Schematic representation of the mass transfer process of volatile compounds on particles (Ristimäki, 2006).

The organic carbonaceous fraction is of particular interest since it includes polycyclic aromatic hydrocarbons (PAH) and their derivatives, with some of them, like benzo(a)pyrene, benzo(b)fluoranthene, benzo(k)fluoranthene and indeno(123cd)pyrene, are known to be responsible for the most of cancerogenic and mutagenic effects in accordance to UNECE POPs protocol (Eastwood, 2008). PAHs is a collective name for a large group of chemicals, which all have in common that they consist of two or more ring structures, where at least one ring has the structure of benzene.

A tiny fraction of the fuel and atomized and evaporated lube oil escape oxidation in cylinder and appears as soluble (or volatile) organic compounds (Rogge et al., 1993a, 1993b) that is later transferred from the gas phase to the particulate phase by adsorption and/or condensation onto the existing 'primary' or on already agglomerated fractal-like particles, resulting in layer of several molecules in thickness (McDow et al., 1996), or by creating separate very small nuclei-particles, i.e. by nucleation (Figure 3), when hot exhaust gas interacts with much cooler ambient or dilution air (fast cooling) since condensation is not able to remove the excess material from the gas phase (Kittelson,

1998; Abdul-Khalek et al., 1999; Khalek et al., 2000). For diesel aerosols the adsorption mechanism seems to dominate in most of the cases (Kittelson and Dolan, 1980) as the surface concentration is large enough and saturation pressure of gaseous organics is relatively low.

Composition of diesel exhaust particles varies significantly with engine design (combustion technology) and with the fuel used. Typical particle composition of 4-stroke heavy-duty diesel engine is composed mostly of carbon, where OC/EC ratio is very load and size dependent (Kittelson, 1998), sulfate fraction, which is roughly proportional to the sulphur content in fuel, inorganic ash and unburned fuel and lubrication oil (SOF), which composition varies with engine design and operating conditions. It can range from less than 10% to 90% by mass and the values are highest for low engine loads when exhaust gas temperature is relatively low (Kittelson et al., 1998). Although, particles emitted by 2-stoke diesel engine will differ remarkably from the ones emitted by 4-stroke engine. And the main reasons are scavenging losses of the fuel and loss of fuel-oil mixture lubrication employed, so the composition of 2-stroke diesel emitted aerosols is usually contains high concentrations of both unburned fuel and lubrication oil, where lube oil seems to be dominating contributor (Sugiura and Kagaya, 1977; Ålander, 2006).

2.1.2. Soot formation mechanism

In general soot is formed due to incomplete combustion of hydrocarbons. Hence, soot could appear as an indicator of combustion completeness along with CO and organic compounds that also include PAHs. Radiative energy loss, i.e. dissipation, associated with soot presence in combustion chamber (Ray and Wichman, 1998), in diesel engines steals from useful work, and so is detrimental to fuel economy (Struwe and Foster, 2003). Additionally, an intriguing circularity arises here, wherein soot is forming: that's how lowering flame temperature (Smooke et al., 2005). And newly introduced fuel is exposed to the aforementioned heat flux, burns richer and hence is more soot-producing, than otherwise (Hampson and Reinz, 1998). For example, as much as 0.05-0.5% fuel by mass can be converted to soot in heavy-duty diesel engines (Klein et al., 1998).

It should be noted here that soot can vary in its microstructure, according to the fuel burned and type (i.e. premixed or diffusional) of the flame (Vander Wal and Tomasek, 2004). Soot formation commences with fuel molecules that contain 12-22 atoms of carbon, and twice as many hydrogen atoms; soot formation suddenly stops a few milliseconds later with spherules that contain thousands of carbon atoms, and 1/10 as many hydrogen atoms (Eastwood, 2008). What actually happens between these two "boundary" steps is been debated by researches for many decades without any final conclusion and is still remaining an open question. But, conceptually, soot formation is known to follow a step-like route (Burtscher, 1992; Bockhorn, 1994) adumbrated in Figure 4 and is mainly dependent on air-fuel ratio, pressure and temperature.

Pyrolysis of gaseous compounds and construction of soot precursors are followed by nucleation that these precursors undergo with formation of first discernible particles, or nuclei. Then these nuclei undergo surface growth by surface reactions when material is transferred from surrounding gas phase onto nuclei, until spherules emerge at approximately 20-50 nm. During this growth the spherules themselves coagulate and agglomerate, with surface growth occurring in parallel (Eastwood, 2008). And oxidation opposes all other mechanisms, but in fact can cull the soot at any of the stages mentioned above. It should be also noted that some researches indeed on including one more step in this process – carbonization stage (not depicted on Figure 4), when the layers of polyaromatics are aligned and amorphous carbon is transformed into the form of graphitic carbon (Richter and Howard, 2000).
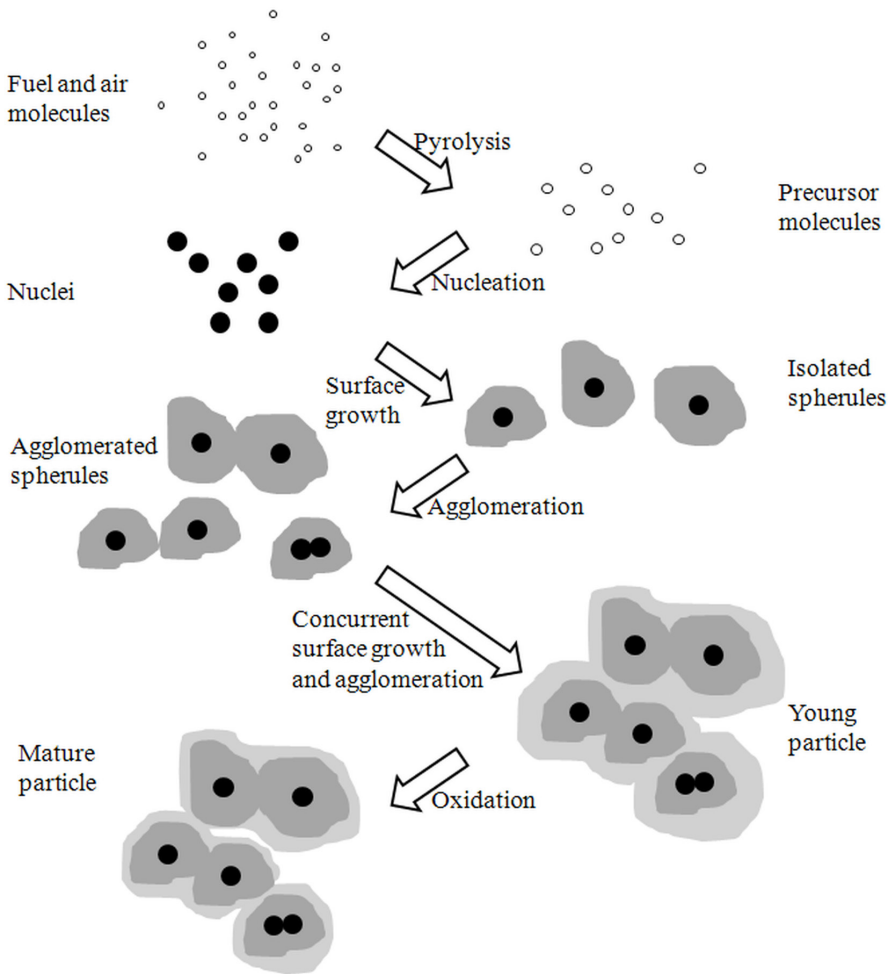
Figure 4:   Conceptual scheme for soot formation process (Adapted from Eastwood, 2008).

It is known that soot appears at some critical air-fuel ratios and from this point of view it is natural to choose the global reaction scheme as a starting point; for instance, when considering C, H_2 and CO as intermediate products, we can get (Li and Wallace, 1995):

$$C_\alpha H_\beta + xO_2 \rightarrow \alpha CO + \left(\frac{\beta}{2} - \frac{\alpha(1-\gamma)}{\gamma}\right)H_2 + \left(\frac{\alpha(1-\gamma)}{\gamma}\right)H_2O + \left(x - \frac{\alpha}{2\gamma}\right)O_2$$

when $\left(\dfrac{\alpha}{2x}\right) \leq \gamma$ (2.1)

$$C_\alpha H_\beta + xO_2 \rightarrow 2x\gamma CO + \left(\frac{\beta}{2} - 2x(1-\gamma)\right)H_2 + 2x(1-\gamma)H_2O + (\alpha - 2x\gamma)C_{(Solid)}$$

when $\left(\dfrac{\alpha}{2x}\right) \geq \gamma$ (2.2)
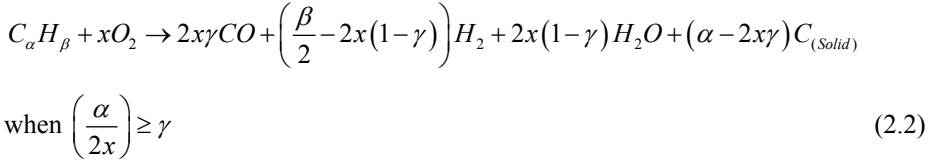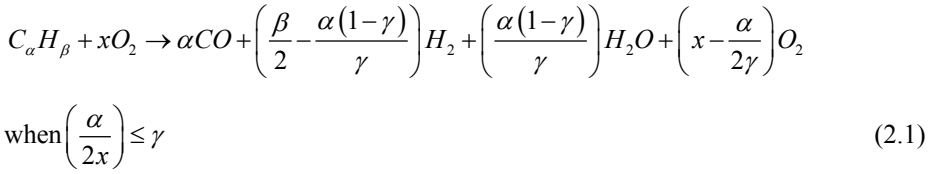
From these equations one might suggest that the critical C/O ratio is unity, when every carbon atom is at least able to find one oxygen atom, and hence form CO, so when this ratio exceeds unity, some carbon atoms appear as soot. Although, this is not necessary true and critical ratios are often less than unity and soot formation has been experimentally proved to be possible at C/O=0.5-0.8 with critical carbon-to-oxygen ratios strongly dependent on fuel composition, flame type and temperature (Haynes and Wagner, 1981).

More detailed description of soot particle formation mechanisms and experimental methods used for studies of soot in the field of internal combustion engines reader can find reported in number of earlier comprehensive studies (e.g. Santoro and Miller, 1987; Flagan and Seinfeld, 1988; Burtscher, 1992; Bockhorn, 1994; Lighty et al., 2000) and also in earlier papers (e.g. Khan, 1969; Khan et al., 1971; Henein, 1976, Duggal et al., 1978, Kadota et al., 1980).

2.1.3. Soluble fraction

Basically, upon heating some material evaporates, and some does not; or in other way, some materials dissolve in certain solvents, but some does not. This principle subdivides the particulates into ones that are volatile or soluble, and that which are non-volatile or insoluble. Hence, by extraction or dissolution in some special organic solvent

or by heating or volatilisation, the fractions contributing to the total particle composition can be called soluble organic fraction (SOF) and volatile organic fraction (VOF) correspondingly. Luckily, the SOF mass is usually quite close to the VOF mass, although, the separation processes are based on different properties, so final result will not necessary be the same. In current work the term SOF will be of main use unless of any special need.

While some relation between fuel composition and soot production is known (de Lucas et al., 2001), there is no any clear relation between fuel (and lubricant) and SOF composition. The effect of SOF on combustion and/or gasification process is also a question for debates (Ciambelly et al., 1990; Querini et al., 1998; Stanmore et al., 1999; Stanmore et al., 2001).

By its nature and origin, SOF is a tiny fraction of fuel and atomized and evaporated lubrication oil which escape the process of oxidation. Some authors suggest that SOF is more a product of lubrication oil and its derivatives, rather than fuel (Clague et al., 1999; de Lucas et al., 2001). The content of soluble organic fraction is known to vary with engine operating conditions and in all over 50% of the measured particulate mass can be volatile or in other words, be a SOF (Kerminen et al., 1997; Ålander et al., 2004).

Composition of organic fraction of SOF is quite complex and contains several hundred, or perhaps several thousand compounds, many of which lie at the threshold of detection. Most of the major chemical families are represented, although their proportions vary significantly: alkenes, alcohols, alkanes, ethers, ketons, acids, esters and aromatics (Eastwood, 2008). And since light compounds from C_4 to C_8 are found as well that theoretically should be in gas phase, then strong surface interactions can be expected.

As shown on Figure 2, the soluble fraction incorporates some more groups of chemical compounds in addition to organics: sulphate and nitrate fractions. The sulphate fraction is the one that concerns water-soluble sulfates, or the SO_4^{2-} ion, but the main component is certainly sulphuric acid, H_2SO_4. And the interesting fact that water content of the

particulate matter often varies only with the sulphate content, because the particulate-bound water is found predominantly with the sulphuric acid (Eastwood, 2008). Since it is widely known that a distinctive property of sulphuric acid is its eager association with water. So, what 'sulphates' really means is the acid and the water. From these facts we can draw two main conclusions, which are, first, that the mass of water is not negligible; and second, it is variable, depending on the humidity in the immediate environment of the filter. Hence, prior to gravimetric analysis all filters must be conditioned (equilibrated) for a certain period of time in a closely defined environment – otherwise the result is meaningless.

The term nitrate fraction denotes water-soluble nitrates, or NO_3^- ion, but the main component is nitric acid, HNO_3. This fraction is quite small and perhaps this fact explains the lack of attention it receives in literature, although it is normally reported by many emission laboratories. In general, HNO_3 forms via reaction that occurs between NO_2 and water; so it seems that nitrate chemistry is connected to the NO_x chemistry. The detailed mechanisms are not known, certain associated chemical reactions were reported in literature (e.g. Villinger et al., 2002).

2.1.4. Ash fraction

The last, but not the least important, fraction that we definitely should mention is ash fraction. The four sources of ash are discernible; first, there are components of lubrication oil (Abdul-Khalek et al., 1998), perhaps naturally present namely phosphorus, zinc, calcium and magnesium. They do not necessary experience the hottest conditions, and in fact are subjected to a range of temperatures, depending on their entry point, for example, valve-stem seals, piston rings, and other (e.g. Hill and Sytsma, 1991). So oil compounds can escape the chemical breakdown and hence appear in exhaust in their native forms.

Second, there exists airborne inorganic debris, or dust, brought in the air, of which silicon (silica) is an example. The third group is wear metals, mainly iron, but with some others like, magnesium (piston rings), copper and lead (bearings), aluminum

(pistons), with some minor presence of manganese, molybdenum (Raux et al., 2005), nickel and chromium (Kimura et al., 2006). There are also particles released by fuel pumps, for instance, ferrous particles – from high-pressure fuel pump, and graphite particles correspondingly from low-pressure fuel pump (Macián et al., 2006). It should be noted that these wear particles are usually quite big, i.e. several microns in size. And hence these supermicron particles carried along by the fuel (of course, if they evade retention by the fuel filter) should behave rather differently in the combustion chamber than metals which are truly dissolved in the fuel used.

Finally, the fourth group is composed from inorganic compounds and elements present in fuel. It is obvious that fuel carries inorganic compounds quite naturally, courtesy of the crude, and unintentially, such as through contamination in the fuel distribution network. Fuel ash emission can be considered as forgotten pollutant as it is usually very poorly reported in fuel analyses. For example, in diesel fuel containing no additives, twenty ashing elements was present at discernible levels, for instance, Si at 46 mg/liter, Zn at 5.6 mg/liter and Fe at 27 mg/liter (Eastwood, 2008). Tailpipe emission rates were fully accounted for by fuel concentration; emissions of crustal elements (Al, Ca, Fe, Mg and Si) appeared several times higher than anthropogenic elements (Ag, Ba, Cd, Cr, Cu, et.) emissions. Such emission rates, if being accounted for whole vehicle population, may exceed those ones from coal-fired power plants (Wang et al., 2003). It should be, however, mentioned that concentrations of fuel-borne ashing elements vary significantly from one country of origin to another (Lim et al., 2007). However, sometimes inorganic, or organometallic, components are admixed in the fuel to improve certain properties of the fuel like combustion characteristics.

One comment should be stated here about the components within the ash fraction that some of them could have a multi-sourced origin (Eastwood, 2008): for example, chlorine can be found in lubrication oil (Mayer et al., 1997), is a relic of catalyst manufacture (Neyestanaki et al., 2004) and is ingestible as road salt (Clarke et al., 1996) and/or salt in sea water spray. At the same time, silicon also might be detected in fuel (Owen and Coley, 1995) and in lubricants (Caines et al., 2004) as a silicon antifoaming agent, so can contribute to particulate emissions (Tomiyasu et al., 2006).

2.2. Aerosol Size Distributions

Figure 5 shows the idealized diesel aerosol number, surface area and mass weighted size distributions (Kittelson, 2006). The distributions are trimodal and lognormal in form. The concentration of particles in any size range is proportional to the area under the corresponding curve in that range (Kittelson, 1998). Most of the particle mass is found in so-called accumulation mode within 0.05-1.0 μm diameter range. This size range is usually composed of carbonaceous agglomerates with corresponding adsorbed materials. The nucleation mode particles are usually in the 0.005-0.050 μm diameter range and consist mostly of volatile organic and sulphur compounds which are formed during exhaust gas cooling and/or dilution, along with solid carbon (De Filippo and Maricq, 2008) and metal compounds originating from lube oil (Abdul-Khalek et al., 1998) as shown in Paper II. The third mode called coarse mode consists of particles in the diameter range of 1-10 μm or even bigger. This mode is actually composed of accumulation mode particles that had been deposited on the walls of cylinder or exhaust system and later reentrained. The nucleation mode typically contains 1-20 % of particulate mass and more than 90 % of the particle number with approximately 5-20 % of total surface area. The accumulation mode could contain the majority of particle mass and greatest part of surface area, i.e. 60-95 % of the PM mass and approximately the same quantity of surface area. Finally, course mode contains 5-20 % in terms of particle mass and contributes very little to the total PN and surface area (Kittelson, 1998).
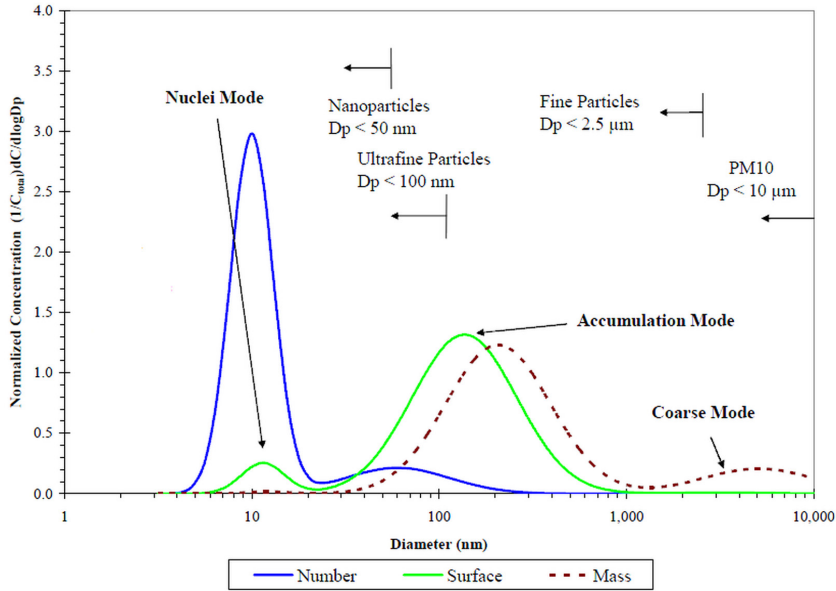
Figure 5: Typical engine exhaust particle size distribution by mass, number and surface area (Adapted from Kittelson, 2006).

Also some definitions that are usually used to define PM are shown on Figure 5: PM_{10} (thoracic fraction), the particles less 10 μm in diameter; fine particles (EPA, 2007), or $PM_{2.5}$ (respirable fraction) are particles with $D_p < 2.5$ μm; ultrafine particles (UFP or UP), $D_p < 100$ nm (Brunshidle et al., 2003); and finally, nanoparticles, $D_p < 50$ nm, however, definitions of ultrafine and nanoparticles are not universally agreed upon. Note that PM_{10}-$PM_{2.5}$ is the difference of PM_{10} and $PM_{2.5}$, so that it only includes the coarse fraction of PM_{10}. These are the formal definitions. Depending on the context, alternative definitions may be applied. In some specialized settings, each fraction may exclude the fractions of lesser scale, so that PM_{10} excludes particles in a smaller size range, e.g. $PM_{2.5}$, usually reported separately in the same work (Brunshidle et al., 2003). Such a case is sometimes emphasized with the difference notation, e.g. PM_{10}-$PM_{2.5}$. Other exceptions may be similarly specified. This is useful when not only the upper bound of a fraction is relevant to a discussion.

3.   Particle emission measurements from diesel engines

Process of exhaust gas conditioning, including sampling, transport and especially dilution, are discussed in current section as are extremely important for accurate and reproducible measurements of diesel exhaust particulates. Certain PM measurement methods most relevant to the study are also reviewed.

3.1. Conditioning of sample gas

Exhaust gas temperature as well as particle and vapor concentration, is high in the tailpipe, so dilution is required both to reduce particle concentration and also to cool down the exhaust sample. Another main task of dilution process is to resemble the real physical and chemical processes that occur when hot exhaust gasses mix with much cooler ambient air. In real world, the dilution ratio of 1000-2000 can be achieved by exhaust gas just several seconds after exiting the tailpipe (Kittelson et al., 2002). Dilution can be performed by means of different dilution systems, which in general can be divided into two categories: full-flow and partial-flow dilution units (Vouitsis et al., 2003). In all types of dilutors exhaust gas is mixed up with clean air in such a way that dilution ratio can be determined (either from flow rates or from concentrations).

To overcome the cost and size problems normally associated with full-flow dilution method, where the whole exhaust is firstly conditioned and then sampled for PM analysis, microdilution (so-called partial-flow dilution) systems have been extensively tested for the measurement of particulates and became popular among the researchers in the recent years. These systems firstly appeared in early 1980s and were applied both to heavy engines and light duty vehicles (MacDonald et al., 1980). In such systems, a small - but proportional to the total flow - fraction of the total exhaust is sampled and used for the determination of the PM emission rate. In such systems both dilution air temperature and dilution ratios (DR) can be controlled more easily with higher achievable DR and providing more flexibility in control of nucleation particle formation process (Virtanen, 2004).

3.1.1. Sampling and transport

In partial-flow dilution systems the sample of exhaust gas should be firstly drawn from engine tailpipe and transported to dilution unit by means of transfer line, making sampling and transport steps especially important, hence they should be arranged in a way to minimize any particle losses in exhaust as may result in some misleading findings. The actual design of sampling probe is closely related to conditions of exhaust gas. ISO standard foresees four possible sampling probe designs: 1) an open tube facing upstream; 2) an open tube facing downstream; 3) a multiple hole probe; and 4) a 'hatted' probe facing upstream (so-called 'Chinese hat' probe). The open-ended sampling probe facing upstream is not recommended for measurements from highly sooting engines unless a pre-classifier is used, while the other three alternatives are believed to prevent excessive loading by large particles by their design only.

The transfer line is of concern mainly because of possible particle deposition on its wall surfaces and the distortions that such deposition can impose on particle measurement results. Two major deposition mechanisms are diffusion and thermophoresis (Kittelson et al., 1999). Diffusion is a function of residence time, and hence of transfer line length and gas flow rate (Silvis et al., 2002), while thermophoretic effects are dependent on radial thermal gradients in the line and are exacerbated by the high volume-to-surface ratio of the transfer tube (Eastwood, 2008). Diffusional losses can be minimized by reducing length of the line and increasing gas flow rates and thermophoretic deposition can be suppressed or even eliminated by transfer line heating and its proper insulation (e.g. Kittelson and Johnson, 1991; Hinds, 1999).

Nevertheless, losses not only due to diffusion and thermophoresis, but also because of inertial impaction and other mechanisms (e.g. Hinds, 1999), should be taken into account for any sampling set-up employed. So in current study the correction procedure based on well-known correlations obtained in literature (Baron and Willeke, 2005) was used for particulate data correction in Paper II-VI and is described in details in Appendix B.

3.1.2. Dilution

A partial-flow-type 2-stage dilution unit composed of primary porous tube diluter and secondary ejector diluter was used in current study and the overall particle sampling-measurement set-up is shown on Figure 6.
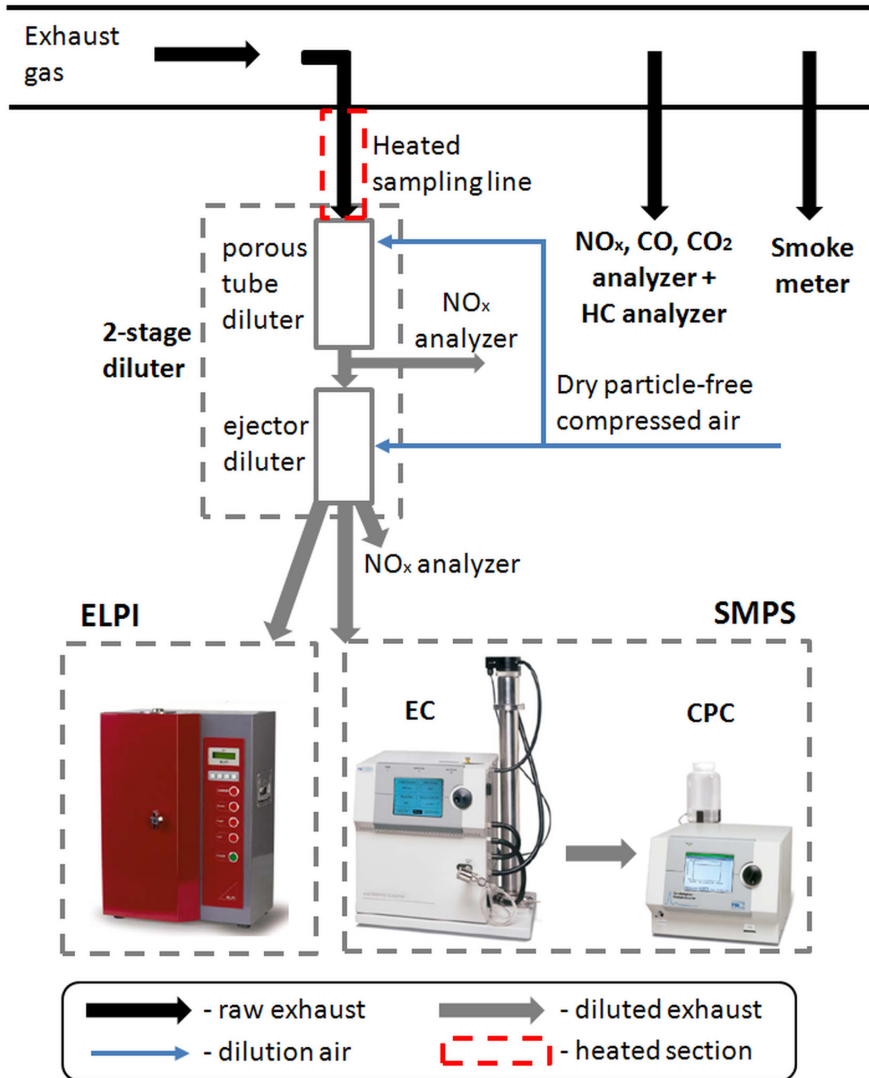
Figure 6:   Sampling and particle measurement set-up used (Paper V).

Exhaust gas dilution process has no effect on solid soot (accumulation mode) fraction, which is formed inside the engine cylinder(s), but is very important for soluble fraction, composed mainly of HC compounds and sulfur with associated bound water (e.g. Kittelson, 1998; Schneider et al., 2005). Depending on dilution parameters, like dilution ratio, dilution air temperature and humidity and residence time in dilution unit, gas-to-particle conversion process of SOF (or VOF) compounds may occur (e.g. Abdul-Khalek et al., 1998, 1999; Khalek et al., 2000; Mathis et al., 2004). Gas-phase material may be adsorbed and/or condensed on the surface of existing solid particles (heterogeneous nucleation) or can form separate small nuclei particles (homogeneous nucleation) in the size range of 3-50 nm. The contribution of nucleation mode particulates to overall PM mass is rather small, but they can dominate the total particle number if homogeneous nucleation occurs. The tendency for nucleation has been also connected to high sulfur and/or high HC content in exhaust gas (e.g. Vaaraslahti et al., 2005; Rönkkö, 2008), so nuclei-particle formation process indirectly depends on engine operating parameters, fuel and lube oil composition and presence of exhaust aftertreatment systems.

Porous tube diluter

In such type of diluter dilution air is directed through a porous tube (pore size of around 20 µm) into the inner tube where it mixes with exhaust gas (see Figure 7a), thus due to such design is sheathing the aerosol flow from deposition and thermophoresis (Auvinen et al., 2000; Lyyränen et al., 2004). The temperature of dilution air can be controlled by using air heater, while dilution ratio can be varied by adjusting the sample flow, making it is rather easy to control the nucleation mode formation (Virtanen, 2004). But at the same time, it was reported (e.g. Lyyränen et al., 2004) that porous tube-type diluters have conditions not favourable for nucleation process due to mixing occurring somewhat slower than, for example, in ejector diluters. Despite this, porous tube diluters are widely used for combustion aerosols conditioning and mainly applied as primary dilutors (Virtanen, 2004; Rönkkö et al., 2007; Rönkkö, 2008; Högström et al., 2012). Their main advantages and disadvantages can be found in number of earlier studies (Mikkanen et al., 2001; Ntziachristos et al., 2004; Mathis et al., 2004).

Ejector diluter

In ejector-type diluter (Koch et al., 1988) the sample gas in drawn into diluter by a pressure drop caused by dilution air flow passing through the ejector nozzle with high velocity (Figure 7b). This partial-flow diluter is often used in combustion studies (e.g. Moisio, 1998; Ristimäki et al., 2002; Virtanen, 2004; Ristimäki, 2006; Rönkkö, 2008) and in current research was used for secondary dilution (Heikkila et al., 2009). Ejector diluter has a constant dilution ratio, which is independent of total exhaust flow rate, a short residence time and hence a rather efficient mixing.
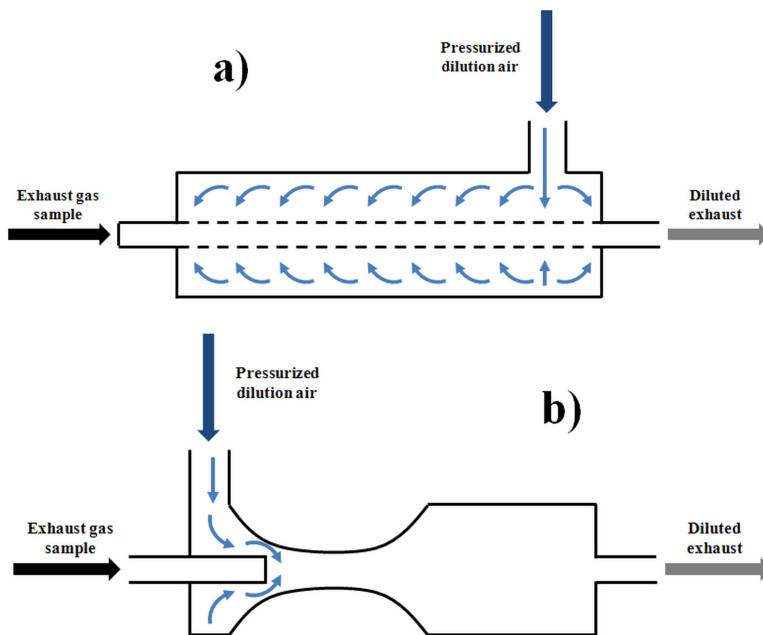
Figure 7:   Schematics of porous tube diluter (a) and ejector diluter (b).

3.2.   Particulate matter measurement

In general, most measurement techniques used in aerosol science can be divided in two categories: 1) collection of PM on a substrate, such as filter, for subsequent laboratory measurement; and 2) real-time or near-real-time measurements of particles. Historically, collection on filter was widely used, but is associated with several disadvantages like

possibility of particles being modified during transport and collection processes, and its non-real-time and time-averaged nature (Baron and Willike, 2005). On the other hand, real-time techniques can provide much quicker measurements, but at the same time the degree of particle characterization can be limited.

3.2.1. Total PM mass

Most of current PM regulations and measurement standards are based on particle mass measurements. Gravimetrical analysis of particle filters is mainly used for that purpose (Paper III and IV), but PM mass is also can be estimated from measured particle size distributions (Paper II, V and VI) or from mass distributions that can be obtained with inertial impactors (e.g. Virtanen, 2004).

Gravimetric analysis

A preliminary diluted and cooled to ≤52 °C sample of particle-laden exhaust gas is transported to a holder that contains appropriate filter medium where particles are separated from the gas. This process is dependent on type of filter media, filter face velocity, particle loading on filter (e.g. Vouitsis et al., 2003; Swanson and Kittelson, 2009; Högström et al., 2012) and other factors. Air drawn through the filter then passes to a flow measurement device like mass flow meter or rotameter (Baron and Willike, 2005), into a flow-regulating device and finally goes to pump or any other flow-moving device. Hence, proper arrangement of filter collection system is crucial to collecting a representative sample of particles on the filter.

The filter is weighted blank and after collection, so accumulated PM mass can be calculated. When collection time, dilution ratios, engine operating parameters and accumulated particle mass are known, the emission factor in mg/km (light-duty engines) and in g/kWh (heavy-duty engines) can be found. Even despite that there is number of various filter materials, none of them can be considered superior for gravimetric measurements as they all are prone to certain filter artifacts including adsorption and deposition of moisture by the filter or previously collected material, adsorption of gases

and vapours from the airstream, evaporation of volatile and semi-volatile materials collected by filter, and particle bounce rather than adhesion during contact with filter material (Baron and Willike, 2005). In Paper IV effects of filter media are considered in details, as well as effect of post-test filter conditioning time.

PM mass estimation from number distribution measurements

Another way to estimate overall PM mass is to use particle number distributions obtained with *in suti* instruments. These distributions together with appropriate assumptions regarding particle shape and density are sufficient to calculate the considered particulate mass. The assumption of spherical particles with unit density is a fairly good one for combustion aerosols (e.g. Amann and Siegla, 1982; Kittelson et al., 1991; Giechaskiel et al., 2010). At the same time, unity density assumption is best appropriate for droplet-like particulates, while soot particles are known to have fractal-like structure and densities decreasing when particle size increases (Burtscher, 2005). This can be taken into account by using concept of effective density which takes depends on porosity (shape and structure) of particulates (Kelly and McMurry, 1992; Hinds, 1999).

3.2.2. Particle number size distributions

Particle size is likely the most important particle property determining its behavior in a gas medium; particles of different sizes behave differently and can be governed by different physical laws. For spherical particles (many atmospheric PM) the diameter is normally a universal measure, while for non-spherical PM (fibers and agglomerates) a universal characteristic measure is much harder to find (Baron and Willeke, 2005), so in such cases concept of equivalent diameter is used. Two important diameter definitions having an important role in this work are aerodynamic equivalent and mobility equivalent (equivalent is often left out for simplicity) diameter. The aerodynamic diameter is defined as the diameter of spherical particle of unit density having the same terminal settling velocity as real particle. This diameter concept is used in measurement devices that employ inertial separation principles (cyclones, cascade impactors) and

depend on particle density. On the other hand the mobility diameter can be determined as the diameter of spherical particle moving with the same speed and experiencing the same drag force as particle in question. This diameter concept depends on the particle motion in the force field (in electrical field it depends on charge level and mobility size) and does not depend on particle density (Virtanen, 2004, Ristimaki, 2006) and is used in differential mobility analyzers. Nevertheless, the aerodynamic and mobility equivalent diameter concepts can be linked through the following expression:

$$d_a^2 C(d_a) \rho_0 = d_m^2 C(d_m) \rho_{eff} \qquad (3.1)$$

where $C(d)$ is Cunningham slip correction factor for aerodynamic diameter d_a and mobility diameter d_m respectively, ρ_0 is unit density and ρ_{eff} is effective density, which depends on PM material density, porosity, particle shape and was investigated in number of studies (e.g. Kelly and McMurry, 1992; Hinds, 1999; Ristimaki et al., 2002; Virtanen et al., 2004; Ristimaki and Keskinen, 2006).

The aerosol PM is very seldom uniform in size and typically consists of particles distributed over a certain range. A differential size distribution which is basically a histogram with fine interval resolution is commonly used to describe particle population, and is called number distribution if ordinate on the plot is number of particles. There is a variety of devices used for particle number size distribution measurements which detailed description and operating principles can be found in literature (e.g. Hinds, 1999; Baron and Willike, 2005). Two most commonly used to study diesel aerosols instruments called Scanning Mobility Particle Sizer (SMPS; Wang and Flagan, 1990) and Electrical Low Pressure Impactor (ELPI; Keskinen et al., 1992) are used in current work and described below.

Scanning Mobility Particle Sizer (SMPS)

The main particle size distribution results in current study were obtained using SMPS (Wang and Flagan, 1990) which includes Differential Mobility Analyzer (DMA; Knudson and Whitby, 1975) and Condensation Particle Counter (CPC; e.g. Bicard et al.,

1976; Sem, 2002). The main purpose of DMA is to extract a known size fraction of submicrometer particles from the incoming polydisperse aerosol. First, particles are charged by bipolar ions, so equilibrium charge state (Boltzmann charge distribution) is reached. Then the charged aerosol passes from the neutralizer into the main portion of the DMA shown in Figure 8a. The size classifier consists of two concentric metal cylinders (rods). Both polydisperse aerosol and sheath air are introduced at the top of DMA and flow down the annular space between the cylinders in such a way that aerosol surrounds the inner core of sheath air, and these flows pass down the annulus with no mixing of the two laminar streams (TSI, 2010). The inner cylinder or the collecting rod is maintained at a controlled negative voltage, while the outer cylinder is electrically grounded, which creates an electric field between the two cylinders. This field causes positively charged particles to be attracted through the sheath air to the negatively charged collector rod, so that they deposit on its surface. The settling location of deposited particles depends on the particle electrical mobility, the DMA flow rates, and the size classifier geometry. Particles with a high electrical mobility are precipitated along the upper portion of the rod; particles with a low electrical mobility are collected on the lower portion of the rod (Baron and Willeke, 2005). This technique allows particles within a narrow range of electrical mobility exit with the monodisperse air flow through a small port located at the bottom part of the collector rod.

These monodisperse particles are then transferred to CPC to determine the particle concentration, where the submicrometer particles are artificially enlarged by condensation of a supersaturated vapour (n-butanol in current study) into droplets that measure several micrometers in diameter. The droplets pass through a lighted viewing volume where they scatter light. These scattered-light pulses are then collected by a photodetector and converted into electrical pulses (TSI, 2007). These pulses are counted with their rate being a measure of particle concentration.

SMPS software (Wang and Flagan, 1990) allows continuous change of DMA collecting rod voltage from low to high values, while particle concentration is determined by CPC. So the scanning time can be as low as 1-2 minutes, while PM size distribution results can be obtained within measurement range with a rather high resolution.
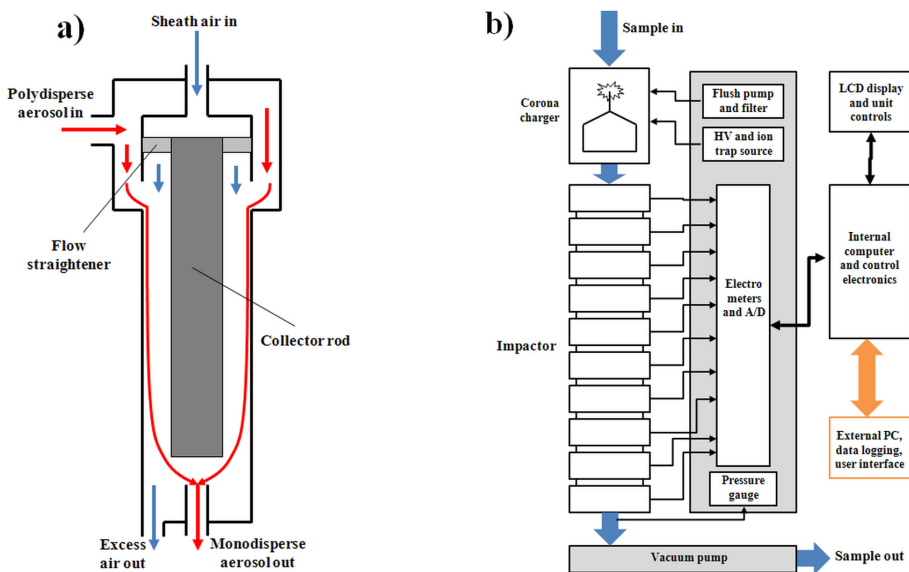
Figure 8:   Schematics of DMA (a) and ELPI (b).

Electrical Low Pressure Impactor (ELPI)

As seen from Figure 8b, the ELPI consists of corona charger and multistage cascade (12 stages + filter stage) impactor assembly, which detailed operation principles are described in literature (e.g. Keskinen et al., 1992; Baron and Willike, 2005) and multistage electrometer. The operating principle of ELPI is based on particle charging, inertial classification in a cascade impactor, and the electrical detection of charged aerosol particles (Dekati, 2008). At first, particles are charged by a unipolar positive-polarity corona charger with charging efficiency being the function of particle mobility size (Marjamäki et al., 2000). After charging, particles are size-classified from 7 nm (with filter stage; Marjamäki et al., 2002) to 10 μm by their aerodynamic diameter in a low-pressure impactor. Classification is achieved by turning the gas flow and capturing particles with high inertia, while particles with less inertia remain in gas stream. The charged PM that is collected by an impactor stage produces electrical current which is measured by an electrometer connected to each of the insulated impactor stages. The measured current value is proportional to the number of collected particles, and thus to

the particle concentration in the particular size, hence providing the required aerodynamic size distribution results (Dekati, 2008).

In ELPI the current is measured from the whole impactor stage, not only from collection substrate (Virtanen, 2004). The results might be affected by small particles collected to stage walls due to secondary collection mechanisms like diffusion and space charge and by bigger particle losses arising from particle bouncing when stage is overloaded. These losses mechanisms can significantly affect measured particle number concentration, so should be avoided. The losses associated with smallest particles are taken into account in calculation procedure (Virtanen et al., 2001), while bigger particle losses can be minimized using sintered collection plates that prevent overloading while added vacuum oil (capillary forces) prevents from bouncing.

The size resolution of ELPI is rather coarse as it has only 12 stages, but its fast response (less than 1-2 sec) making it extremely valuable instrument for transient test measurements and for continious real-time particle number concentration monitoring when is employed together with other instruments having higher size resolution, like SMPS. So far, ELPI was extensively used in many combustion application studies including vehicle emission investigations (e.g. Shi et al., 1999; Moisio, 1999; Mohr et al., 2000; Maricq et al., 2000, 2002; Shi and Harrison, 2001; Virtanen, 2004; Ristimaki and Keskinen, 2006; Giechaskiel et al., 2010 and others).

4.   Marine engines and fuels

Whereas for on-road vehicles only 4-stroke engines (gasoline and diesel) are applied, both 2-stroke and 4-stroke diesel-type engines are used for marine applications, although serving for different purposes. In this context, engines intended for use on a marine vessel (usually with bore size larger than 200 mm) are referred as marine diesel engines (MDE). Small 4-stroke medium speed (300-1000 rpm) or high-speed MDEs (>1000 rpm), with the power output in the range of 30-3000 kW, usually serve as auxiliary engines on-board, while large ones – for passenger transportation (ferries, cruise ships). At the same time, 2-stroke diesel engines generally power seagoing vessels intended for transportation of goods. This splitting of operational fields is mainly due to 4-stroke engines operating more smoothly than 2-stroke engines, which makes them more suitable for transportation of passengers (Kasper et al., 2007). Also the trunk piston 4-stroke engines (in contrast to 2-stroke crosshead engines) require less space on the vessel and are appropriate for smaller engine rooms. The 2-stroke engines have larger displacement volumes and therefore are more powerful than 4-stroke MDEs with similar bores, making them an ideal choice for fast and reliable transportation of goods by sea. Although it should be stated that most of cargo ships are equipped with two kinds of engines, where the main engine (normally 2-stroke) is running the ship and is mainly operated on heavy fuels, and the auxiliary engine (4-stroke), firing typically on distillate fuels, generates electricity for onboard consumers supply and is used to run manoeuvre systems in ports. So the auxiliary engines are in principle always in use, only turned off when land-based electricity replaces the generated electricity, and at sea if generators are connected to the main engine (Janhall, 2007). Passenger ships have a larger need of electricity maintaining the indoor climate onboard and thus often have larger auxiliary engines than typical cargo ships. The auxiliary engines in port areas are used mainly on ships that are unable / unwilling to use land based electricity and, as it was already stated above, for manoeuvring during arrival and departure to/from port.

At the same time the differences between on-road (and off-road) and marine diesel engines are quite significant. In addition to already overviewed preferences in

operational cycles (4-stroke for automotive engines and 2-stroke – for marine), the geometrical dimensions, engine operating parameters and types of fuels used are also very different (Kasper et al., 2007). The fuel effect, at the same time, might be the most important one as majority of the fuels used by the international fleet today are different variants of heavy fuel oil (HFO). This fuel typically contains residual compounds left after distillation of crude oil and is highly viscous, so requires heating before use onboard. In addition to viscosity this fuel type is characterized by its very high sulfur content, high density as well as high content of aromatic compounds and minerals respectively (e.g. Cooper et al., 1996; King et al., 2001). According to some sources (e.g. Ahlbom and Duus, 2006) residual oils contain about 7-20% of polycyclic aromatic hydrocarbons (PAHs) and an average of 2.7% of sulphur. The other category of marine fuels is marine distillates, which contains mainly well-refined products like marine gas oil (MGO), but its certain classes can include some fractions of residues.

It should be obvious that fuel composition has a great impact not only on the total level of emitted PM (Bonk and Lange, 1994), but also on particulate matter number distribution and particle composition emitted by marine diesel engines (e.g. Lyyränen et al., 1999). Moreover, there are not many studies related to the topic of particulate matter emissions from sea shipping (e.g. Kasper et al., 2007; Fridell et al., 2008; Petzold et al., 2008; Moldanova et al., 2009), especially from medium-speed MDEs.

4.1. PM emissions from medium-speed marine diesel engines

The effect of fuel type, as well as engine operating parameters (speed and load) and engine cycle on particulate matter emission characteristics of medium-speed MDEs was studied and results are presented in Paper I.

The study was particularly oriented on measurements of mainly solid PM and revealed significant differences in PM size distributions from 2-stroke and 4-stroke engines operating on both distillate and residual fuels as can be seen from Figure 9. The number size distributions for 2-stroke Wärtsilä WX28B engine operated on both fuels showed a bimodal structure consisting of load-independent accumulation (soot) mode and

nucleation mode decaying as load increases. This nucleation mode is believed to compose primarily of metal compounds originating from high lube oil emissions (Sakurai et al., 2003) caused by specific engine design and non-optimized lubrication oil supply system. The size distributions from 4-stroke Rolls-Royce engine at all load conditions were unimodal with pronounced accumulation mode. Soot mode PM observed in the study is likely composed of carbonaceous agglomerates due to incomplete fuel combustion during MGO operation and of soot together with incombustible fuel ash species in case of HFO firing (Lyyränen et al., 1999; Kasper et al., 2007; Moldanova et al., 2009; Popovicheva et al., 2009). This ash compounds (mainly metals) can also explain the registered increase in total particle number and number of nanoparticles (smaller 50 nm) observed when changing from MGO to HFO fuel. For example, during HFO firing nanoparticles corresponded in average 80-90 % from total PM number concentration.
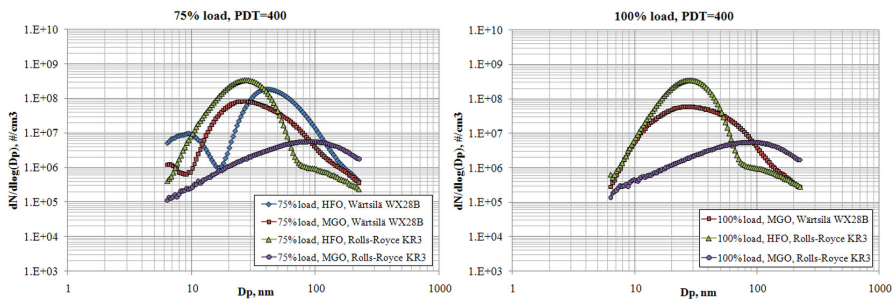
Figure 9:   Particle number distribution characteristics at various operating conditions for 2-stroke Wärtsilä WX 28B and 4-stroke Rolls-Royce KR3 engines operated on MGO and HFO fuels (Paper I).

Comparison of particle number distributions from MDEs to that from heavy-duty (HD) engine was performed and revealed a surprisingly good agreement in PM emission characteristics between automotive and 4-stroke marine engines. This result is rather hard to explain, especially if differences in engine geometrical dimensions and operating parameters are taken into account. At the same time, 2-stroke engine showed an accumulation mode at around 30 nm, which is much smaller than known for automotive engines (50-150 nm; for Euro I – Euro III engine design), but agrees well

with findings from studies related to particulate matter emissions of 2-stroke MDEs (e.g. Kasper et al., 2007).

Morphology analysis of PM samples, collected from MGO fuel, revealed several distinct particle classes: 1) carbonaceous agglomerates consisted of spherical primary carbon particles (found in wide size range); 2) very small separate spherical carbon particles and irregular-shape metal PM, more likely originated from lube oil; 3) big supermicron particles formed from fuel oil droplet residue and metal particles formed due to mechanical abrasion. Three main particle origins have been confirmed: fuel, oil and mechanical wear of moving cylinder parts.

4.2. Characterization of particulate matter from low-sulfur marine fuel

The study was performed on heavy-duty engine operated under steady-state modes based on ECE R49 cycle with test fuel being conventional low-sulfur MGO. Gaseous emissions, particle number size distributions and total concentrations were measured, while PM mass was estimated from number size distributions. Details of the study, including experimental set-up description, test conditions and detailed results are given in Paper II.

At both intermediate and full engine speed with load (fuel/air ratio) increase, the corresponding combustion (exhaust gas) temperature increased (air excess ratio decreased) resulting in increased NO_x and CO_2 concentration and corresponding decrease of HC and CO levels. PM mass and total particle number concentrations also showed increase with load that is mainly due to increase in number of accumulation (solid carbon) mode particles and caused by increased amount of injected fuel and associated more locally rich combustion zones, formed inside the cylinders, which are primarily responsible for soot formation (Tobias et al., 2002; Mathis et al., 2004).

The registered particle number size distribution at intermediate engine speed (1080 rpm) changed its shape from bimodal (only at low load) to unimodal form. Nucleation mode

appeared to be non-volatile and likely originates from heavy hydrocarbons and/or lube oil metal compounds and is typical for such low load conditions (Abdul-Khalek et al., 1998), while accumulation mode is believed to compose of soot agglomerates. At full speed (1800 rpm) only unimodal-shape number size distributions were observed with corresponding carbonaceous accumulation mode. The calculated count median diameter (CMD) values were almost independent of load at this speed and were 25% smaller than those for intermediate speed operation. This observation can be explained by higher exhaust flow rates at high engine speed, and hence smaller residence time available for particles to coagulate to bigger sizes.

Different settings for primary dilution air temperature (PDT) indicated significant contribution of volatile organic and sulfur compounds to overall PM emissions, both in terms of mass and number of emitted particulates (e.g. Baumgard, 1995), with this contribution being maximal at low loads (Ristimaki et al., 2010). Different aspects of dilution process are considered in greater details in Paper IV. At the same time separate nucleation mode was not observed, so heterogeneous nucleation of volatile compounds on the surface of existing solid particles is assumed to be prevailing mechanism.

4.3. Effect of high sulfur content

The sole effect of high sulfur content in marine fuels on PM emission characteristics was investigated in details in Paper III. To isolate the pure effect of sulfur from other influencing fuel components, like ash and metal sediments, the low-sulfur MGO, used as a reference fuel, was artificially doped by dimethyl disulfide (DMDS) at certain blending ratios. This resulted in fuels containing 2% and 4% of sulfur (by mass) representing typical sulphur levels that can be found in marine heavy fuel oils.

A strong correlation between fuel sulphur level and both number and mass of emitted particulates was observed as indicated by Figure 10 and Figure 11 respectively. The nucleation mode particles appeared to be the most affected as compose mainly of condensed/nucleated HC and sulphur compounds that dominate at low load conditions (e.g. Ristimaki et al., 2010). Heterogeneous nucleation (Kittelson, 1998; Shi and

Harrison, 1999) was dominating at these conditions and was additionally enhanced by availability of high amount of vapour-phase semivolatile (mainly sulphur) compounds available for condensation/adsorption when 2% and 4% sulphur fuels are used. These nuclei-mode particles comprised up to 80-90% from total PM concentration, but their contribution to PM mass was not so pronounced, although clearly visible.

At the same time, accumulation mode PM, composed of carbonaceous agglomerates formed during combustion process (Tobias et al., 2001), dominates the particle mass. This mode is independent of dilution conditions, but is affected by engine operating conditions, such as load and speed.
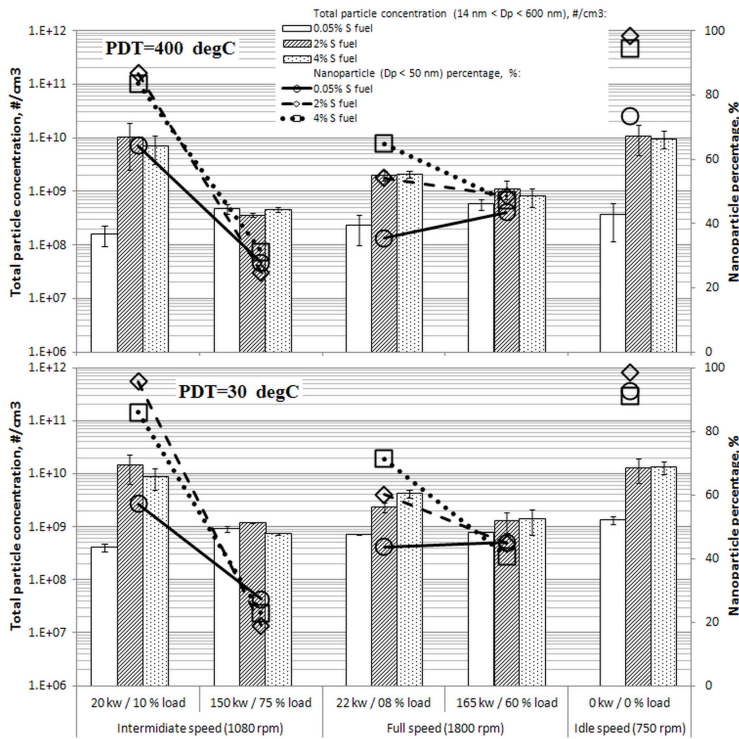
Figure 10: Effect of high sulphur content on total particle concentration and percentage of nanoparticles (<50 nm) at various operating conditions and PDT=400/30 °C (Paper III).

The effect of "hot dilution" (PDT=400 °C) on nucleation mode was rather moderate, while it was negligible for accumulation mode particles. Increase in PDT causes increase in saturation vapour pressures of volatile components, hence is slowing down nucleation (Abdul-Khalek et al., 1999). Although, as seen here for high sulphur fuels, it did not allow to entirely suppress nucleation, and can be likely explained by too high concentration of vapour-phase semivolatile compounds (too low primary dilution ratio employed) or by presence of solid core PM (Rönkkö et al., 2007; Lähde et al., 2010).
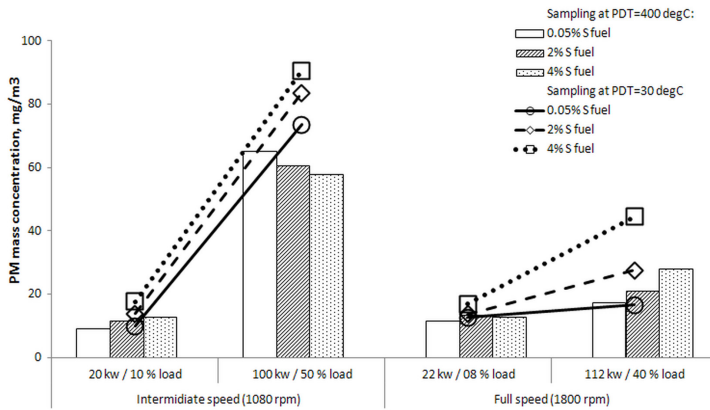
Figure 11: Effect of high sulphur level on PM mass measured gravimetrically at different engine load and speed conditions and PDT=400/30 °C (Paper III).

In addition, the PM mass concentrations found from gravimetric analysis of filter samples were compared to that estimated from ELPI number size distributions. Essentially a fairly good correlation between the data was observed, although number of potential error components, such as filter artefacts (e.g. Samara, 1995; Eastwood, 2008) and particle unit density assumption (e.g. Burtscher, 2005; Kasper et al., 2007; Giechaskiel et al., 2010), should be kept in mind.

4.4. Effects of dilution conditions on PM emissions in case of high-sulphur fuels

The effect of primary dilution ratio (PDR) and primary dilution temperature (PDT) on particle emission characteristics from low- and high-sulphur (artificially doped) marine

fuels, while operating a heavy-duty diesel at certain representative low and high load conditions of full engine speed, was investigated and main observations and findings are summarized in Paper IV. In addition, the importance of PM sampling filter media type and filter conditioning time are considered in the paper.

Both particle size distributions and mass concentrations were severely affected by the studied dilution parameters as reflected in Figure 12-14. Particle number size distributions were mainly unimodal (only accumulation mode), while bimodal shape was observed only at low-load conditions for 3% S fuel. It can be explained by the use of primary diluter of a porous tube-type, known not favouring heterogeneous nucleation due its rather low turbulence level (Lyyränen et al., 2004).

As seen from Figure 12 the PDT has especially large effect on nucleation mode particles which are believed to compose mainly of sulphuric acid and HC compounds (Kittelson, 1998). Increase of PDT causes saturation pressures of volatile compounds to increase, hence is suppressing nucleation process (Ristovski et al., 2006). The accumulation mode soot PM is believed to be independent of PDT, and the registered change in their concentration can be likely associated with a high amount of revolatilizing vapour-phase condensable matter during heat treatment. These compounds upon condensation can create a layer on the surface of existing soot PM (Abdul-Khalek et al., 1998) if sufficient amount of solid-core nucleus is available or can form rather big purely semivolatile particles. Moreover, PDT variation revealed a considerable contribution of temperature-sensitive semivolatile compounds to PM mass for 3% S fuel.

For both low- and high-sulphur fuels the found accumulation mode was not affected by changes in primary dilution ratio (e.g. Abdul-Khalek et al., 1998; 1999), when PDR ≥ 6-8, while for the case of PDR=3 a significant increase in particle mass and number concentration was observed (see Figure 13 and Figure 14 respectively). The only reasonable explanation might suggest a possible water-vapour condensation that can occur, as suggested by earlier studies (e.g. Ristimaki et al., 2010), when DR<4 are applied. The possibility and severity of such artefact should be considered by researchers in future and higher PDR values should be used.

In case of 3% S fuel low load conditions, which exhibited a pronounced nucleation mode peak, the increase of PDR showed a significant effect on nucleation mode particles decreasing their tendency to nucleate. Partial pressure of volatile species is reduced when PDR is increased (e.g. Mathis et al., 2004), hence is decreasing the driving force for nucleation.
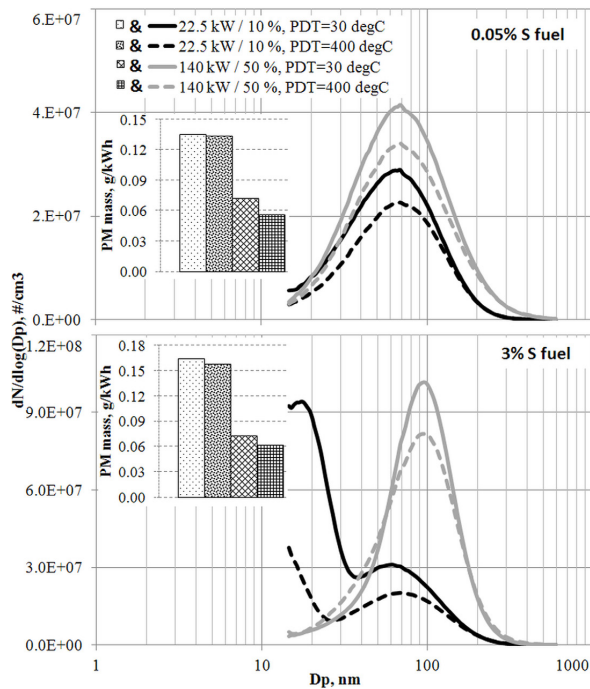
Figure 12: Effect of PDT on particle size distribution and mass concentrations at full engine speed for 3% sulphur (S) fuel. PDR values were remained in the range of 6-8 (Adopted from Paper IV).

The effect of filter media type was found to be vital, particularly in case of high sulphur fuels, as affinity of vapour-phase molecules very much depends on the filter surface composition. No filter type, including a commonly used and most-appreciated glass fiber filter (Khalek, 2007), was found overwhelmingly superior for gravimetric PM analysis due to various positive and/or negative artifacts that should be kept in mind. In

addition, a standard 24 hour filter conditioning time might be insufficient to reach complete PM sample equilibrium, so longer conditioning period can be required.
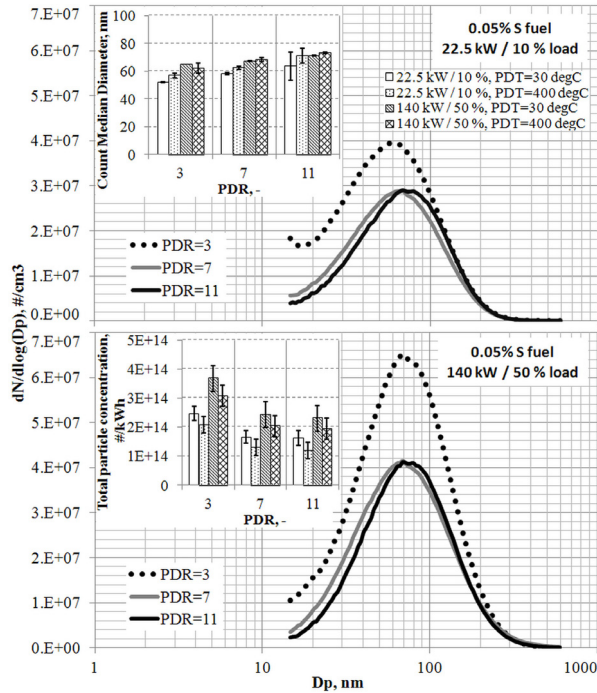
Figure 13: Effect of PDR on particle size distribution and total concentrations at full engine speed high-load conditions for conventional MGO fuel at PDT=30 °C (Adopted from Paper IV).
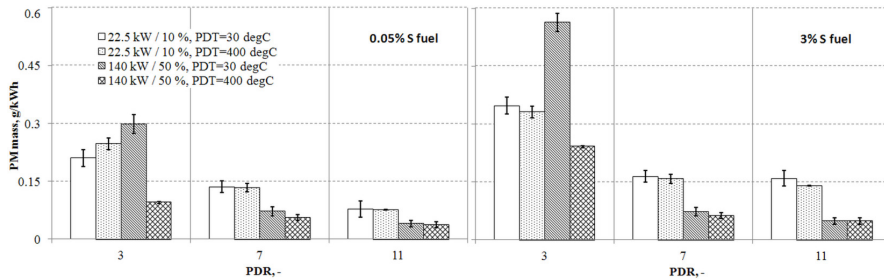
Figure 14: Influence of PDR on gravimetrically-measured PM mass collected at PDT=30 °C while operating engine at full speed (Paper IV).

5.   Emission reduction potential of alternative marine diesel fuels

The world's population is continuously growing, hence the demand for energy supply is also increasing. Nowadays it is mainly covered from petroleum, gas and coal sources, which are non-renewable by nature and may approach depletion within next 100 years (Monyem and Gerpen, 2001). At the same time, excessive use of fossil fuels is known to cause severe local, regional and global environmental problems like: local – air pollution, regional – acid rain and airborne pathogens (i.e. infections, particles and chemicals), global – greenhouse effect (Agarwal, 2007; Gill et al., 2011) with biggest contributor to atmospheric pollution being from transportation sector (Agarwal, 2007) that also includes transport by sea (sea-shipping).

Diesel engines are almost exclusively used as power sources for transportation purposes because of their advantages in fuel efficiency (also CO_2 reduction) and maximum power output in comparison with spark ignition engines (Soltic et al., 2009). But there still remains a challenge to control NO_x and PM emissions simultaneously to the levels allowed by regulations (Tree and Svensson, 2007). Two ways in solving this problem can be proposed: advanced emission abatement technologies like reformed exhaust gas recirculation (REGR), selective catalytic reduction (SCR) and diesel particulate filters (DPF) or use of alternative fuels like biofuels or synthetic fuels such as Fischer-Tropsch (FT) fuels (Abu-Jrai et al., 2006).

Biofuels are renewable sources of energy and can be potentially derived from various sources like plant matter, animal waste, agricultural crops and residues, municipal waste, and industrial effluents (e.g. Bozell et al., 2004; Jayasinghe and Hawboldt, 2012). Bio-oils are obtained from biomass, mainly from edible and non-edible crops like rapeseed, palm, sunflower, corn, safflower, canola, mahua and jatropha (e.g. Boyd et al., 2004; Raheman and Ghadge, 2006). At the same time, the evidence of food vs. fuel trade-off normally limits the use of food crops for fuel production (Jayasinghe and Hawboldt, 2012). In this case, biofuels derived from waste biomass are becoming

advantageous with fish oil (FO) being one such example (Blythe, 1996; Steigers, 2003). As all biofuels, it is renewable and can reduce dependency on fossil fuel. It has no aromatic compounds, almost no sulfur, but contains oxygen embedded in fuel molecules which may help to reduce CO, HC, and PM emissions (e.g. Ballesteros, 2002; Lapuerta et al., 2008). However, this fuel has number of drawbacks when compared to conventional diesel, like worse low temperature properties (Pegg and Joshi, 2007), lower lubricity and some other factors (e.g. Graboski and McCormick, 1998). The main concern is typically associated with observed excessive cylinder wear and reported deposit formation in exhaust tailpipes (Steigers, 2003). Despite that FO has demonstrated good ignition properties and excellent combustion characteristics in comparison with conventional diesel fuel (Blythe, 1996) and also require minimal processing time (Godinagur et al., 2010).

Synthetic fuels can offer another promising path for converting a variety of feedstocks to liquid fuels. The conversion technology for that is called Fischer-Tropsch process (e.g. Fischer and Tropsch, 1926; Dry, 2002; Leckel, 2009) and different feedstock sources can be used for raw material supply. In case the feedstock is natural gas, the product can be called GTL (gas-to-liquid) fuel. In comparison to conventional diesel fuel that contains a number of hydrocarbons, aromatics, napthens, and paraffins, the GTL is a paraffinic fuel that has a high cetane number, very low sulfur and aromatic (low C/H ratio) content, so pronounced emission reduction benefits from GTL can be expected (e.g. Alleman and McCormick, 2003; Heikkilä et al., 2009). However, it should be mentioned that these F-T fuels have a rather poor lubricity properties which can be improved either by using commercially available additives or by adding fatty acid methyl esters (FAME), i.e. biofuels (Alleman and McCormick, 2003).

5.1. GTL and FO fuels

Environmental benefits of using FO and GTL as potential alternatives to conventional MGO fuel in a diesel engine were investigated in Paper V and Paper VI respectively. The test engine (heavy-duty high-speed DI) was operated under modes of propulsion and generator operation, i.e. under E3 and E2 marine cycles respectively. The detailed

summary of gaseous, smoke and PM mass and number concentration results is given in Table 1 for FO biofuel and in Table 2 for GTL.

Table 1:   Gaseous, smoke and PM emissions for MGO and FO fuels.

Fuel	NO_x, g/kWh	CO, g/kWh	CO_2, g/kWh	THC, g/kWh	FSN, -	PM, g/kWh	N(total), #/cm^3	N(nano), #/cm^3
Propulsion mode								
25% load								
MGO	6.34	0.55	538.5	0.083	0.445	0.103	1.63×10^9	4.38×10^8
FO	6.56	0.36	530.8	0.035	0.085	0.030	6.38×10^8	2.11×10^8
Change: FO/MGO	**3.5%**	**-34.5%**	**-1.4%**	**-57.8%**	**-80.9%**	**-70.9%**	**-60.8%**	**-51.8%**
50% load								
MGO	5.87	0.86	537.6	0.078	1.095	0.148	2.05×10^9	4.65×10^8
FO	6.06	0.38	531.2	0.024	0.175	0.042	1.07×10^9	3.47×10^8
Change: FO/MGO	**3.2%**	**-55.8%**	**-1.2%**	**-69.2%**	**-84.0%**	**-71.6%**	**-47.8%**	**-25.3%**
75% load[1]								
MGO	3.97	0.29	565.9	0.099	0.455	0.095	1.68×10^9	5.38×10^8
FO	3.96	0.22	566.3	0.055	0.070	0.020	5.57×10^8	2.32×10^8
Change: FO/MGO	**~0%**	**-24.1%**	**~0%**	**-44.5%**	**-84.6%**	**-79.0%**	**-66.9%**	**-56.9%**
Generator mode								
25% load								
MGO	4.53	0.77	622.0	0.142	0.545	0.200	2.70×10^9	8.28×10^8
FO	4.79	0.63	623.6	0.061	0.115	0.070	1.58×10^9	7.14×10^8
Change: FO/MGO	**5.7%**	**-18.2%**	**0.3%**	**-57.1%**	**-78.9%**	**-65%**	**-41.4%**	**-13.9%**
50% load								
MGO	4.21	0.42	570.9	0.097	0.980	0.186	2.64×10^9	6.61×10^8
FO	4.39	0.30	567.6	0.050	0.160	0.051	1.53×10^9	6.24×10^8
Change: FO/MGO	**4.3%**	**-28.6%**	**-0.6%**	**-48.5%**	**-83.7%**	**-72.6%**	**-42.1%**	**-5.6%**

---

[1] Operating conditions for 75% load point of propulsion and generator modes are equal, i.e. common maximum (due to brake limitations) load point

Table 2: Gaseous, smoke and PM emissions for MGO and GTL fuels.

Fuel	NO_x, g/kWh	CO, g/kWh	CO_2, g/kWh	THC, g/kWh	FSN, -	PM, g/kWh	N(total), #/cm^3	N(nano), #/cm^3
Propulsion mode								
25% load								
MGO	6.23	0.50	511.0	0.088	0.345	0.048	8.24×10^8	1.95×10^8
GTL	5.72	0.53	500.3	0.096	0.389	0.057	1.08×10^9	2.48×10^8
Change: GTL/MGO	**-8.2%**	**6.0%**	**-2.1%**	**9.1%**	**12.8%**	**18.8%**	**31.6%**	**27.4%**
50% load								
MGO	5.92	0.69	514.4	0.074	0.865	0.113	1.71×10^9	4.20×10^8
GTL	5.00	0.56	490.8	0.087	0.770	0.110	2.21×10^9	5.48×10^8
Change: GTL/MGO	**-15.6%**	**-18.9%**	**-4.6%**	**17.6%**	**-11.0%**	**-2.7%**	**28.8%**	**30.3%**
75% load[2]								
MGO	4.07	0.28	549.1	0.092	0.400	0.064	1.48×10^9	5.66×10^8
GTL	3.29	0.28	527.6	0.105	0.290	0.054	1.85×10^9	7.95×10^8
Change: GTL/MGO	**-19.2%**	**0%**	**-3.9%**	**14.1%**	**-27.5%**	**-15.6%**	**25.0%**	**40.4%**
Generator mode								
25% load								
MGO	4.50	0.78	599.2	0.147	0.460	0.104	1.49×10^9	4.13×10^8
GTL	3.84	0.60	576.7	0.124	0.445	0.118	1.97×10^9	5.80×10^8
Change: GTL/MGO	**-14.7%**	**-23.1%**	**-3.8%**	**-15.7%**	**-3.3%**	**13.5%**	**32.7%**	**40.2%**
50% load								
MGO	4.29	0.40	554.4	0.095	0.790	0.137	2.28×10^9	6.11×10^8
GTL	3.64	0.39	528.5	0.100	0.580	0.116	2.62×10^9	7.88×10^8
Change: GTL/MGO	**-15.2%**	**-2.5%**	**-4.7%**	**5.3%**	**-26.6%**	**-15.3%**	**15.1%**	**29.0%**

---

[2] Operating conditions for 75% load point of propulsion and generator modes are equal, i.e. common maximum (due to brake limitations) load point

Analysis of combustion process revealed that fish oil fuel has almost identical or even better ignition and combustion properties when compared to MGO. In addition, as seen from Table 1, FO can significantly reduce CO, THC, smoke and PM emissions (in terms of particle mass and number concentration) both under modes of propulsion and generator operation. These effects can be attributed to its lack of aromatic compounds and presence of considerable amount of fuel-bound oxygen (Blythe, 1996; Steigers, 2003; Lapuerta et al., 2008), which results in better fuel-air mixing properties, hence minimizing the volume of fuel-rich regions, mainly responsible for HC, smoke and PM production (e.g. Ballesteros, 2002; Lapuerta et al., 2008; Mancaruso and Vaglieco, 2012). At the same time, measured NO_x concentration slightly increased, while CO_2 concentration slightly decreased, but the observed changes did not exceed 5%, so can be considered marginal. In addition, FO fuel is free of sulphur, so contribution of sulphuric compounds to PM fraction is negligible. Moreover, during whole experiment no additional deposits, clogging or excessive engine wear, which are often of high concern, were observed when engine was operated on fish oil biofuel (Jayasinghe and Hawboldt, 2012).

In case of GTL fuel, as highlighted in Table 2, the emitted NO_x concentrations can be pronouncedly reduced. The reason for that is its high cetane number, which results in shortened ignition delay (e.g. Abu-Jrai et al., 2006) and thus in less pronounced pre-mixed combustion. This gives lower NO_x formation rates with GTL fuel. Lack of aromatics in gas-to-liquid fuel also contributes to lower adiabatic flame temperature, which was reported to be lower for paraffinic compounds than for aromatic ones (e.g. Glaude et al., 2010). High cetane number and very low aromatic content can likely help in explaining observed carbon monoxide reduction (e.g. Wu et al., 2007). CO_2 reduction of around 4% in case of GTL fuel is believed to arise from its higher H/C ratio (Gill et al., 2011). At the same time, measured THC concentrations increased, and can be explained by higher GTL fuel volume flow rates that were increased to compensate for its lower fuel density (lower volumetric energy content) resulting in possible higher incidence of wall-wetting that contributes to HC emissions (Schaberg et al., 2002). Besides GTL negligible aromatic and nearly zero sulphur content are responsible for PM reduction (Ntziachristos et al., 2000; Xinling and Zhen, 2009) registered at medium

and high loads, while at low loads (Ristimaki et al., 2010) these effects are diminished by higher level of HC compounds emitted by GTL fuel due to possible fuel impingement on cylinder surfaces. This may also explain the observed increase in emitted particle number concentrations. Possible injection system modification/tuning for operation especially on GTL fuel and/or shift to more advanced common rail system might be proposed for further reduction of gaseous (especially THC) and PM emissions.

6.   **Summary and conclusions**

The interest in diesel aerosols is enhanced by the found correlation between human morbidity and mortality and the exposure to fine particles. Transportation sector is known to be one of the biggest contributors of particulate matter emissions to the atmosphere. In contrast to PM emissions from industry and road transport, which are steadily decreasing due to implemented strict PM regulations, the particulate matter emitted by sea shipping is expected to increase because of increased amount of goods transported by sea and due to absence of any direct particle emission regulation. In fact, the sea shipping can itself contribute as much PM emissions as road traffic, so can be considered a significant contributor of PM. Big marine diesel engines operated primarily on residual fuels are the main power-producers used for ship propulsion and there are only few research studies investigating their PM characteristics. Current thesis has focused on the measurement and characterization of diesel exhaust particles emitted by diesel engines operating on conventional marine fuels and their potential alternatives.

As presented in Paper I the particle size distributions emitted by 2-stroke and 4-stroke marine diesel engines are very different in shape, resulting in difference observed for total particle mass and number concentration and indicating the importance of engine technology. This finding is valid for both MGO and HFO fuels, although the emitted solid PM levels are higher for HFO fuel operation mainly due to its significantly higher ash content. Three different particle classes related to main origins of PM, such as fuel, lubrication oil and mechanical wear, were identified from PM morphology analysis.

A strong correlation between fuel sulphur level and both number and mass of emitted particulates was revealed as seen in Paper III. The contribution of fuel sulphur to PM mass was pronouncedly higher than is known for automotive fuels. Heterogeneous nucleation dominated at medium and high loads, while homogeneous (separate small nuclei formation) nucleation was observed only at low loads, which can be a consequence of a rather slow and not perfect mixing occurring in primary porous tube diluter. Both primary dilution temperature and primary dilution ratio can significantly

affect the measured PM results, as reported in Paper II and Paper IV for low-sulphur and high-sulphur fuel respectively. At the same time these parameters affect only the condensation/nucleation process of semivolatile HC and sulphur compounds, while carbonaceous PM concentration is not affected by changes in dilution settings. Too low (below 4) PDR should be avoided in case of marine fuels as water condensation may occur. The increase in PDR leads to reduction in partial pressure of semivolatile compounds, while increasing PDT results in increase of saturation vapour pressure of these compounds, hence is decreasing their tendency to nucleate.

The effect of filter media type was considered to be especially significant when high-sulphur marine fuels are used (Paper IV) as the importance of possible positive and/or negative filter measurement artifacts should be taken into account. No filter type was considered overwhelmingly superior for gravimetric analysis.

Both fish oil biofuel and gas-to-liquid Fischer-Tropsch fuel indicated a big potential in reducing gaseous and particulate matter emissions and at the same time keeping a fairly good ignition and combustion properties as presented in Paper V and Paper VI for FO and GTL fuel respectively. These fuels can be considered potential substitutes for conventional MGO, although additional experiments to validate rheological, cold temperature properties and its oxidation stability of FO might be required. In addition, engine injection system modification/tuning or shift to common rail arrangement can help to reduce gaseous (especially THC) and PM emissions from GTL fuel even further.

It should be finally stated that one additional aim of this thesis was also to pin-point the importance of marine fuels (and their high sulphur levels) as contributor of PM to air pollution and to encourage the development of regulations to control particulate matter emissions from marine diesel engines, i.e. from shipping.

6.1. Contributions of the thesis

The output of the research study can be summarized as follows:

C1: Commercially available particle sampling and dilution setup was adapted and validated for robust and reliable measurement of PM from marine diesel engines (Paper I) and fuels (Paper I-IV).

C2: The effect of dilution parameters (PDR and PDT) on particle emission from low- and high-sulphur marine fuels was thoroughly investigated (see Paper II and Paper IV). High-temperature dilution (PDT=400 °C) was shown to be an easy and reliable way to measure solid PM. Very low PDR (below 4) was found to lead to water condensation artefact, hence should be avoided in future.

C3: The sole effect of high-sulphur level in marine fuels was studied by sulphur doping of MGO fuel (Paper III) and revealed a significant contribution of sulphate-phase PM both to particle mass and number concentrations. As far as author knows, there were no similar studies done before where such high sulphur content (up to 4% by mass) was simulated by sulphur dopant addition.

C4: A method to calculate PM mass concentration from particle size distribution results obtained by ELPI was proposed, developed and rather successfully validated (for marine fuels) against filter-based PM mass data (Paper II-III). Such method can be used on-board of the ships for preliminary PM mass estimation and does not require dilution tunnel, although has several limitations that are discussed in Paper III.

C5: The potential of fish oil biofuel and Fischer-Tropsch GTL fuel as alternative to conventional MGO in terms of reduction of gaseous and PM emissions were investigated in Paper V and Paper VI respectively. Both these fuels indicated pronounced environmental benefits when were tested under propulsion and generator mode marine cycles, although further analysis of certain fuel properties might be required.

C6: The detailed assessment of particle losses during sampling and exhaust sample transport for used PM sampling setup was performed by the author based on various literature sources (Appendix B). The spreadsheet was created and applied for particle

losses correction in Paper II-VI, which resulted in significant increase in accuracy of reported PM results. With minor modifications this spreadsheet can be used to estimate losses in almost any sampling setup.

6.2. Recommendations for future work

It should be mentioned that the area of diesel particulate matter emissions from maritime industry (shipping) is not well investigated and requires more attention. From author's perspective it can be interesting to investigate particle growth process (coagulation of particles) in the engine exhaust system, which may help to identify the most optimal location of the sampling point (especially important in case of on-board experiments). Comparison of particle emission characteristics from modern and old-technology marine engines (e.g. Tier I vs. Tier II) on its turn can help to quantify the effectiveness of various technologies used for PM (both mass and number) reduction in maritime sector. Nevertheless, the most interesting topic for further detailed study can be to perform ambient PM measurements on ship's deck and in harbor areas and compare these results with ones presented in current thesis. There were no studies trying to find correlation between laboratory and field PM measurement results from marine engines, so the results can be very valuable.

7.   References

Abdul-Khalek, I.S., Kittelson, D.B., Brear, F. (1998). Diesel trap performance: particle size measurements and trends. *SAE Technical Paper* 982599.

Abdul-Khalek, I.S., Kittelson, D.B., Brear, F. (1999). The influence of dilution conditions on diesel exhaust particle size distribution measurements. *SAE Technical Paper* 1999-01-1142.

Abu-Jrai, A., Tsolakis, A., Theinnoi, K., Cracknell, R., Megaritis, A., Wyszynski, M.L., Golunski, S.E. (2006). Effect of gas-to-liquid diesel fuels on combustion characteristics, engine emissions, and exhaust gas fuel reforming. Comparative study. *Energy and Fuels*, 20, 2377-2384.

Agarwal, A.K. (2007). Biofuels (alcohols and biodiesel) applications as fuels for internal combustion engines. *Progress in Energy and Combustion Science*, 33, 233-271.

Ahlbom, J. and Duus, U. (2006). *Claen solutions for ships – examples from the port of Göteborg.* Grönn kemi, *www.gronkemi.se*. Göteborg, Sweden: Länsstyrelsen Västra Götalands Län, SE-403 40.

Alleman, T.L. and McCormick, R.L. (2003). Fischer-Tropsch diesel fuels e properties and exhaust emissions: a literature review. *SAE Technical Paper* 2003-01-0763.

Amann, C.A. and Siegla, D.C. (1982). Diesel particles – what they are and why. *Journal of Aerosol Science and Technology*, 1, 72-101.

Asariotis, R., Benamara, H., Hoffmann, J., Núñez, E., Premti, A., Valentine and Vincent, V. (2009). *Review of maritime transport 2009*. New York and Geneva, United Nations Conference on Trade and development (UNCTAD).

Auvinen A., Lehtinen K.E.J., Enriquez J., Jokiniemi J.K., Zilliacus R. (2000). Vaporization rates of CsOH and CsI in conditions simulating a severe nuclear accident. *Journal of Aerosol Science,* 31, 1029-1043.

Ålander, T. (2006). *Carbon composition and volatility characteristics of the aerosol particles formed in internal combustion engines*. Ph.D. Thesis. University of Kuopio, Finland.

Ålander, T.J.A., Leskinen, A.P., Raunemaa, T.M., Rantanen, L. (2004). Characterization of diesel particles: Effects of fuel reformulation, exhaust aftertreatment, and engine operation on particle carbon composition and volatility. *Environmental Science and Technology*, 38, 2707-2714.

Ballesteros, R. (2002). *Analisis experimental de las emisiones de particulas de un motor Diesel con combustibles convectionales y alternatives*. PhD Thesis. Universidad de Castilla-La Mancha, Spain.

Ban-Weiss G.A., Lunden M.M., Kirchstetter T.W., Harley, R.A. (2010). Size resolved particle number and volume emission factors for on-road gasoline and diesel motor vehicles. *Journal of Aerosol Science*, 41, 5-12.

Baron, P.A. and Willeke, K. (2005). *Aerosol measurement: Principles, techniques, and applications, 2nd edition*. New Jersey: John Wiley & Sons Inc., 1131 pp.

Baumgard, K. (1995). *The effect of fuel and engine design on diesel exhaust particle size distributions*. PhD Thesis. Michigan Technological University, USA.

Bicard, J., Delattre, P., Madelaine, G., Pourprix, M. (1976). Detection of ultra-fine particles by means of continuous flux condensation nucleus counters. In *Aerosol generation, measurement, sampling, and analysis*. Academic Press, New York, pp. 565-580.

Blythe, N.X. (1996). Fish oil as an alternative fuel for internal combustion engines. 1996 spring technical conference. *ASME*, 3, 85-92.

Bockhorn, H.E. (1994). *Soot formation in combustion*. Berlin: Springer-Verlag. 593 pp.

Bonk, N. and Lange, J. (1994). Einflüsse von Kraftstoffkomponenten und motorischen Massnahmen auf die Abgaszusammentsetzung an einem schwerölbetribenen Schiffsdieselmotor. *Abgasemission von Schiffsdieselmotoren bei Schwerölbetrieb II (ASS II) 18 S 00117*. IFKO, Universität Hannover. 149 pp. (in German).

Boyd, M., Murray-Hill, A., Schaddelee, K. (2004) *Biodiesel in British Columbia – feasibility study report*. WISE Energy Co-op/Eco-Literacy Canada.

Bozell, J., Moens, L., Peterson, E., Tyson, K.S., Wallace, R. (2004). *Biomass oil analysis: research needs and recommendations*. NREL Technical Report.

Brunshidle, T.P., Konowalchuk, B., Nabeel, I., Sullivan, J.E. (2003). A review of the measurement, emission, particles: Characteristics and potential human health impacts of ultrafine particle. Available at: *http://enhs.umn.edu/5103/particles/character.html.*

Burtscher, H. (1992). Measurement and characteristics of combustion aerosols with special consideration of photoelectric charging and charging by flame ions. *Journal of Aerosol Science,* 23, 549-595.

Burtscher, H. (2005). Physical characterization of particulate emissions from diesel engines: a review. *Journal of Aerosol Science,* 36, 896-932.

Caines, A.J., Haycock, R.F., Hillier, J.E. (2004). *Automotive lubricants reference book.* SAE International and Professional Engineering Publishing. 760 pp.

Chambers, L.A., edited by Stern, A.C. (1976). *Air pollution, volume 1: Air pollutants, their transformations and transport.* New York: Academic Press Inc. 715 pp.

Ciambelli, P., Corbo, P., Parrella, P., Scialò, M., Vaccaro, S. (1990). Catalytic oxidation of soot from diesel exhaust gases: 1. Screening of metal oxide catalysts by TG-DTG-DTA analysis. *Thermochimica Acta*, 162, 83-89.

Clague, A.D.H., Donnet, J.B., Wang, T.K., Peng, J.C.M. (1999). A comparison of diesel engine soot with carbon black. *Carbon*, 37, 1553-1565.

Clark, N.N., Atkinson, C.M., McKain, D.L., Nine, R.D., El-Gazzar, L. (1996). Speciation of hydrocarbon emissions from a medium duty diesel engine. *SAE Technical Paper* 960322.

Cofala, J., Amann, M., Heyes, C., Wagner, F., Klimont, Z., Posch, M., Schöpp, W., Tarasson, L., Johnson, J.E., Whall, C., Stavrakaki, A. (2007). *Analysis of policy measures to reduce ship emissions in the context of the revision of the National Emissions Ceiling Directive* (Final report). Laxenburg, Austria: International Institute for Applied Systems Analysis (IIASA).

Cooper, D.C. and Alley, F.C. (1986). *Air pollution control: a design approach.* Boston: PWS publishers, 630 pp.

Cooper, D.A., Peterson, K., Simpson, D. (1996). Hydrocarbon, PAH and PCB emissions from ferries: A case study in the Skagerak-Kattegatt-Öresund region. *Atmospheric Environment*, 30, 2463-2473.

Corbett, J.J., Winebrake, J.J., Green, E.H., Kasibhatla, P., Eyring, V., Lauer, A. (2007). Mortality from ship emissions: a global assessment. *Environmental Science and Technology*, 41, 8512-8518.

De Filippo, A. and Maricq, M.M. (2008). Diesel nucleation mode particles: semivolatile or solid? *Environmental Science and Technology,* 42, 7957-7962.

Dekati (2008). *ELPI, User manual, ver. 4.10*. Dekati Ltd.: Tampere, Finland.

de Lucas, A., Durán, A., Carmona, M., Lapuerta, M. (2001). Modelling diesel particulate emissions with neural networks. *Fuel*, 80, 539-548.

Dockery, D., Pope, C.A., Xu, X., Spengler, J., Ware, J., Fay, M., Ferris, B., Speizer, F. (1993). An association between air pollution and mortality in six U.S. cities. *New England Journal of Medicine*, 329, 1753-1759.

Donaldson, K., Beswick, P. H., Gilmour, P. S. (1996). Free radical activity associated with the surface of particles: A unifying factor in determining biological activity? *Toxicology Letters*, 88, 293–298.

Doyle, M., and Dorling, S. (2002). Visibility trends in the UK 1950-1997. *Atmospheric Environment*, 36, 3161-3172.

Dry, M. (2002). The Fischer-Tropsch process: 1950-2000. *Catalysis Today*, 71, 227-41.

Duggal, V.K., Priede, T., Khan, I.M. (1978). A study of pollutant formation within the combustion space of a diesel engine. *SAE Technical Paper* 780227. *SAE Transactions,* 87.

Eastwood, P. (2008). *Particulate emissions from vehicles*. Chichester, England: John Wiley & Sons Ltd. 493 pp.

EPA (2007). Report on the environment: Science report (SAB review draft). Available at: *http://cfpub.epa.gov/ncea/cfm/recordisplay.cfm?deid=140917* obtained 25.03.11.

Eyring, V., Kohler, H.W., van Aardenne, J., Lauer, A. (2005). Emissions from international shipping: 1. The last 50 years. *Journal of Geophysical Research*, 110, D17305.

Fischer, F. and Tropsch, H. (1926). The synthesis of petroleum at normal pressure. "Verfahren zur Gewinnung mehrgliedriger Paraffinkohlenwasserstoffe aus Kohlenoxygen und Wasserstoff auf katalytischem Wege", in D.R.G. Patent, DPR 484337, Germany.

Flagan, R.C., Seinfeld, J.H. (1988). *Fundamentals of air pollution engineering*. Englewood Cliffs, N.J.: Prentice Hall. 542 pp.

Forsberg, B., Hansson, H.-C., Johansson, C., Areskoug, H., Persson, K., and Järvholm, B. (2005). Comparative health impact assessment of local and regional particulate air pollutants in Scandinavia. *Ambio*, 34, 11.

Fridell, E., Steen, E., Peterson, K. (2008). Primary particles in ship emissions. *Atmospheric Environment*, 42, 1160-1168.

Giechaskiel, B., Chirico, R., DeCarlo, P.F., Clairotte, M., Adam, T., Martini, G., Heringa, M.F., Richter, R., Prevot, A.S.H., Baltensperger, U., and Astorga, C. (2010). Evaluation of the particle measurement programme (PMP) protocol to remove the vehicles exhaust aerosol volatile phase. *Science of the Total Environment*, 408, 5106-5116.

Ghio, A.J., Kim, C., Devlin, R.B. (2001). Concentrated ambient air particles induce mild pulmonary inflammation in healthy human volunteers. *American Journal of Respiratory and Critical Care Medicine*, 162, 981-982.

Giechaskiel, B., Chiroco, R., DeCarlo, P.F., Clairotte, M., Adam, T., Martini, G., Heringa, M.F., Richter, R., Prevot, A.S.H., Baltensperger, U., Astorga, C. (2010). Evaluation of the particle measurement programme (PMP) protocol to remove the vehicles exhaust aerosol volatile phase. *Science of the Total Environment*, 408, 5106-5116.

Gill, S.S., Tsolakis, A., Dearn, K.D., Rodriguez-Fernandez, J. (2011). Combustion characteristics and emissions of Fischer-Tropsch diesel fuels in IC engines. *Progress in Energy and Combustion Science*, 37, 503-523.

Glaude, P.-A., Fournet, R., Bounaceur, R., Moliere, M. (2010). Adiabatic flame temperature from biofuels and fossil fuels and derived effect on NOx emissions. *Fuel Processing Technology*, 91, 229-235.

Godiganur, S., Murthy, C.S., Reddy, R.P. (2010). Performance and emission characteristics of a Kirloskar HA394 diesel engine operated on fish oil methyl esters. *Renewable Energy*, 35, 355-359.

Graboski, M.S. and McCormick, R.L. (1998). Combustion of fat and vegetable oil derived fuels in diesel engines. *Progress in Energy and Combustion Science*, 24, 125-164.

Haagen-Smith, A.J., Wayne, L.G., edited by Stern, A.C. (1976). *Air pollution, volume 1: Air pollutants, their transformations and transport*. New York: Academic Press Inc. 715 pp.

Hampson, G.J., Reitz, R.D. (1998). Two-colour imaging of in-cylinder soot concentration and temperature in a heavy-duty DI diesel engine with comparison to multidimensional modeling for single and split injections. *SAE Technical Paper* 980524.

Haynes, B.S., Wagner, H.G. (1981). Soot formation. *Progress in Energy and Combustion Science*, 7, 229-273.

Heikkilä, J., Virtanen, A., Rönkkö, T., Keskinen, J., Aakko-Saksa, P., Murtonen, T. (2009). Nanoparticle emissions from a heavy-duty engine running on alternative diesel fuels. Environmental Science and Technology, 43, 9501-9506.

Henein, N.A. (1976). Analysis of pollutant formation and control and fuel economy in diesel engines. *Progress in Energy and Combustion Science*, 1, 165-207.

Heywood, J.B. (1988). *Internal combustion engine fundamentals*. New York: McGraw-Hill Inc. 930 pp.

Hill S.H. and Sytsma, S.J. (1991). A systems approach to oil consumption. *SAE Technical Paper* 910743.

Hinds, W.C. (1999). *Aerosol technology: Properties, behavior, and measurement of airborne particles, 2nd edition*. Canada: John Wiley & Sons Inc. 483 pp.

Högström, R., Karjalainen, P., Yli-Ojanperä, J., Rostedt, A., Heinonen, M., Mäkela, J.M., Keskinen, J. (2012). Study of the PM gas phase filter artefact using a setup for mixing diesel like soot and hydrocarbons. Submitted to *Aerosol Science and Technology*.

IPCC (2001). *Climate change 2001: Synthesis report*. Available at: *http://www.grida.no/publications/other/ipcc_tar/*, accessed 04.05.2010.

Janhall, S. (2007). *Particle emissions from ships*. Report. The Alliance For Global Sustainability.

Jayasinghe, P. and Hawboldt, K. (2012). A review of bio-oil from waste biomass: Focus on fish processing waste. *Renewable and Sustainable Energy Reviews*, 16, 798-821.

Kadota, T., Henein, N.A., Lee, D.U. (1980). A new approach to study the formation of soot particulates in diesel sprays. *The Spring Meeting, Central States Section of the Combustion Institute.* March 1980.

Kasper, A., Aufdenblatten, S., Forss, A., Mohr, M., Burtscher, H. (2007). Particulate emissions from a low-speed marine diesel engine. *Aerosol Science and Technology*, 41, 24-32.

Kelly, W.P. and McMurry, P. (1992). Measurement of particle density by inertial classification of differential mobility analyzer-generated monodisperse aerosol. *Aerosol Science and Technology,* 17, 199-212.

Kennedy, I.M. (2007). The health effects of combustion-generated aerosols. *Proceedings of the Combustion Institute*, 31, 2757-2770.

Kerminen, V.-M., Mäkelä, T.W., Ojanen, C.H., Hillamo, R.E., Vilhunen, J.K., Rantanen, L., Havers, N., von Bohlen, A., Klockow, D. (1997). Characterization of the particulate phase in the exhaust from a diesel car. *Environmental Science and Technology*, 31, 1883-1889.

Keskinen, J., Pietarinen, K., Lehtimäki, M. (1992). Electrical low pressure impactor. *Journal of Aerosol Science*, 23, 353-360.

Khalek, I.A. (2007). *Diesel particulate measurement research. CRC E-66, Final Report*. Phase 1. May, 2007.

Khalek, I.A., Kittelson, D.B., Brear, F. (2000). Nanoparticle growth during dilution and cooling of diesel exhaust: experimental investigation and theoretical assessment. *SAE Technical Paper* 2000-01-0515.

Khan, I.M. (1969). Formation and combustion of carbon in a diesel engine. *Proceedings of the Institution of Mechanical Engineers*, 184, 36-43.

Khan, I.M., Wang, C.H.T., Langridge, B.E. (1971). Coagulation and combustion of soot particles in diesel engines. *Combustion and Flame*, 17, 409-419.

Kimura, K., Lynskey, M., Corrigan, E.R., Hickman, D.L., Wang, J., Fang, H.L., Chatterjee, S. (2006). Real world study of diesel particulate filter ash accumulation in heavy-duty diesel trucks. *SAE Technical Paper* 2006-01-3257.

King, D., Bradfield, M., Falkenback, P., Parkerton, T., Peterson, D., Remy, E., Toy, R., Wright, M., Dmytrasz, B., Short, D. (2001). Environmental classification of petroleum substances - summary data and rationale. Brussels, CONCAWE.

Kittelson, D.B. (1998). Engines and nanoparticles: a review. *Journal of Aerosol Science*, 29, 575-588.

Kittelson, D.B. (2006). *Ultrafine particles formation mechanisms* (Report). Minneapolis, MN, USA: University of Minnesota. 37 pp.

Kittelson, D.B. and Johnson, J.H. (1991). Variability in particle emission measurements in the heavy duty transient test. . *SAE Technical Paper* 910738.

Kittelson, D.B., Reinertsen, J., Michalski, J. (1991). Further studies of electrostatic collection and agglomeration of diesel particles. *SAE Technical Paper 910329*.

Kittelson, D.B., Watts, W.F., Arnold, M. (1999). *Review of diesel particulate matter sampling methods*. Final report. Minneapolis, MN, USA: University of Minnesota. 64 pp.

Kittelson D.B., Watts W.F., Johnson J. (2002). *Diesel aerosol sampling methodology*. Final Report # CRC-E43. University of Minnesota: Minneapolis, MN.

Klein, H., Lox, E., Kreuzer, T., Kawanami, M., Ried, T., Bächmann, K. (1998). Diesel particulate emissions from passenger cars – New insights into structural changes during the process of exhaust aftertreatment using diesel oxidation catalysts. *SAE Technical Paper* 980196.

Knudson, E.O. and Whitby, K.T. (1975). Aerosol classification by electric mobility: apparatus, theory, and application. *Journal of Aerosol Science*, 6, 443-451.

Koch, W., Lödding, H., Mölter, W., Munzinger, F. (1988). Verdünnungssystem fü die Messung hochkonzentriet Aerosole mit Optischen Partikelzählern. *Staub-Reinhaltung der Luft*, 48, 341-344.

Lapuerta, M., Rodriguez-Fernandez, J., Agudelo, J.R. (2008). Diesel particulate emissions from used cooking oil biodiesel. *Bioresource Technology*, 99, 731-740.

Leckel, D. (2009). Diesel production from Fischer-Tropsch: the past, the present, and new concepts. *Energy and Fuels*, 23, 295-330.

Lewandowska, A., Falkowska, L., Murawiec, D., Pryputniewicz, D., Burska, D., Beldowska, M. (2010). Elemental and organic carbon analysis in aerosols over urbanized coastal region (southern Baltic Sea). *Science of the Total Environment*, 408, 4761-4769.

Li, X., Wallace, J.S. (1995). A phenomenological model for soot formation and oxidation in direct injection diesel engines. *SAE Technical Paper* 952428.

Lighty, J.S., Veranth, J.M., Sarofim, A.F. (2000). Combustion aerosols: factors governing their size and composition and implications to human health. *Journal of the Air and Waste Management Association*, 50, 1565–1618.

Lim, M.C.H., Ayoko, G.A., Morawska, L., Ristovski, Z.D., Jayarante, E.R. (2007). The effects of fuel characteristics and engine operating conditions on the elemental composition of emissions from heavy duty diesel busses. *Fuel*, 86, 1831-1839.

Lyyränen, J., Jokiniemi, J., Kauppinen, E.I., Joutsensaari, J. (1999). Aerosol characterisation in medium-speed engines operating with heavy fuel oils. *Journal of Aerosol Science,* 30, 771.

Lyyränen, J., Jokiniemi, J., Kauppinen, E.I., Backman, U., Vesala, H. (2004). Comparison of different dilution methods for measuring diesel particle emissions. *Aerosol Science and Technology,* 33, 239-260.

Lähde, T., Rönkkö, T., Virtanen, A., Solla, A, Kytö, M., Söderström, C., Keskinen, J. (2010). Dependence between nonvolatile nucleation mode particle and soot number concentrations in an EGR equipped heavy-duty diesel engine exhaust. *Environmental Science and Technology*, 44, 3175-3180.

MacDonald, J.S., Plee, S.L., D'Arcy, J.B., Schreck, RM. (1980). Experimental measurements of the independent effects of dilution ratio and filter temperature on diesel exhaust particle samples. *SAE Technical Paper* 800185.

Macián, V., Payri, R., Tormos, B., Montoro, L. (2006). Applying analytical ferrography as a technique to detect failures in diesel engine fuel injection system. *Wear*, 260, 562-566.

Mancaruso, E. and Vaglieco, B.M. (2012). Premixed combustion of GTL and RME fuels in a single cylinder research engine. *Applied Energy*, 91, 385-394.

Maricq M.M., Chase R.E., Xu N., Laing P.M. (2002). The effects of the catalytic converter and fuel sulfur level on motor vehicle particulate matter emissions: light duty diesel vehicles. *Environmental Science and Technology*, 36, 283-290.

Maricq, M.M., Podsiadlik, D.H., Chase, R.E. (2000). Size distributions of motor vehicle exhaust PM: A comparison between ELPI and SMPS measurements. *Journal of Aerosol Science and Technology*, 33, 239-260.

Marjamäki, M., Keskinen, J., Chen, D.-R., Pui, D.Y.H. (2000). Performance evaluation of electrical low-pressure impactor (ELPI). *Journal of Aerosol Science*, 31, 249-261.

Marjamäki, M., Ntziachristos, L., Virtanen, A., Ristimäki, J., Keskinen, J., Lappi, M. (2002). Electrical filter stage for the ELPI. *SAE Technical Paper* 2002-01-0055.

Mathis, U., Ristimäki, J., Mohr, M., Keskinen, J., Ntziachristos, L., Samaras, Z., Mikkanen, P. (2004). Sampling conditions for the measurement of nucleation mode particles in the exhaust of diesel vehicle. *Journal of Aerosol Science and Technology*, 38, 1149-1160.

Mayer, A., Czerwinski, J., Scheidegger, W., Kieser, D., Bigga, E., Wyser, M. (1997). VERT – clean diesel engines for tunnel construction. *SAE Technical Paper* 970478.

McDow, S.R., Jang, M., Hong, Y., Kamens, R.M. (1996). An approach to studying the effect of organic composition on atmospheric aerosol photochemistry. *Journal of Geophysical Research*, 101, 19593-19600.

McKenna, J.D., Turner, J.H., McKenna Jr., J.P. (2008). *Fine particle (2.5 microns) emissions. Regulation, measurement, and control*. John Wiley & Sons Inc.: Hoboken, New Jersey.

Mikkanen P., Moisio M., Keskinen J., Ristimäki J., Marjamäki M. (2001). Sampling method for particle measurements of vehicle exhaust. *SAE Technical Paper* 2001-01-0219.

Mohr, M., Steffen, D., Forss, A.M. (2000). Particulate emissions of gasoline vehicles and influence of the sampling procedure. *SAE Technical Paper* 2000-01-1137.

Moisio, M. (1999). *Real time size distribution measurement of combustion aerosols*. Ph.D. Thesis. Tampere University of Technology: Finland.

Moldanová, J., Fridell, E., Popovicheva, O., Dimirdjian, B., Tishkova, V., Faccinetto, A., Focsa, C. (2009). Characterisation of particulate matter and gaseous emissions from a large ship diesel engine. *Atmospheric Evironment*, 43, 2632-2641.

Monyem, A. and van Gerpen, J.H. (2001). The effect of biodiesel oxidation on engine performance and emissions. *Biomass and Bioenergy*, 20, 317-325.

Neyestanaki, A.K., Klingstedt, F., Salmi, T., Murzin, D.Y. (2004). Deactivation of postcombustion catalysts, a review. *Fuel*, 83, 395-408.

Ntziachristos, L., Samaras, Z., Pistikopoulos, P., Kyriakis, N. (2000). Statistical Analysis of Diesel Fuel Effects on Particle Number and Mass Emissions. *Environmental Science and Technology*, 34, 5106-5114.

Ntziachristos L., Giechaskiel B., Pistikopoulos P., Samaras Z., Mathis U., Mohr M., Ristimaki J., Keskinen J., Mikkanen P., Casati R., Scheer V., Vogt R. (2004). Performance evaluation of a novel sampling and measurement system for exhaust particle characterization. *SAE Technical Paper* 2004-01-1439.

Oberdörster, G. (2000). Toxicology of ultrafine particles: In vivo studies. *Philosophical Transactions of the Royal Society Series A*, 258, 2719–2740.

Owen, K. and Coley, T. (1995). *Automotive fuels reference book*. SAE International. 976 pp.

Pandis, S.N., Harley, R.A., Cass, G.R., Seinfeld, J.H. (1992). Secondary organic aerosol formation and transport. *Atmospheric Environment*, 26A, 2269-2282.

Pegg, M.J. and Joshi, R.M. (2007). Flow properties of biodiesel fuel blends at low temperatures. *Fuel*, 86, 143-151.

Petzold, A., Hasselbach, J., Lauer, P., Baumann, R., Franke, K., Gurk, C., Schlager, H., Weingartner, E. (2008). Experimental studies on particle emissions from cruising ship, their characteristic properties, transformation and atmospheric lifetime in the marine boundary layer. *Atmospheric Chemistry and Physics*, 8, 2387-2403.

Pietropaoli, A.P., Frampton, M.W., Hyde, R.W., Morrow, P.E., Oberdörster, G., Cox, C. et al. (2004). Pulmonary function, diffusing capacity and inflammation in healthy and asthmatic subjects exposed to ultrafine particles. *Inhalation Toxicology*, 16 (suppl. 1), 59–72.

Pope III, C.A. (2000). Epidemiology of fine particulate air pollution and human health: Biologic mechanisms and who's at risk? *Environmental Health Perspectives*, 108 (Suppl.), 713–723.

Pope III, C.A., Burnett, R.T., Thun, M.J., Calle, E.E., Krewski, D., Ito, K., Thurnston, G.D. (2002). Lung cancer, cardiopulmonary mortality, and long-term exposure to fine particulate air pollution. *Journal of American Medical Association*, 287, 1132-1141.

Pope III, C.A., Burnett, R.T., Thurston, G.D., Thun, M.J., Calle, E.E., Krewski, D. et al. (2004). Cardiovascular mortality and long-term exposure to particulate air pollution. Epidemiological evidence of general pathophysiological pathways of disease. *Circulation*, 109, 71–77.

Pope, C.A. and Dockery, D.W. (2006). Health effects of fine particulate air pollution: lines that connect. *Journal of the Air and Waste Management Association*, 56, 709-742.

Pope III, C.A., Thun, M.J., Namboodiri, M.M., Dockery, K.S., Evans, J.S., Speizer, F.E., Heath Jr., C.W. (1995). Particulate air pollution as a predictor of mortality in a prospective study of US adults. *American Journal of Respiratory and Critical Cardiac Care Medicine*, 151, 669-674.

Popovicheva, O., Kireeva, E., Shonija, N., Zubareva, N., Persiantseva, N., Tishkova, V., Demirdijan, B., Moldanová, J., Mogilnikov, V. (2009). Ship particulate pollutants: Characterization in terms of environmental implication. *Journal of Environmental Monitoring,* 11, 2077-2086.

Querini, C.A., Ulla, M.A., Requejo, F., Soria, J., Sedrán, U.A., Miró, E.E. (1998). Catalytic combustion of diesel soot particles. Activity and characterization of Co/MgO and Co,K/MgO catalysts. *Applied Catalysis B: Environmental*, 15, 5-19.

Raheman, H. and Ghadge, S.V. (2006). Process optimization for biodiesel production from mahua (*Madhuca indica*) oil using response surface methodology. *Bioresource Technology*, 97, 379-384.

Raux, S., Forti, L., Barbusse, S., Plassat, G., Pierron, L., Monier, R., Momique, J.C., Pain, C., et al. (2005). French program on the impact of engine technology on particulate emissions, size distribution and composition heavy duty diesel study. *SAE Technical Paper* 2005-01-0190.

Ray, A., Wichman, I.S. (1998). Influence of fuel-side heat loss on diffusion flame extinction. *International Journal of Heat and Mass Transfer*, 41, 3075-3085.

Richter, H., Howard, J.B. (2000). Formation of polycyclic aromatic hydrocarbons and their growth to soot – a review of chemical rection pathways. *Progress in Energy and Combustion Science*, 26, 565-608.

Ristimäki, J. (2006). *Sampling and measurement methods for diesel exhaust aerosol*. Ph.D. Thesis. Tampere University of Technology: Finland.

Ristimäki, J. and Keskinen, J. (2006). Mass measurement of non-spherical particles: TDMA-ELPI setup and performance tests. *Journal of Aerosol Science and Technology,* 40, 997-1001.

Ristimäki, J., Virtanen, A., Marjamäki, M., Rostedt, A., Keskinen, J. (2002). On-line measurement of size distribution and effective density of submicron aerosol particles. *Journal of Aerosol Science,* 33, 1541-1557.

Ristimäki, J., Hellen, G., Lappi, M. (2010). Chemical and physical characterization of exhaust particulate matter from a marine medium speed diesel engine. *CIMAC Congress 2010, Bergen, Norway*. Paper #73, 11 pp.

Ristovski, Z.D., Jayaratne, E.R., Lim, M., Ayoko, G.A., Morawska, L. (2006). Influence of diesel fuel sulfur on nanoparticle emissions from city busses. *Environmental Science and Technology*, 40, 1314-1320.

Rogge, W.F., Hildemann, L.M., Mazurek, M.A., Cass, G.R., Simoneit, B.R.T. (1993a). Sources of fine organic aerosols. 2. Noncatalyst and catalyst-equipped automobiles and heavy-duty diesel trucks. *Environmental Science and Technology*, 27, 636-651.

Rogge, W.F., Mazurek, M.A., Hildemann, L.M., Cass, G.R., Simoneit, B.R.T. (1993b). Quantification of urban organic aerosols at a molecular level: identification, abundance and seasonal variation. *Atmospheric Environment*, 27A, 1309-1330.

Rothen-Rutishauser, B.M., Schürch, S., Haenni, B., Kapp, N., Gehr, P. (2006). Interaction of fine particles and nanoparticles with red blood cells visualized with advanced techniques. *Environmental Science and Technology,* 40, 4353-4359.

Ruckerl, R., Ibald-Mulli, A., Koenig, W., Schneider, A., Woelke, G., Cyrys, J. et al. (2006). Air pollution and markers of inflammation and coagulation in patients with coronary heart disease. *American Journal of Respiratory and Critical Cardiac Care Medicine*, 173, 432-441.

Ryall, D.B., Derwent, R.G., Manning, A.J., Redington, A.L., Corden, J., Millington, W., Simmonds, P.G., Doherty, S.O., Carslaw, N., Fuller, G.W. (2002). The origin of high particulate concentrations over the United Kingdom, March 2000. *Atmospheric Environment*, 36, 1363–1378.

Rönkkö, T. (2008). *Diesel exhaust particles: On-road and laboratory studies*. Ph.D. Thesis. Tampere University of Technology: Finland.

Rönkkö, T., Virtanen, A., Kannosto, J., Keskinen, J., Lappi, M., Pirjola, L. (2007). Nucleation mode particles with a non-volatile core in the exhaust of a heavy duty diesel vehicle. *Environmental Science and Technology,* 41, 6384-6389.

Sakurai, H., Tobias, H.J., Park, K., Zarling, D., Docherty, K.S., Kittelson, D.B., McMurry, P.H., Ziemann, P.J. (2003). On-line measurements of diesel nanoparticle composition, volatility, and hygroscopicity. *Atmospheric Environment*, 37, 1199-1210.

Samara, C. (1995). Analysis of organic matter. In *Airborne Particle Matter*, Volume 4, Part D. Kouimtzis, T., Samara, C. (eds.). Springer, 233-252 pp.

Santoro, R.J., Miller, J.H. (1987). Soot particle formation in laminar diffusion flames. *Langmuir*, 3, 244-254.

Schaberg, P., Botha, J., Schnell, M., Hermann, H.O., Pelz, N., Maly, R. (2002). Emissions performance of GTL diesel fuel and blends with optimized engine calibrations. *SAE Technical Paper 2002-01-2727*.

Schneider, J., Hock, N., Weimer, S., Borrmann, S., Kirchner, U., Vogt, R., Scheer, V. (2005). Nucleation particles in diesel exhaust: composition inferred from *in suti* mass spectrometer analysis. *Environmental Science and Technology,* 39, 6153-6161.

Seaton, A. (1999). Airborne particles and their effects on health. In *Particulate matter: Properties and effects upon health*. Maynard, R.L., Howard, C.V. (editors). Bios Scientific Publishers, pp. 9-18.

Sem, G.J. (2002). Design and performance characteristics of three continuous-flow condensation particle counters: a summary. *Atmospheric Research*, 62, 267-294.

Shi, J.P. and Harrison, R.M. (1999). Investigation of ultrafine particle formation during diesel exhaust dilution. *Environmental Science and Technology,* 33, 3730-3736.

Shi, J.P., Harrison, R.M., Brear, F. (1999). Particle size distribution from a modern heavy duty diesel engine. *Science of the Total Environment*, 235, 305-317.

Silvis, W.M., Marek, G., Kreft, N., Schindler, W. (2002). Diesel particulate measurement with partial flow sampling systems: a new probe and tunnel design that correlates with full flow tunnels. *SAE Technical Paper* 2002-01-0054.

Smith, R.G. (1981). Fundamentals of soot formation in flames with application to diesel engine particulate emissions. *Progress in Energy and Combustion Science*, 7, 275-291.

Smooke, M.D., Long, M.B., Connelly, B.C., Colket, M.B., Hall., R.J. (2005). Soot formation in laminar diffusion flames. *Combustion and Flame*, 143, 613-628.

Soltic, P., Edenhauser, D., Thurnheer, T., Schreiber, D., Sankowski, A. (2009). Experimental investigation of mineral diesel fuel, GTL, fuel, RME and neat soybean and rapeseed oil combustion in a heavy-duty on-road engine with exhaust gas aftertreatment. *Fuel*, 88, 1-8.

Stanmore, B., Brilhak, J.-F., Gilot, P. (1999). The ignition and combustion of cerium doped diesel soot. *SAE Technical Paper* 1999-01-0115.

Stanmore, B., Brilhak, J.-F., Gilot, P. (2001). The oxidation of soot: A review of experiments, mechanisms and models. *Carbon*, 39, 2247-2268.

Stern, A.C., Wohlers, H.C., Boubel, R.W., Lowry, W.P. (1973). *Fundamentals of air pollution*. New York: Academic Press Inc. 492 pp.

Steigers, J.A. (2003). *Demonstrating the use of fish oil in a large stationary diesel engine*. Steigers Corporation.

Struwe, F.J., Foster, D.E. (2003). In-cylinder measurement of particulate radiant heat transfer in a direct injection diesel engine. *SAE Technical Paper* 2003-01-0072.

Sugiara, K., Kagaya, M. (1977). A study of visible smoke reduction from a small two-stroke engine using various engine lubricants. *SAE Technical Paper* 770623.

Suzuki, H., Toyooka, T., Ibuki, Y. (2007). Simple method to evaluate uptake potential of nanoparticles in mammalian cells using a flow cytometric light scatter analysis. *Environmental Science and Technology*, 41, 3018-3024.

Swanson J., Kittelson D.B. (2009). Factors influencing mass collected during 2007 Diesel PM filter sampling. *SAE Technical Paper* 2009-01-1517.

Tobias, H.J., Beving, D.E., Ziemann, P.J., Sakurai, H., Zuk, M., McMurry, P.H., Zarling, D., Waytulonis, R., Kittelson, D.B. (2002). Chemical analysis of diesel engine nanoparticles using a nano-DMA/thermal desorption particle beam mass spectrometer. *Environmental Science and Technology*, 35, 2233-2243.

Tomiyasu, B., Owari, M., Nihei, Y. (2006). TOF-SIMS measurements of the exhaust particles emitted from gasoline and diesel engine vehicles. *Applied Surface Science*, 252, 7026-7029.

Tree, D.R. and Svensson, K.I. (2007). Soot processes in compression ignition engines. *Progress in Energy and Combustion Science*, 33, 272-309.

TSI (2010). *Series 3080 Electrostatic classifiers. Operation and service manual*. Revision H, April 2008. TSI Inc.: Shoreview, MN.

TSI (2007). *Model 3775 Condensation particle counter. Operation and service manual*. Revision D, April 2007. TSI Inc.: Shoreview, MN.

Turpin, B.J. and Huntzicker, J.J. (1995). Identification of secondary organic aerosol episodes and quantification of primary and secondary organic aerosol concentration during SCAQS. *Atmospheric Environment,* 29, 3527-3544.

Vaaraslahti K., Virtanen A., Ristimaki J., Keskinen J. (2004). Nucleation mode formation in heavy-duty diesel exhaust with and without a particulate filter. *Environmental Science and Technology*, 38, 4884-4890.

Vander Wal, R.L., Tomasek, A.J. (2004). Soot nanostructure: Dependance upon synthesis conditions. *Combustion and Flame*, 136, 129-140.

Villinger, J., Federer, W., Praun, S. (2002). Continuous pre- and post-catalyst hydrocarbon and nitrogen compounds-monitoring of various DeNO$_x$ reactions by twin chemical ionization spectrometry. *SAE Technical Paper* 2002-01-1679.

Virtanen, A. (2004). *Physical characterization of diesel soot particles*. Ph.D. Thesis. Tampere University of Technology: Finland.

Virtanen, A., Marjamäki, M., Ristimäki, J., Keskinen, J. (2001). Fine particle losses in electrical low-pressure impactor. *Journal of Aerosol Science,* 32, 389-401.

Virtanen, A., Ristimäki, J., Keskinen, J. (2004). Method for measuring effective density and fractal dimension of aerosol agglomerates. *Journal of Aerosol Science and Technology,* 38, 437-446.

Vouitsis, E., Ntziachristos, L., Samaras, Z. (2003). Particulate matter mass measurements from low emitting diesel powered vehicles: what's next? *Progress in Energy and Combustion Science*, 29, 635-672.

Wang, S.C. and Flagan, R.C. (1990). Scanning Electrical Mobility Spectrometer. *Aerosol Science and Technology,* 13, 230-240.

Wang, Y.-F., Huang, K.-L., Li, C.-T., Mi, H.-H., Luo, J.-H., Tsai, P.-J. (2003). Emissions of fuel metals content from a diesel vehicle engine. *Atmospheric Environment*, 37, 4637-4643.

Watkinson, W.P., Campen, M.J., Nolan, J.P., Kodavanti, U.P. et al. (2000). In *Relationships between acute and chronic effects of air pollution. Cardiovascular effects following exposure to particulate matter in healthy and cardiopulmonary*

compromised rat. Heinrich, U., Mohr, U. (editors). Washington, DC: ILSI Press, pp. 447-463.

Xinling, L. and Zhen, H. (2009). Emission reduction potential of using gas-to-liquid and dimethyl ether fuels on a turbocharged diesel engine. *Science of the Total Environment*, 407, 2234-2244.

Appendix A: Selected publications

Paper I

Particulate emission characteristics from medium-speed marine diesel engines

Sergey Ushakov, Harald Valland, Jørgen B. Nielsen, Erik Hennie

The Proceedings of the PACIFIC 2012 International Maritime Conference

31 January – 02 February 2012, Sydney, Australia

Particulate Emission Characteristics from Medium-Speed Marine Diesel Engines

Sergey Ushakov, Norwegian University of Science and Technology, Norway
sergey.ushakov@ntnu.no
Harald Valland, Norwegian University of Science and Technology, Norway
Jørgen B. Nielsen, MARINTEK AS, Norway
Erik Hennie, MARINTEK AS, Norway

Particulate matter (PM) emissions from diesel engines are of major concern due to their adverse health effects. While PM emissions from the automotive sector have been regulated for decades, there have been no direct regulations on PM from sea-going vessels. The engines used in maritime sector are significantly different from automotive engines not only regarding their size, but also in regard to power output and fuels used.

This study presents results from exhaust particle emission measurements from two different medium-speed turbocharged marine diesel engines: 2-stroke Wätrsilä WX28B and 4-stroke Rolls-Royce KR3. The engines were tested according to ISO 8178-4 E2 and E3 cycles, using two typical marine fuels: marine gas oil (MGO) and heavy fuel oil (HFO). The size distributions were obtained using Scanning Mobility Particle Sizer (SMPS) and Electrical Low Pressure Impactor (ELPI), operated simultaneously.

The obtained number distributions for 2-stroke engine are mainly bimodal with the pronounced nucleation mode, representing mainly non-volatile species originating from lubrication oil, and found below 20 nm and accumulation mode at 20-60 nm, referred to carbonaceous agglomerates, while for 4-stroke engine only accumulation mode was observed, and appeared to be insensitive to changes in load conditions. Additionally, results revealed a surprisingly good agreement both in total particle number and mean count median diameter values between 4-stroke Rolls-Royce KR3 and 4-stroke heavy-duty diesel engine for MGO fuel, while results from a 2-stroke Wätrsilä WX28B engine were very different.

1. INTRODUCTION

During the last decades the particulate matter emissions have become a topic of significant interest. A number of toxicological and epidemiological studies (e.g. Dockery et al., 1993; Pope, 2000; Pope at al., 2002) confirmed the existence of statistical correlation between the daily mortality and morbidity and the exposure to small particles. Diesel engine PM emissions are known as a major source of fine particles in the environment with the majority of them being in nanoparticle (i.e. below 50 nm) size range (Kittelson, 1998). Modern medical investigations showed the possibility of nanoparticles to penetrate into the human body cells (Suzuki et al., 2007) causing structural damage and can have a potential to cross the blood-brain barrier (Oberdörster et al., 2004). So the awareness of the probable adverse health effects associated with aerosol particles became the main driving force to limit diesel PM mass emissions. The regulations originally restricted the total suspended particulate (TSP) mass, but later shifted their main attention to mass of particles having aerodynamic diameter smaller than 10 μm and 2.5 μm respectevely, resulting in corresponding PM10 and PM2.5 standards, as more strong evidences of smaller particle effect on human health have been found (e.g. Goo and Kim, 2003). Although, not all researchers agree that PM mass is the best appropriate metric to assess the negative effects of diesel PM on human health. Other

suggestions are, for example, surface area (e.g. Oberdörster et al., 1996) or/and particle number concentration (Ferin et al., 1992) to be more appropriate.

A number of studies comprehensively investigated PM mass, number concentrations and size distributions from automotive light- and heavy-duty diesel engines (e.g., Kittelson, 1998; Kittelson et al., 2006). The diesel PM emissions normally range from 3 nm to approximately 1 μm in diameter with characteristic bimodal-shape size distribution with two distinctive modes. The nucleation mode representing the particles smaller 50 nm is believed to be semivolatile and consisting mainly of hydrocarbons and sulphuric acid PM formed during the dilution process (Kittelson et al., 1999), but could also contain non-volatile species originated from lubrication oil (e.g. Tobias et al., 2001; Sakurai et al., 2003), while accumulation mode is usually associated with carbonaceous agglomerates larger than 50 nm in size with volatile compounds adsorbed on the surfaces of these solid particles.

Despite the large number of studies concerning automotive engine PM, there were only few ones (e.g. Lyyränen et al., 1999; Kasper et al., 2007) related to particle emissions from marine diesel engines (MDE), which are believed to be as significant PM source as road traffic (Eyring et al., 2005) with corresponding adverse health effects resulting in number of serious diseases and decrease of life expectancy (e.g. Corbett et al., 2007). And while the particle emissions from in-land sources continuously decrease due to stricter environmental standards applied, the amount of PM emitted by sea-shipping can either decrease as the permittable sulfur content in marine fuels will be reduced and a wider use of LNG fuel is expected or it can increase because of significantly increasing ship traffic and absence of any direct regulation of particle emissions from marine diesel engines. This is still a hot topic for debates and up to now none of these theories has been validated.

There are several principal differences between automotive and marine diesel engines, which should be pointed out here. Firstly, they operate on highly different types of fuel with cars and trucks using a well-refined, high-quality products, and MDEs operating mostly on heavy fuels. It means the latter type of engines has to burn fuels with relatively large content of sulphur, ash and other residual contaminants, i.e. the compounds that are avoided in auto diesel fuel. Secondly, engines' geometrical dimensions and size also differ significantly, which may have effect on engine thermodynamical performance substantively. Thirdly, operating characteristics are not the same for automotive engines and MDEs. So taking into account all the mentioned differences, it can be expected that there will be also a pronounced difference in PM emission characteristics.

In this study the formation of particles, their physical properties and morphology were investigated from two very different marine diesel engines, operating on marine gas oil and low-grade residual fuel oil. Essentially the same instrumentation and measurement techniques as used for automotive PM characterization were applied here, allowing intercomparison of the results. Additionally, particle morphology and composition were assessed using scanning electron microscopy (SEM) with additional energy-dispersive X-ray (EDX) spectroscopy.

2. EXPERIMENTAL
2.1. Test engines, fuels and operating conditions

Two engines were evaluated in the current study: a 2-stroke Wätrsilä WX 28B and a 4-stroke Rolls-Royce KR3. They are both turbocharged medium-speed, direct-injection (DI) marine diesel engines with the detailed technical specification provided in Table 1. For

relative comparison, the main specifications for a turbocharged 4-stroke DI heavy-duty engine are shown in the right column highlighting the engine differences discussed before. Both engines during the experiment were operated on two totally different types of fuel: low-sulphur marine gas oil (MGO), which can be considered as the cleanest fuel used in maritime industry, and heavy fuel oil (HFO) that is pure or nearly pure residual fuel oil. The major fuel specifications are presented in Table 2. In fact, HFO is the main fuel used in sea-shipping, since it is much cheaper comparing to other fuel types, but at the same time contains such undesirable residuals like ash, asphaltenes and metal sediments. The sulphur content of marine fuels is much more significant, reaching up to 4.5% by mass, than in well-refined fuels used in on-road diesel vehicles that normally use diesel fuel with around 10 ppm of sulphur in most European counties. The high sulphur content could lead to the formation of large amounts of sulfate particles, as well as to high SO_x emission concentrations. Additional factor influencing diesel PM level and composition is the content of sulphur, ash and metal compounds in lubrication oil used (Kittelson et al., 2008).

Table 1 Specifications of the test engines.

Engine type/specification	Loop-scavenged 2-stroke Wätrsilä WX 28B	4-stroke Rolls-Royce KR3	4-stroke Scania DC1102
Application	Ship propulsion	Ship propulsion/ Electricity generation	Truck engine
Number of cylinders	1	3	6
Cylinder bore, mm	280	250	127
Piston stroke, mm	360	300	140
Displ. per cylinder, l	22.2	14.7	1.8
Power, kW	300	500	280
Speed, rpm	600	750	1800
MEP, bar	13.5	18.1	15.4

Table 2 Major fuel specifications.

Fuel type/parameters	Marine Gas Oil	Heavy Fuel Oil
Viscousity@50 °C, cSt	2,5	380
Density@15 °C, kg/m^3	845	991
Sulphur content, % by mass	0,05	1,5
Vanadium, mg/kg	<1	300
Aluminum + silicium, mg/kg	<1	80
Zinc, mg/kg	<1	15
Phosphor, mg/kg	<1	15
Calcium, mg/kg	<1	30
Ash content, % by mass	<0,01	0,15
Water content, % by volume	0,01	0,5

There are currently no standard test cycle for marine diesel engines when measuring PM emissions. And the legislative body, International Maritime Organization (IMO), is limiting only NO_x emissions and allowed fuel sulphur content. Therefore, the same fixed operating conditions as used for NOx emission certification in accordance with the rules of IMO NO_x Technical Code (as stated in Annex VI of the MARPOL 73/78 convention) were adopted for current study to obtain PM size distributions. Due to different applications, the investigated MDEs were operated on different test cycles with 2-stroke Wätrsilä WX 28B tested over ISO 8178-4 E3 cycle for propeller-law-operated engines and ISO 8178-4 E2 test

cycle for constant-speed main propulsion application used for a 4-stroke Rolls-Royce KR3 engine. Load, speed and corresponding exhaust gas temperatures (after turbocharger) are listed in Table 3. It should be noted that due to the PM data acquisition system problem the PM emission results from a 2-stroke engine operated on HFO at maximum load were lost and there were no possibility to repeat the experiment due to a turbocharger change.

Table 3 Test points with corresponding measured exhaust gas temperature.

Engine type/spec.		2-stroke Wätrsilä WX 28B				4-stroke Rolls-Royce KR3			
Load, %		100	75	50	25	100	75	50	25
MGO	Speed, rpm	659	600	523	415	750	750	750	750
	Exhaust gas temp., ° C	258	267	249	236	367	353	330	277
HFO	Speed, rpm	659	600	523	415	750	750	750	750
	Exhaust gas temp., ° C	261	270	253	240	326	321	317	287

2.1. Particulate matter sampling and measurement set-up

All exhaust gas samples during this study were extracted from the engine tailpipe with the help of "chinese hat" probe fitted near the centerline of the exhaust pipe. This special type of sampling probe was chosen to prevent the sampling system from overloading especially by big particles. After been sampled the extracted gas was transported to the dilution system by means of 1.5 m-long sampling line that was kept heated up to 400 °C. The heating was applied as it firstly prevents volatile species in the gas stream from condensation and, secondly eliminates the PM losses caused by thermophoretic forces.

Schematic representation of PM sampling-measurement set-up used in the study is provided in Figure 1. A commercially available Dekati two-stage ejector dilutor was used to dilute the sampled gas with properly conditioned particle-free dry air. This process roughly simulates the actual physical sub-processes and chemical reactions that occur when hot combustion products mix with much cooler atmospheric air. It was decided to study only solid particles, so barely "hot" dilution with applied primary dilution temperature (PDT) of as high as 400 °C was used. In reality the exhaust gas is diluted with much cooler ambient air which causes condensation of vapour-phase semi-volatile hydrocarbons and sulphuric acid via homogeneous or heterogeneous nucleation (Khalek et al., 2000; Kittelson et al., 1999). The total dilution ratio (DR) was kept in the range of 50-80 during the experiment for all test points. Its value was calculated as the ratio of NO_x concentration in the raw exhaust to that in the diluted exhaust. The applied method normally gives a more precise value of the dilution ratio than the one where values of DR is calculated based on the measured diluent and inlet flow rates (De Filippo and Maricq, 2008).
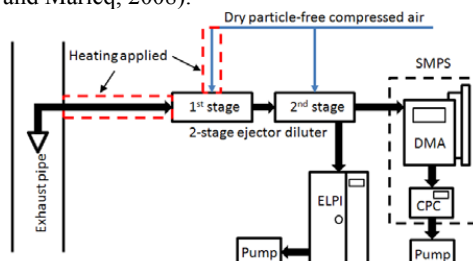

Figure 1 Schematic diagram of particle sampling-measurement set-up.

Scanning mobility particle sizer (SMPS) and electrical low-pressure impactor (ELPI) were used to obtain the required particle number and size distributions in the study. They were arranged to work in tandem increasing the measurement system capability. SMPS spectrometer (Knudson and Whitby, 1975) provided the main number size distribution results as it has a very high particle size resolution, but on the other hand its slower response makes it applicable only for steady-state measurements. The studied particle size range was approximately 6-215 nm, which was dictated by instrument flow rate settings. A 12-channel ELPI (Keskinen et al., 1992), as all cascade impactors, has a drawback of a much coarser size resolution, but at the same time has several great advantages like high time-resolution of 2-3 sec, and also can cover a very wide size range from 17 nm to 10 μm. It can be also used to collect PM mass for gravimetric and/or composition analysis. In this study, 47-mm thin aluminium foils, greased with Apiezon L vacuum grease to avoid particle bouncing, were installed on ELPI collection plates were used to collect the particles for further scanning electron microscope (SEM) and energy-dispersive X-ray (EDX) analysis. Several selected films, containing PM mass, were later analyzed with SEM/EDX techniques by Jeol JXA-8500F instrument, which is a high-performance thermal field emission electron probe micro analyser combining high SEM resolution with high quality X-ray analysis of submicron areas.

3. RESULTS AND DISCUSSION
3.1. PM emission characteristics for various fuels and operating conditions

Particle size distributions from a 2-stroke Wätrsilä WX 28B and a 4-stroke Rolls-Royce KR3 engines operated on MGO and HFO were obtained for various operating conditions using SMPS in rather narrow size range of 6-215 nm. The results were plotted on log-log scale and are presented on Figure 2. All the results were acquired with the "hot" dilution settings with corresponding PDT=400 °C, meaning that they reflect the distributions of mainly solid, non-volatile particles in diesel exhaust. The "hot" dilution allowed to keep the volatile species, normally comprised of light semi-volatile hydrocarbons and sulphuric acid (Kittelson, 1998; Tobias et al., 2001), in the vapour phase as they were beyond the main scope of the study. At the same time, authors want to highlight the significant contribution of the mentioned volatile components to PM emission, especially in terms of particle number, but were comprehensively studied elsewhere (e.g. Khalek et al., 2000; Kittelson et al., 2006).

The size number distributions from the 2-stroke Wätrsilä WX 28B engine showed a pronounced bimodal shape both on MGO and HFO for all operating conditions, except the maximum load where the distribution shape was unimodal (only accumulation mode). As expected and seen on Figure 4, the total particle concentration was higher when operating on residual HFO than on MGO with the highest difference of around an order of magnitude occurred at low load. The marked distinction occurred in the size range of the smallest particles that contributed from approximately 65% to 90% of total PM on all the fuels as seen in Figure 5, while there was particularly no difference in number concentrations above 100 nm due to fuel quality at any of the test points. The mean CMD values shown on Figure 3 increase from 18.3 nm to 19.9 nm and from 30.8 nm to 42.6 nm at 25% and 75% load respectively when shifting from MGO to HFO, which is in accordance to observations from other researchers (Ristimaki et al., 2010). All this can be probably explained by the significant difference in fuel composition with special emphasis on ash content between MGO and HFO (Lyyränen et al., 1999), but not the decaying nature of the nucleation mode with the load, especially when applying "hot" dilution. The earlier observations from this engine indicated the high lub oil consumption (especially below 50% load) which can result in additional production of non-volatile nucleation mode particles (Sakurai et al., 2003). The high lub oil

consumption is more likely caused by specific engine design characterized by 'valveless' cylinder cover and exhaust port located in the bottom part of the cylinder, which is more typical for V-type engines. So authors do believe that observed nuclei mode on both fuels is composed primarily from metal compounds originated from lubrication oil (Sakurai et al., 2003). The accumulation mode formed when running on MGO is believed to compose mainly of carbonaceous agglomerates due to incomplete fuel combustion, while on HFO it is composed of carbon particles together with incombustible species originated from fuel ash.
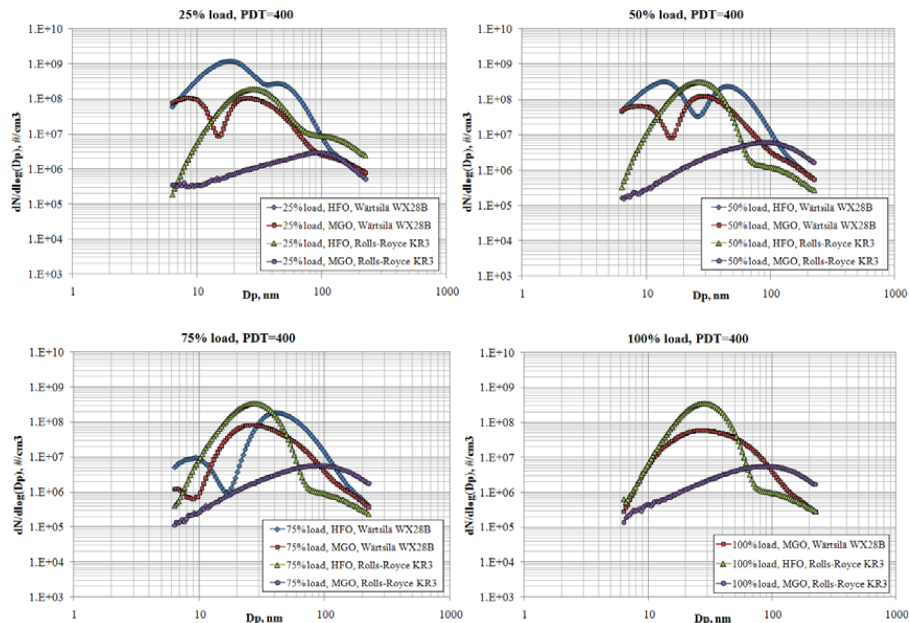
Figure 2 Particle number distribution characteristics at various operating conditions for 2-stroke Wätrsilä WX 28B and 4-stroke Rolls-Royce KR3 operated on MGO and HFO.

For all load conditions on both MGO and HFO the particle size distributions from a 4-stroke Rolls-Royce KR3 engine showed only a unimodal-shape without the lubrication oil-dependent nuclei mode as observed for Wätrsilä WX 28B engine. But the difference in the total number of particles between the fuels was dramatic and found to be around two orders of magnitude as shown on Figure 4. The total number of particles showed a slight increase for all tested fuels while increasing the load. This can probably be explained by the small increase in carbonaceous particle number due to increased amount of injected fuel and associated more locally rich combustion zones inside the cylinders (Tobias et al., 2001). At the same time the mean CMD values showed no dependence to load conditions and was around 25-30 nm and 60-70 nm for HFO and MGO respectively. Contribution of nanoparticles to the total PM number was above 90% while operating on HFO, but on MGO it was only around 25-35% as shown on Figure 5, which is more typical for automotive heavy-duty diesel engines. Results suggest that accumulation mode on MGO is mainly consist of carbonaceous fraction, while on HFO it is comprised of elemental (black) carbon aggregate particles and PM originated from the incombustible fuel ash species (Lyyränen et al., 1999; Kasper et al., 2007), which are mainly composed of vanadium, aluminum, calcium, silicium, asphaltenes and other sediments as given in Table 2 with heavy fuel oil specification.
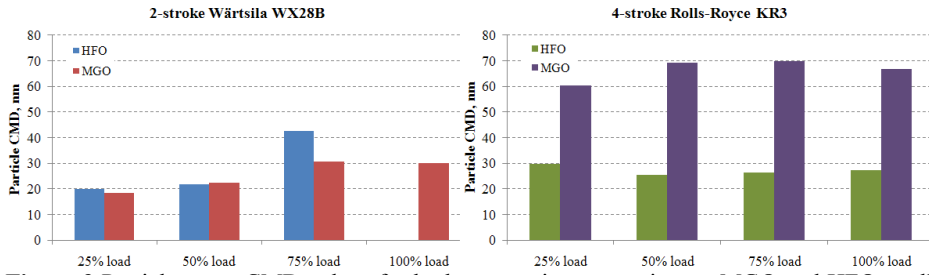
Figure 3 Particle mean CMD values for both test engines operating on MGO and HFO at all operational modes.
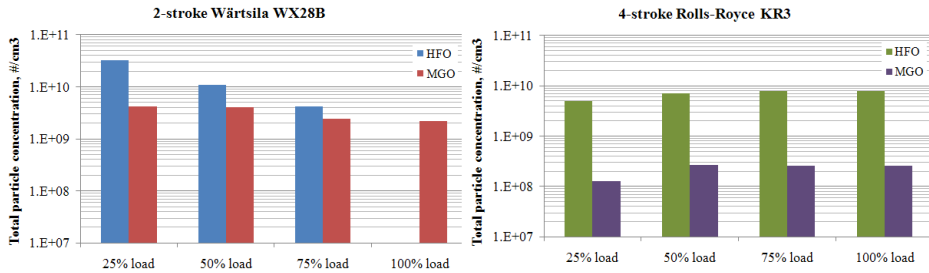
Figure 4 Total particle number concentration as calculated from SMPS data in the size range of 6-215 nm.
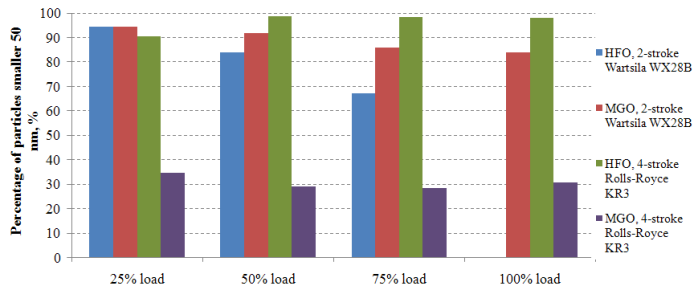
Figure 5 Mean percentage of particles smaller 50 nm in the SMPS scans at each operational mode with PDT of 400 °C.
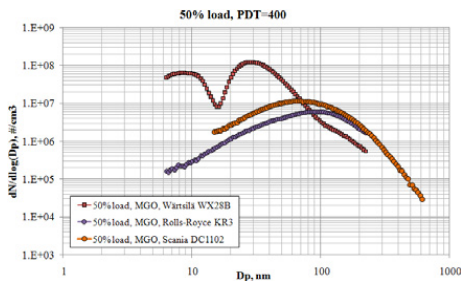
Figure 6 Comparison of PM size distributions from MDEs and heavy-duty engine at 50% load on marine gas oil fuel.
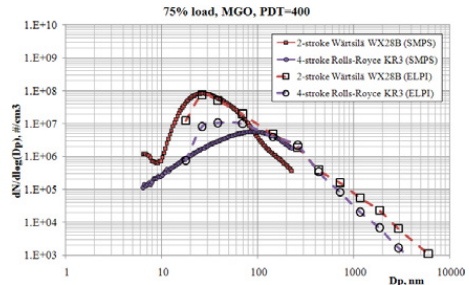
Figure 7 Comparison of number size distributions measured by SMPS and ELPI at 75% load while operating on MGO fuel.

As particle emission characteristics from a 4-stroke Rolls-Royce KR3 while operating on MGO showed an interesting behavior, very different from other results, it was considered to compare obtained PM characteristics with ones from a 4-stroke heavy-duty DI diesel engine. The results of comparison are shown on Figure 6 for all engines run on MGO at 50% load and suggest that total particle number emitted by a 2-stroke MDE is significantly higher than one from automotive engine, even if not take into account the nuclei PM associated with engine lub oil. This and also the fact that PM size distribution emitted by MDE shows a distinct accumulation mode at around 30 nm, which is much smaller than is known from automotive engines (50-150 nm) are in accordance to the findings of other researchers (Kasper et al., 2007). At the same time, results revealed an interesting feature, i.e. that PM size distribution from a 4-stroke MDE was almost identical to one from a 4-stroke HD engine in the range of result overlap (as different instrument settings were used). Small difference in PM number was registered for particles below 100 nm in size, while almost perfect coincidence was observed for sizes above 100 nm and even means CMD values were similar between MDE and HD engine with corresponding 69.1 nm and 66.3 nm respectively. This good agreement is difficult to explain, especially if the significant difference between the engines in terms of geometrical dimensions and operating conditions is taken into account.

A nice agreement between ELPI and SMPS PM size distributions were obtained for all tested fuels and operating conditions, as shown on Figure 7 for 75% load, MGO fuel case. It also showed that a significant number of particles exist above 1 μm. They are denoted as coarse particles and consist from accumulation mode ones that have been deposited on cylinder and exhaust system surfaces and later reentrained. Nevertheless, one should not ignore the fact that ELPI and SMPS operate on very different working principles and even the size axis has a different meaning for them. For SMPS, where particles are segregated in electrical field, the distributions are a function of electrical mobility diameter, while for ELPI, where particles are separated by impaction, they are a function of an aerodynamic diameter.

3.2. Particle morphology and composition analysis

The scanning electron microscopy and energy-dispersive X-ray analysis were performed for the PM samples collected with the help of ELPI, which cascade impactor configuration allows it obtaining size-selected particle samples. Due to its complexity and time consumption the detailed morphology analysis was performed only for particles collected from a 4-stroke Rolls-Royce KR3 when operating on MGO at 75% load conditions.

The particles were classified into several groups based on morphology and elemental composition. The majority of observed particles were carbon agglomerates, or aggregates, exhibited a complex, branched morphology as seen on Figure 8a, and consisted of spherical carbon particles with mean diameters between 30 and 90 nm. These agglomerates were observed in all sizes, containing approximately from ten to as many as several thousands of primary carbon particles (Kocbach et al., 2005). Some carbonaceous particles were also found as separate spherules in the smallest particle size range together with irregular-shaped ones (sharp-edged particles as seen on Figure 8b), which were mainly composed of Ca, Na, Fe, K and Si as revealed the EDX spectroscopy (Figure 8c) and are believed to originate from lubrication oil. Some particles formed from fuel oil droplet residue and the particles indicating mechanical abrasion were found in the coarse mode size. It should be noticed here that PM morphology results from a 4-stroke Rolls-Royce KR3 MDE appeared to be very similar to results from automotive diesel PM morphology and composition studies as found in literature (e.g. Berube et al., 1999; Kocbach et al., 2005).
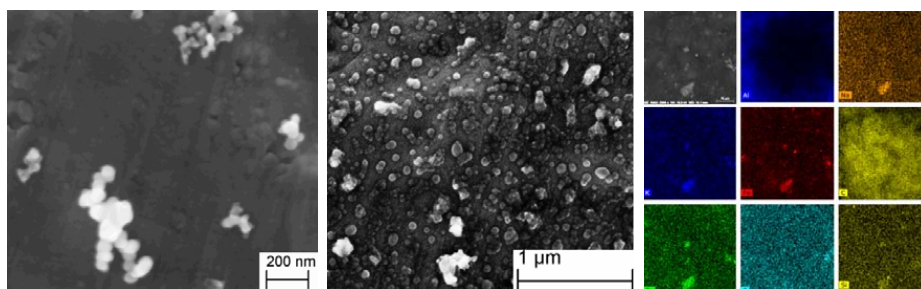
Figure 8 (a-b) Representative SEM micrographs of particles collected from a 4-stroke Rolls-Royce KR3 MDE operating on MGO at 75% load. (c) Elemental analysis of metallic particles with the help of EDX spectroscopy.

4. CONCLUSIONS

The combined ELPI-SMPS set-up showed a good stability and repeatability during the experiments performed under "hot" dilution conditions which allowed to study only solid, non-volatile particles. For a 2-stroke Wätrsilä WX 28B the obtained distributions for both MGO and HFO were bimodal, comprised of a pronounced load-independent accumulation mode and a nucleation mode which decayed with the load increase. The total particle number concentrations for both fuels were dominated by nanoparticles and decreased with the load, but was considerably higher for HFO in comparison to MGO with the biggest difference occurred at low load conditions. The observed load-dependent, for both the fuels, nuclei mode is believe to compose primarily of metal compounds and originated from high lub oil emissions, which are more likely caused by a specific engine design. At the same time, the accumulation mode on MGO is represented almost entirely by carbonaceous agglomerates formed due to incomplete combustion, while on HFO the mentioned carbon particles are found together with considerable amounts of incombustible residual fuel ash species. For all load conditions on both tested fuels the particle size distributions from a 4-stroke Rolls-Royce KR3 marine diesel engine were barely unimodal with pronounced accumulation mode. The maximal difference in total PM number between HFO and MGO was around two orders of magnitude. The total particle number increased with load, which can be explained due to increased amount of fuel injected and associated more locally rich combustion zones formed inside the cylinder. The calculated mean CMD values were fairly constant at all loads and were around 25-30 nm for HFO and 60-70 nm for MGO respectively. Contribution of nanoparticles to total PM number was above 90% on HFO, but only 25-35% on MGO fuel.
The surprisingly good agreement not only in overall shape, but also in terms of total PM number and mean CMD values were found between automotive and 4-stroke marine engine. This interesting finding is hard to explain and it probably needs separate, more detailed investigation. At the same time, total particle number concentration from a 2-stroke MDE was considerably higher than from automotive HD engine. In addition, Wätrsilä WX 28B engine showed a distinct accumulation mode at around 30 nm, which is much smaller than is known from automotive engines (50-150 nm), but is completely in accordance to the findings from the studies of MDE particulate emissions.

Several distinct particle classes were observed during PM morphology analysis: the carbonaceous agglomerates consisted of spherical carbon particles with mean diameters between 30 and 90 nm were observed in a very wide size ranges. Among the smallest particles the separate spherical carbon particles together with irregular-shaped metal ones,

which could originate from lubrication oil, were found. Some supermicron particles formed from fuel oil droplet residue and the particle indicating mechanical abrasion were also observed. Hence, three main origins of PM as fuel, lubrication oil and mechanical wear due to friction of moving parts have been confirmed.

REFERENCES

Berube, K.A., Jones, T.P., Williamson, B.J. et al. (1999) Physicochemical characterization of diesel exhaust particles: factors for assessing biological activity, Atmos. Environ. 22, 1599–1614.

Corbett, J.J., Winebrake, J.J., Green, E.H., Kasibhatla, P., Eyring, V., Lauer, A. (2007) Mortality from Ship Emissions: A Global Assessment. Environ. Sci. Technol. 41, 8512-8518.

De Filippo, A. and Maricq, M.M. (2008) Diesel nucleation mode particles: semivolatile or solid? Environ. Sci. Technol. 42, 7957-7962.

Dockery, D., Pope, C.A., Xu, X., Spengler, J., Ware, J. et al. (1993) An association between air pollution and mortality in six U.S. cities. New England Journal of Medicine 329, 1753-1759.

Ferin, J., Oberdörster, G., Penney, D.P. (1992). Pulmonary retention of ultrafine and fine particles in rats. Am. J. Respir. Cell Mol. Biol. 6, 535-542.

Goo, J.H. and Kim, C.S. (2003) Theoretical analysis of particle deposition in human lungs considering stochastic variations of airway morphology. J. Aerosol Sci. 34, 585-602.

Kasper, A., Aufdenblatten, S., Forss, A.,Mohr, M., Burtscher, H. (2007) Particulate Emissions from a Low Speed Marine Diesel Engines. Aerosol Sci. Technol. 41, 24-32.

Keskinen, J., Pietarinen, K., Lehtimäki, M. (1992) Electrical low pressure impactor. J. Aerosol Sci. 23, 353-360.

Khalek, I.A., Kittelson, D.B., Brear, F. (2000) Nanoparticle growth during dilution and cooling of diesel exhaust: experimental investigation and theoretical assessment. SAE Paper 2000-01-0515.

Kittelson, D.B. (1998) Engines and nanoparticles: a review. J. Aerosol Sci. 29, 575-588.

Kittelson, D.B., Arnold, M., Watts, W.F. (1999) Review of diesel particulate matter sampling methods. Final Report. University of Minnesota: Minneapolis, MN.

Kittelson, D. B., Watts, W. F. et al. (2008) Effect of Fuel and Lub Oil Sulfur on the Performance of a Diesel Exhaust Gas Continuously Regenerating Trap. Environ. Sci. Technol. 42, 9276-9282.

Kittelson, D.B., Watts, W.F., Johnson, J. (2006) On-road and laboratory evaluation of combustion aerosols – Part 1: Summary of diesel engine results. J. Aerosol Sci. 37, 913-930.

Knudson, E.O. and Whitby, K.T. (1975) Aerosol classification by electric mobility: apparatus, theory, and application. J. Aerosol Sci. 6, 443-451.

Kocbach, A., Johansen, B.V. et al. (2005) Analytical electron microscopy of combustion particles: a comparison of vehicle exhaust and residential wood smoke. Sci. Total Environ. 346, 231–243.

Lyyränen, J., Jokiniemi, J., Kauppinen, E.I., Joutsensaari, J. (1999) Aerosol Characterization in Medium-Speed Diesel Engines Operating with Heavy-Fuel Oils. J. Aerosol Sci. 30, 771-784.

Oberdörster, G., Sharp, Z., Atudorei, V., Elder, A., Gelein, R., Kreyling, W., Cox, C. (2004) Translocation of inhaled ultrafine particles to the brain. Inhal. Toxicol. 16, 437-445.

Oberdörster G., Finkelstein J., Ferin J. et al. (1996) Ultrafine particles as a potential environmental health hazard. Studies with model particles. Chest 109 (Suppl. 3), 68–9.

Pope III, C.A. (2000) Epidemiology of fine particulate air pollution and human health: Biologic mechanisms and who's at risk? Environ. Health Perspect. 108 (Suppl.), 713–723.

Pope, C.A. III., Burnett, R.T., Thun, M.J., Calle, E.E. et al. (2002) Lung cancer, cardiopulmonary mortality, and long-term exposure to fine particulate matter. JAMA. 287, 1132-1141.

Ristimaki, J., G., Hellen, et al. (2010) Chemical and physical characterization of exhaust particulate matter from a marine medium speed diesel engine. CIMAC Congress, Paper # 73.

Sakurai, H., Tobias, H.J., Park, K., Zarling, D. et al. (2003) On-line measurements of diesel nanoparticle composition, volatility, and hygroscopicity. Atm. Env., 37, 1199-1210.

Suzuki, H., Toyooka, T., Ibuki, Y. (2007) Simple method to evaluate uptake potential of nanoparticles in mammalian cells using a flow cytometric light scatter analysis. Env. Sci. Tech., 41, 3018-3024.

Tobias, H.J., Beving, D.E. et al. (2002) Chemical analysis of diesel engine nanoparticles using a nano-DMA/thermal desorption particle beam mass spectrometer. Environ. Sci. Tech. 35, 2233-2243.

Paper II

Particulate size distributions from heavy-duty diesel engine operated on low-sulfur marine fuel

Sergey Ushakov, Harald Valland, Jørgen B. Nielsen, Erik Hennie

Paper III

Effect of high sulphur content in marine fuels on particulate matter emission
characteristics

Sergey Ushakov, Harald Valland, Jørgen B. Nielsen, Erik Hennie

Submitted to:

***Proceedings of IMarEST Part A: Journal of Marine Engineering and Technology
(2012)***

Paper IV

Effects of dilution conditions on diesel particle size distribution and filter mass measurement in case of marine fuels

Sergey Ushakov, Harald Valland, Jørgen B. Nielsen, Erik Hennie

Submitted to:

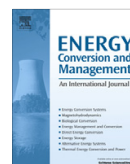***Journal of Fuel Processing Technology (2012)***

Paper V

Combustion and emission characteristics of fish oil fuel in a heavy-duty diesel engine

Sergey Ushakov, Harald Valland, Vilmar Æsøy

Energy Conversion and Management

Combustion and emissions characteristics of fish oil fuel in a heavy-duty diesel engine

Sergey Ushakov [a,*], Harald Valland [a], Vilmar Æsøy [b]

[a] Department of Marine Technology, Norwegian University of Science and Technology, Otto Nielsens vei 10, NO-7491 Trondheim, Norway
[b] Department of Product Development and Machinery Systems Design, Aalesund University College (AaUC), Larsgårdsvegen 2, NO-6009 Ålesund, Norway

ARTICLE INFO

ABSTRACT

Residual fish oil, which is basically a by-product of fish processing industry, was tested pure and in 50% v/v blend with conventional low-sulfur marine gas oil in a direct-injection heavy-duty diesel engine. Experiments were performed at various operating conditions under standard propulsion and generator mode marine cycles. Engine performance, exhaust smokiness, gaseous emissions together with particulate matter (PM) size distribution and corresponding total particle number and mass concentrations were measured in all of the tests performed. In general, fish oil showed fairly good combustion and ignition properties, which were very similar to that of marine gas oil. Only slight difference was observed in NO_x and CO_2 levels, while emissions of CO and THC were significantly decreased at all operating conditions. Fish oil also allows reducing smoke (soot) and both total particle number and PM mass concentrations. Fish oil also allows reducing smoke (soot) and both total number and PM mass emissions up to 70–90% with the biggest particles being most affected. Such positive impact on pollutants can be explained by high oxygen content in fish oil fuel and its lack of aromatic compounds, which is promoting more complete fuel oxidation.

© 2012 Elsevier Ltd. All rights reserved.

1. Introduction

The majority of mankind's current energy demand is satisfied from petrochemical, coal and natural gas sources, which are all non-renewable resources and are estimated to approach depletion within next 50–100 years [1]. During last century the worldwide energy consumption showed more than 20-fold increase and is expected to continue its growth in future. All current main energy sources are finite, with the exception of solar, wind, hydroelectricity and nuclear power, as are principally fossil fuel-based and hence continuously boosting oil prices. Moreover, as the demand for energy has grown, so have the adverse environmental effects of its production [2] with NO_x, CO_2, SO_x emissions originating from fossil fuel combustion being primary sources of atmospheric pollution [3]. Carbon dioxide and other greenhouse gases (GHGs), accumulating in atmosphere, bring another concern as they are responsible for global climate change [4], which may have disastrous consequences for the life on our planet.

Renewable energy sources, in their turn, are indigenous, and can not only substantially decrease negative environmental impact associated with fossil fuels, but also reduce dependency on oil and gas, hence increasing security of supply with latter being especially important for oil-importing countries. But it is also important for

oil-exporting countries, for example Norway. Despite being within world's top-10 oil exporters Norway has all its oil and gas fields located off-shore, which are more difficult for production. Besides, all easy-access oil and gas has been already extracted and taking into account fatal consequences of possible ecological disaster, like that caused by *Deepwater Horizon* drilling rig, certain oil/gas fields can be kept for future until more advanced, efficient and safer production technologies will be developed. Meanwhile, more attention should be addressed to renewable energy sources.

One of the most promising renewable sources is biofuels and can be potentially derived from plant matter, animal waste, agricultural crops and residues, municipal waste, and industrial effluents [5,6]. Bio-oils can be obtained from biomass such as edible and non-edible oilseed crops, wood (lignocelluloses), microorganisms, algae, animal waste, and recycled cooking greases [5,7–9]. The most common virgin crops used for bio-oil production are rapeseed, palm, sunflower, soybean, corn, safflower, canola, mustard, jatropha and mahua [7,10]. In addition, corn, wheat, rice straw, sugar cane and sweet sorghum are used for bio-ethanol production. However, food vs. fuel trade-off debates together with other environmental impacts associated with cultivation and conversion can limit the use of food crops for fuels [7,11] with this biofuels source being inapplicable in Norway which has very limited farming lands and inclement northern climate with rather short summer. Wood or lignocelluloses conversion to biofuels is difficult and currently economically unfeasible until more advance technologies enter

Nomenclature

CMD	count median diameter	GHG	greenhouse gas
CO	carbon monoxide	HC	hydrocarbons
CO_2	carbon dioxide	ISO	international standard organization
CPC	condensation particle counter	MGO	marine gas oil
DMA	differential mobility analyzer	NO_x	nitrogen oxides
D_p	particle diameter	PM	particulate matter
ELPI	electrical low pressure impactor	ROHR	rate of heat release
FID	flame ionization detector	SO_x	sulfur oxides
FO	fish oil	SMPS	scanning mobility particle sizer
FSN	filter smoke number	THC	total unburned hydrocarbons

the market. At the same time, large scale oil production is currently challenging with both microalgae and microorganisms, although the lipid content of yeast can be up to 70% [5]. Waste biomass-derived biofuels have a serious advantage of recovering certain by-product from the waste stream [12,13], hence decreasing amount of waste and its toxicity.

One example of such biofuels is fish oil (FO), which is by-product of fish processing industry. In average, waste generated from fish processing plant is approximately 50% from harvested fish mass depending on the type of fish, product and processing techniques [14,15]. The chemical composition of the corresponding effluent depends on the harvesting region, season, type of fish, and type of processing, but is mainly composed of lipids, proteins, metals, carbohydrates and moisture [15,16]. Despite that most of fish oil (56%) was globally used (in 2002) for aqua feed, 30% for edible oils, 2% in pharmaceutical industry and only 12% for industrial purposes [7] and having a rather short history as a fuel, there were several successful projects that demonstrated the possibility of using FO as fuel in internal combustion engines alone, or as a blend with conventional diesel fuel [17,18]. This type of biofuels is more attractive for production in Norway which has strong fishing and aquacultural industries and required fish processing facilities, including fishmeal plants that are of particular interest as the major by-product of this process is waste oil. In addition, FO can appear superior type of biofuel for certain rural and remote communities in Alaska, Atlantic Canada, Greenland, Northern Norway and Russia (Kamchatka) that are dependent on fish processing industry. Its use by community itself and possible in-community production/processing from local materials/wastes can result in reduction of dependency on transportation costs associated with fuel, lower the importance of fossil fuel price fluctuations, boost economic development and reduce overall GHG emissions and other negative environmental and human health impacts [7,9].

In addition to mentioned advantages of using fish oil, such as reduction of CO_2 emissions to atmosphere and dependence on fossil fuel, it is renewable by nature, safer to handle, has no aromatic compounds, practically no sulfur and its fuel molecules inherently contain oxygen atoms which may reduce CO, THC and PM emissions [19–21]. However, FO can present several problems like worse low temperature properties, lower lubricity, and higher viscosity, more acidity and higher flash point compared to conventional diesel fuel. The main concern raised by earlier studies for engines using fish oils were exhaust duct deposits and increased wear of parts that are constantly in contact with the oil [18], with transesterification been proposed to solve these problems. Overall, fish oils and blends have demonstrated similar ignition properties and excellent combustion characteristics comparing to neat diesel oil [17]. Additional advantage of FO is that it requires minimal processing to be made usable as fuel.

Current study aims to compare engine performance and emission characteristics from a diesel engine under modes of propulsion and generator operation when firing both on neat low-sulfur marine gas oil (MGO), fish oil and their 50% v/v blend. The article's major importance was to see the behavior of gaseous, soot and PM emissions when shifting from conventional MGO to fish oil under different operating marine cycles. These results should encourage the use of biofuels in general, and waste fish oils particularly, and show the potential possibility of their application as fuels, for example, for fishing vessels.

2. Experimental

2.1. Test engine, fuels and operating conditions

The test engine was a four-stroke, turbocharged, intercooled, direct injection heavy-duty diesel engine fully complied with Euro 2 emission tier. Engine detailed specification is given in Table 1 and the schematics of the test bed is shown in Fig. 1a. Experimental engine was connected to a dynamometer water brake and equipped with all necessary instrumentation for real-time monitoring and measurements of operating pressures, temperatures and mass flow rates of intake air, exhaust gas, fuel, lube oil, etc. No exhaust gas aftertreatment was used in the study. Cylinder gas pressure data was measured with the help of pressure transducer PCB-M112B11, and combustion process was analyzed through standard rate of heat release (ROHR) calculations based on averaging 10 operating cycles. To study combustion variability, 20 consecutive individual cycles were recorded at each operating condition.

A conventional marine gas oil (diesel fuel), which forms the baseline fuel for the study, was supplied by Norske Shell AS and represents typical low-sulfur MGO. This fuel is almost free of asphaltenes and ash, and contains only 0.05% S. It is the cleanest fuel used in maritime industry and is roughly equivalent to no. 2 diesel fuel. Such type of marine fuel is normally used in coastal and harbor areas to reduce negative environmental impact from diesel emissions.

Fish oil biofuel used in current study was a pure light fraction of residual oil which is a by-product from omega-3 dietary supplement

Table 1
Engine specifications.

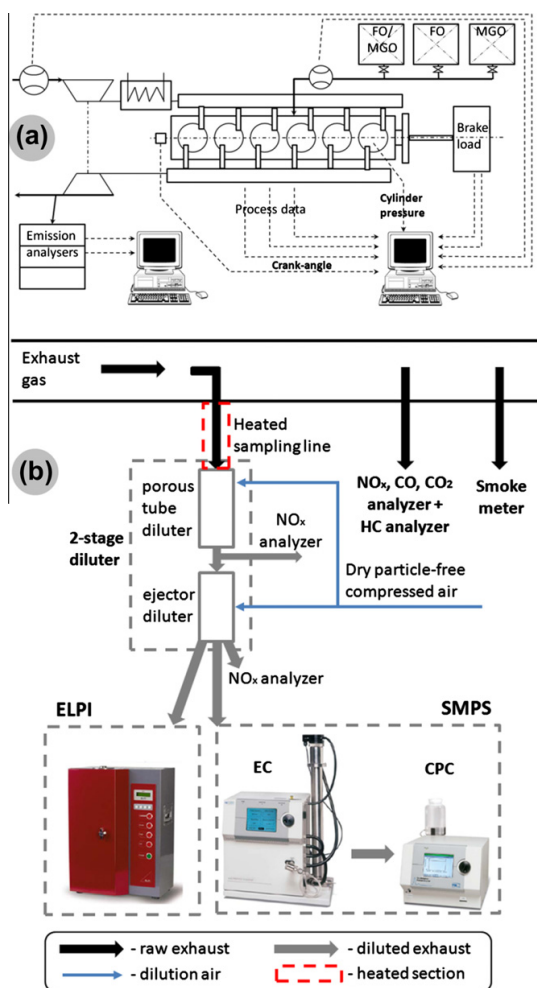|	
Engine model	Scania DC1102
Number of cylinders	6, in-line
Displacement	10.64 l
Bore × stroke	127 × 140 mm
Compression ratio	18:1
Maximum power @ 1800 rpm	280 kW
Maximum torque @ 1080–1500 rpm	1750 Nm
Min. spec. fuel consumption	191 g/kW h
Injection system	Unit injector
Size and number of holes	Ø 0.216 mm × 8
Needle opening pressure	220 bar

Fig. 1. A schematic diagram of the test bed and logging system (a) and experimental setup for gaseous emissions and PM measurements (b).

and functional food production from omega-3 fish oils [9]. This oil was supplied by BASF and was found to contain fatty acids with carbon atoms varying between 14 and 24 (from C14:0 to C24:1) with percentage of long chain fatty acids (C20–C24) did not exceeding 7%. Myristic, palmitic, palmitoleic, oleic and eicosapentaenoic acids were the major fatty acids in the oil as reflected in Table 2 presenting full fatty acid composition of the tested FO biofuel.

Both MGO and FO were tested neat and in 50% v/v blend (FO_50). The main properties of all experimental fuels and blends are summarized in Table 3. Some properties were determined during laboratory analysis and the rest were calculated from fuels composition.

For each of test fuels the investigated engine was operated both on E2 and E3 cycles in accordance to ISO 8178 standard. These marine application cycles are 4-mode ones with E2 cycle (generator mode) simulating constant-speed main propulsion application, while E3 cycle (propeller mode) is used for propeller-law-operated engines in accordance to MARPOL 73/78 Convention. Due to engine brake limitations, there was no possibility to go above 75% load,

Table 2
Fish oil fuel fatty acid composition (wt.%).

Fatty acid	Chemical structure	% Value
Myristic	C14:0	18.75
Palmitic	C16:0	35.12
Hexadecenoic (palmitoleic)	C16:1	16.59
Hexadecatetraenoic	C16:4	3.97
Stearic	C18:0	2.81
Octadecenoic (oleic)	C18:1	10.65
Octadecadienoic (linoleic)	C18:2	1.20
Octadecatrienoic (linolenic)	C18:3	0.73
Octadecatetraenoic	C18:4	3.31
Eicosatetraenoic (arachidonic)	C20:4	0.15
Eicosapentaenoic	C20:5	5.36
Docosahexaenoic	C22:6	0.71
Tetracosenoic (selacholeic)	C24:1	0.64

which hence determined the maximum load point for both test cycles. The actual engine operating parameters related to each of the tested modes are listed in Table 4.

Experiments were performed without any engine modification. For every fuel change, the fuel lines were cleaned and engine was allowed to run at medium load for about 30 min to purge any of the remaining previously tested fuel from the engine fuel system and then another 15 min to stabilize at its new condition.

2.2. Gaseous emissions analysis and smoke measurements

Gaseous emissions were determined in accordance to ISO 8178 standard with exhaust gas sample extracted from the tailpipe through a separate port located 3 m after engine turbocharger. NO_x, CO and CO_2 were measured simultaneously by Horiba PG-250 portable multi-gas analyzer which utilizes chemiluminescence detector for NO_x monitoring and non-dispersive infra-red detection technique for measurement of CO and CO_2 respectively. The concentration of THC was determined with a J.U.M., model 3-200, portable heated flame ionization (FID) analyzer.

A smoke meter AVL 415S was used to measure the smoke opacity (filter smoke number, FSN). Estimation of soot (black carbon) emissions was performed through the recommended correlations [22] as follows:

$$C(soot), \text{mg/m}^3 = 12.222 \cdot FSN \cdot \exp(0.38 \cdot FSN) \qquad (1)$$

2.3. Sampling and dilution procedures

The experimental setup used in the study for gaseous and PM measurement is shown on Fig. 1b. Sample of exhaust gas for

Table 3
Properties of tested fuels and blends.

Fuel properties	MGO	FO_50	FO
Density (g/cm³)	0.849[a]	0.860[a]	0.871[a]
Kinematic viscosity (cSt)	3.16[b]		3.83[b]
Gross heating value (MJ/kg)	45.80	42.95	40.10
Lower heating value (MJ/kg)	43.10	40.40	37.70
Cetane number (–)	47.1	–	–
Initial boiling point (IBP) (°C)	171	–	–
Final boiling point (FBP) (°C)	370	–	–
C (wt.%)	86.32	81.39	76.53
H (wt.%)	13.63	12.98	12.34
O (wt.%)	0	5.61	11.13
S (wt.%)	0.050	0.027	0
Stoichiometric fuel/air ratio (–)	1/14.59[c]	1/13.55[c]	1/12.54[c]
Flash point (°C)	62		161
Pour point (°C)	−33		−3

[a] Measured at 20 °C.
[b] Measured at 40 °C.
[c] Calculated from fuel composition.

Table 4
Engine operation modes.

Mode #	Mode type	Torque (Nm)	Engine speed (rpm)	Power (kW)	Load (% from max.)	BMEP (bar)
2[a,b]	Propulsion/generator	1114.1	1800	210	75	13.16
3[a]	Propulsion	834.5	1602	140	50	9.86
4[a]	Propulsion	515.8	1296	70	25	6.09
3[b]	Generator	742.7	1800	140	50	8.77
4[b]	Generator	371.4	1800	70	25	4.39

[a] Mode # in accordance to ISO 8178 E3 cycle.
[b] Mode # in accordance to ISO 8178 E2 cycle.

particle size distribution measurement was extracted from the engine tailpipe by means of J-shaped open-ended probe through a separate port and was transported to dilution system by means of flexible heated sampling line. The sampling line was 1.5 m-long, electrically heated and insulated to maintain the volatile species in a sampled stream above the dew point and also to reduce particle losses caused by thermophoresis [23].

Dilution of the exhaust gas samples was performed in a two-stage dilution unit, commercially available by Dekati Ltd., Finland. The primary dilution occurred inside a porous tube diluter, where dry particle-free dilution air flows though a porous tube, with pore size of 20 µm, into the inner tube, thus sheathing the aerosol flow from deposition and thermophoresis [24,25]. Advantages and disadvantages of such type of diluter can be obtained from number of earlier comprehensive studies [26,27]. The secondary dilution was carried out in a typical ejector-type diluter [28,29].

The process of dilution is very important as simulates the actual physical and chemical processes that occur when exhaust gas is released from exhaust pipe and mixes with much cooler ambient air. Although dilution issues were beyond the scope of the study, it should be mentioned that dilution parameters, like temperature and humidity of dilution air, residence time and dilution ratio, have significant effect on particle formation especially in nucleation mode range and received a lot of attention reflected in number of publications [26,30–32]. In current work dilution air temperature, used for both primary and secondary dilution, was 30 °C and its relative humidity was maintained below 5%. The overall dilution ratio is a product of primary and secondary dilution and was determined as ratio of NO_x concentration measured in raw exhaust to that in diluted exhaust. Primary dilution ratio slightly varied with load and was around 5–7, while secondary dilution ratio was maintained 10 during the whole experiment. Hence, overall dilution ratio was in the range of 50–70 and remained fairly constant during data acquisition at each of operating points.

2.4. Particulate matter measurements

Particle size distributions were obtained using a scanning mobility particle sizer (SMPS, model 3934) [33] from TSI Inc., consisting of a differential mobility analyzer (DMA, model 3071 with 3081 classifier) [34] and a condensation particle counter (CPC, model 3010) and electrical low-pressure impactor (ELPI) [35] from Dekati Ltd. that operated simultaneously. The measurement particle size range for DMA + CPC was 10–400 nm, while ELPI with filter stage was able to measure real-time size distributions in size range of 7 nm–10 µm.

The total particle mass concentrations were calculated for each operational mode from ELPI particle number distributions assuming spherical particles with unit density [36,37]. Only the lowest seven stages of ELPI were taken into consideration to prevent the coarse mode artifact reported in literature [38]. The total and nano-particle concentration and mean count median diameter (CMD) values of the distributions were calculated by integrating over the considered particle diameter size range of 10–400 nm.

The actual measurements were not started until the engine had completely warmed-up (temperatures are stabilized), and real-time measured particle size distributions are rather stable. It is crucial to ensure that the data obtained is not mixed with possible artefacts from other sources [25]. During any change of operational mode, the system was allowed to stabilize for 10–15 min with stability of aerosol continuously monitored with the help of ELPI that provided real-time particle size distribution results.

3. Results and discussion

3.1. Combustion process and engine performance

Combustion performance is analyzed from the measured process data and results are summarized in Table 5. These results show that combustion properties of the tested fish oil and MGO are very similar. For instance, from Fig. 2 it can be seen that cylinder pressure and rate of heat release show a similar combustion rate when neat FO is compared to MGO. These results comply with the results obtained in similar studies by Mrad et al. [19]. To compare cyclic variations 20 combustion cycles are plotted on Fig. 3, and show that combustion stability of FO is the same or even better than that of MGO.

At low load conditions FO ignites slightly earlier and advances combustion, which might suggest that it has a slightly higher cetane index [39]. Other physical fuel properties, such as density and bulk modulus of compressibility [40], fuel surface tension and viscosity [41], can also affect ignition delay and combustion. Lower volumetric heating value of FO should normally result in increased fuel injection rate given as a longer injection period for each operating cycle. However, combustion duration as seen from Fig. 2 was not affected significantly. This can be explained by the different physical and chemical properties of FO affecting both mass flow rate through injection nozzle, evaporation, mixing and reaction rates in the cylinder and hence compensating for the lower volumetric heating value for the FO (approximately 10% lower than MGO). The pronounced difference in heat release rate in initial premixed combustion phase at low load conditions between FO and conventional MGO is likely associated with pronouncedly higher intermediate distillation temperatures, such as T10, T25 and T50 [20,39], of fish oil, which to some higher extent determine volatility properties of fuel. At the same time, final boiling point of oxygenated biofuels, like FO, and conventional diesel fuel normally do not differ significantly [20,39].

3.2. Gaseous emissions

The results of pollutant emissions measured from the exhaust of the tested diesel engine under both propulsion and generator modes are shown on Fig. 4 for NO_x, CO, CO_2 and THC respectively. The concentration of emitted nitrogen oxides for fish oil was slightly higher than from neat diesel fuel at low and medium loads with the observed increment not exceeding 6%. Higher NO_x emissions from oxygen-rich biofuels and biodiesels have been reported

Table 5
Engine performance characteristics. The data is presented for neat MGO and neat FO fuels with their relative difference given in % in parenthesis.

| Load (% from max.)	Power (kW)	Engine speed (rpm)	Pmax (bar)	Texh (°C)	SFC (MJ/kW h)	Shaft efficiency (%)
MGO/FO (change: FO/MGO, %)						
Propulsion mode						
25	70	1296	79.7/80.6 (1.1%)	356/349 (−2.0%)	8.96/8.84 (−1.4%)	40.2/40.7
50	140	1602	102.3/102.4 (0.1%)	422/415 (−1.7%)	8.65/8.67 (0.2%)	41.6/41.5
75	210	1800	105.4/102.5 (−2.8%)	471/464 (−1.5%)	8.82/8.90 (0.9%)	40.8/40.4
Generator mode						
25	70	1800	66.7/68.6 (2.9%)	305/305 (0%)	10.11/10.21 (1.0%)	35.6/35.3
50	140	1800	87.5/88.6 (1.3%)	406/401 (−1.2%)	9.03/9.07 (0.4%)	39.9/39.7
75	210	1800	105.4/102.5 (−2.8%)	471/464 (−1.5%)	8.82/8.90 (0.9%)	40.8/40.4
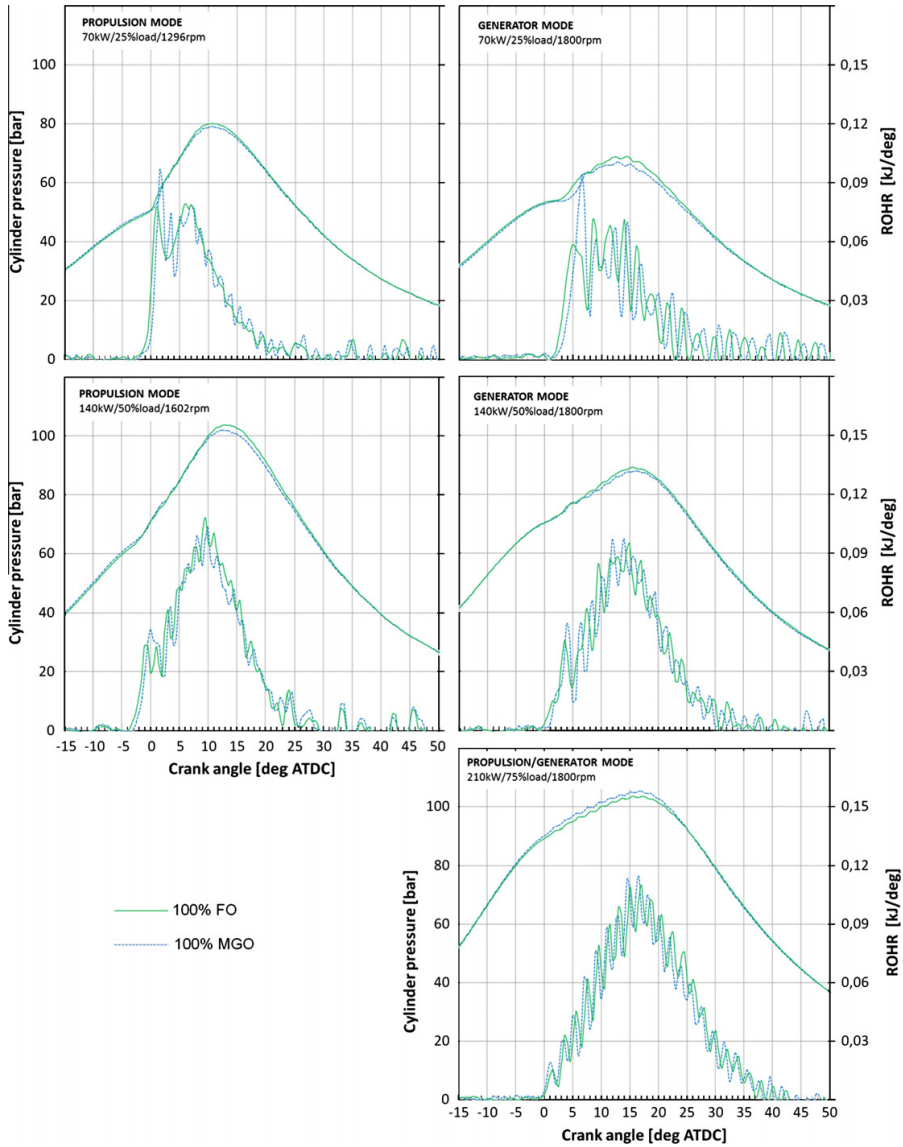
Fig. 2. Cylinder pressure and rate of heat release (ROHR) curves for MGO and FO fuels at various operating conditions.
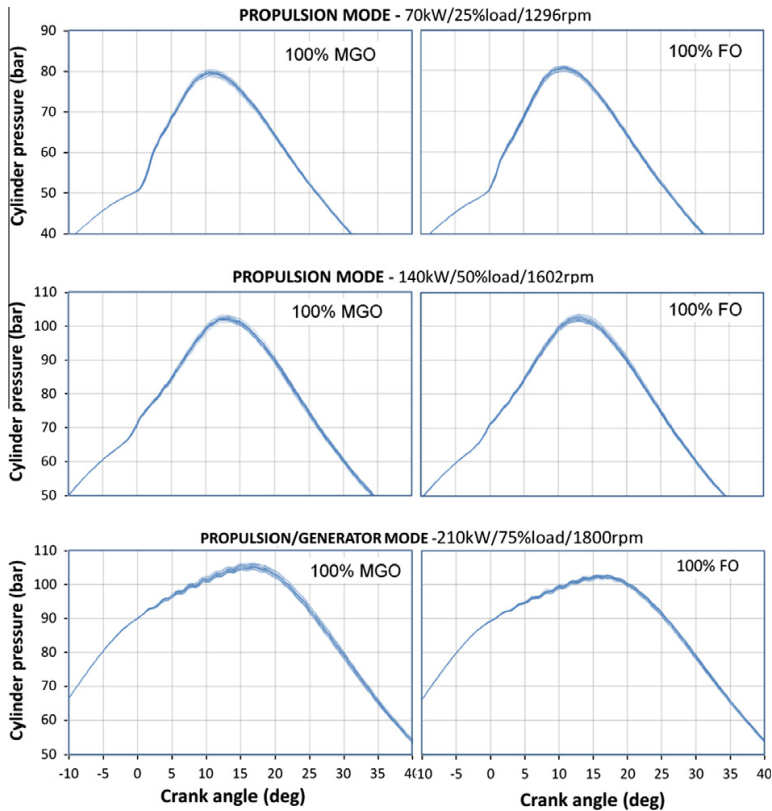
Fig. 3. Cyclic variations in cylinder pressure shown for MGO and FO at low and high load conditions.

earlier [18,42–44] and are normally associated with increase in flame temperature during the combustion process [45–47] due to presence of fuel-bound oxygen. Besides, the roles of density and high distillation area were also considered reasons for increase in NO_x concentration [44]. At the same time, in certain studies [e.g. 48] it is indicated that increasing oxygen content in fuel actually shortens the ignition delay and reduces the amount of fuel burned in premixed combustion phase, hence decreasing the peak burning temperature, which means a certain reduction in NO_x emissions.

The CO emissions from fish oil fuel appeared to be significantly lower than for the corresponding MGO. This effect was more pronounced for propulsion mode and low load conditions. MGO–FO blend lowered CO emission concentrations by 15–35% and 12–15%, while neat fish oil achieved reduction by 24–56% and 18–29%, under propulsion and generator modes respectively. It is generally accepted that CO is resulted from incomplete combustion in fuel-rich regions. Hence, in case of fish oil the combustion in these locally rich zones will be assisted and enhanced by the presence of fuel-bound oxygen which leads to considerable CO reduction [42]. Moreover, absence of aromatic compounds is also known to lighten complete fuel oxidation and thus is desirable. Emissions of CO_2 from FO at the same time were slightly lower than that of MGO, as an outcome of different values for LHV, C/H ratio and fuel conversion efficiency between fish oil and conventional MGO [49,50]. Nevertheless, CO_2 reduction is to be only offset as do not exceed 2% as indicated on Fig. 4.

The THC emissions are known to be strongly affected by fuel quality and contain partially and/or completely unburned fuel from locations with over- and undermixing of air and fuel. Fish oil showed a significant effect on emitted THC concentrations with overall maximum reduction up to 70% when used alone, and up to 37% when blended with MGO. This effect may be attributed to its lack of bi- and poly-aromatic compounds [42] and additionally enhanced by presence of significant amount of oxygen in FO fuel, which results in better fuel–air mixing properties, hence minimizing the volume of fuel-rich regions, mainly responsible for HC production, and resulting in more complete combustion [51,52].

All diesel engine emissions are known to be affected by fuel/air equivalence ratio (relative to stoichiometric conditions). But as seen from Fig. 5, the difference in equivalence ratio value at each operation mode for all tested fuels was very slight, so authors do believe that differences in emission results were caused by different characteristics and composition of tested fuels, but not because of differences in fuel/air equivalence ratio.

3.3. Smoke (soot) emissions

The operating load and speed conditions are known to have strong influence on exhaust emissions, especially for smoke and soot (FSN) formation. The reason for this is that soot is mainly formed in fuel-rich regions downstream of the liquid core of the fuel spray and hence is dependent on the overall fuel/air ratio and spray formation in the combustion chamber, which vary with engine load condition (torque and speed) [53]. Under generator mode the soot oxidation is promoted by lower fuel/air ratio as more air is passing through the cylinder due to higher engine
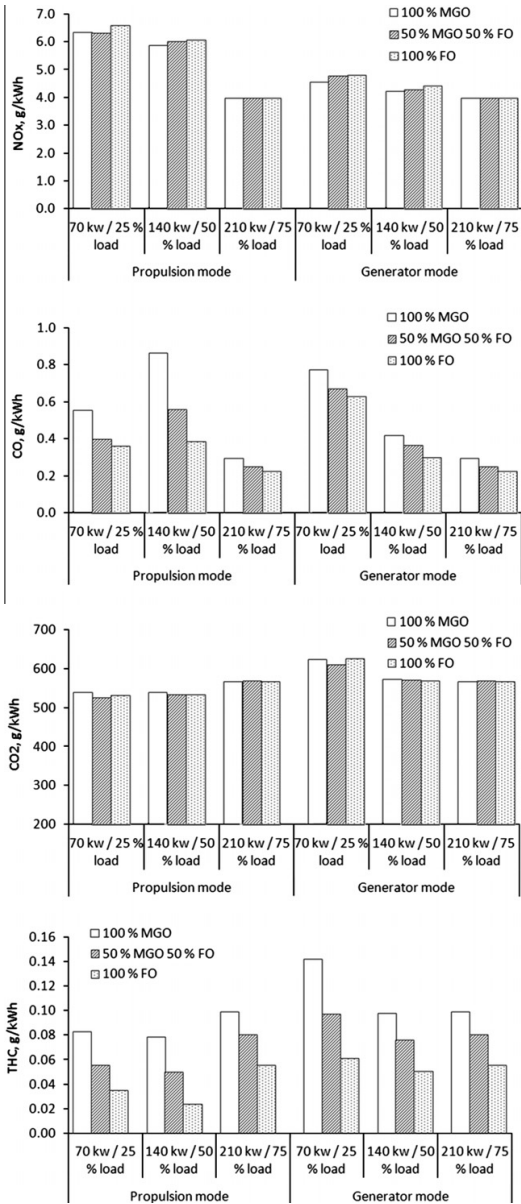
Fig. 4. Concentrations of NO$_x$, CO, CO$_2$ and THC in raw exhaust for different test fuels under propulsion and generator modes.
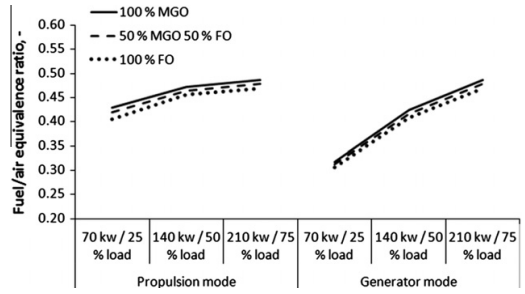

Fig. 5. Fuel/air equivalence ratio for MGO, FO and MGO–FO blend under propulsion and generator modes.

At the same time FO showed significant benefits in reduction of smoke emission with soot concentration decreased up to 63% when used as a blend with MGO and up to 90% when applied neat. This effect is believed to result from several factors. The increased oxygen content in fuel contributes to more complete fuel oxidation in fuel-rich zones mainly responsible for soot production as was reported in number of studies [18,55] and at certain level may result in entirely soot-less combustion [52,56]. In addition, lack of aromatic compounds is also found to decrease smoke emissions [20,57].

3.4. Particulate emissions

The particulate matter number size distributions measured by SMPS, corrected for diffusional losses and multiple particle charging, are presented on Fig. 7 for all studied fuels and different engine operating conditions. All results are plotted on a log–log scale and in all presented cases the distribution is the average of four–six distribution measures.

For all experimental fuels the observed particle number size distributions appeared to be unimodal with pronounced accumulation (soot) mode with corresponding mode diameter being in the range of 50–80 nm. The nucleation mode, which is normally found in size range below 30 nm [58] was not observed. This mode typically consists mainly of HC and sulfur compounds that homogeneously nucleate or condense on existing particles during dilution process [59,60]. At the same time, some studies reported existence of non-volatile nucleation mode [61–63], but the formation mechanism of such particles is still unknown. On the other hand, volatile nucleation mode particles are formed during dilution process, hence are dependent on dilution system arrangement and dilution settings used [30,64,65]. The porous tube-type diluter, used in current study as a primary diluter, is known to have conditions not favorable for nucleation, mainly because of rather slow and not perfect mixing and cooling, which is a consequence of how dilution is taking place [25]. Moreover, the presence of high amount of soot particles is known to enhance the adsorption of existing volatile material on the carbon particle surfaces [66]. So accumulation mode particles reported here are assumed to compose of soot agglomerated with a thin layer of condensed HC compounds formed upon them. It should be also stated that nucleation mode particles are often smaller than 10 nm [44,63], so can appear beyond the measured particle size range.

As seen from Fig. 7, PM size distributions were significantly affected by the sole use of fish oil and its addition to marine gas oil. The distributions remained their diesel log-normal shape and were fairly unimodal. However, the observed accumulation mode magnitudes were pronouncedly lower indicating clear reduction of emitted soot particle number with the biggest particles being most

speed. More air and hence possible better mixing allows unburned and partially burned fuel molecules to oxidize, but simultaneously the time available for the combustion process to complete is shorter at high engine speed. The observed FSN, as shown on Fig. 6, is rather low which is in line with other studies [54] showing that total PM, which is comparable approximately to smoke plus HC [53], is dominated by HCs. The combustion efficiency is known to increase with load which is attributed to decrease of FSN (soot) when changing from medium to high load.

Fig. 6. Smoke opacity (AVL 415S measurements) in FSN (left) and g/kW h (right).
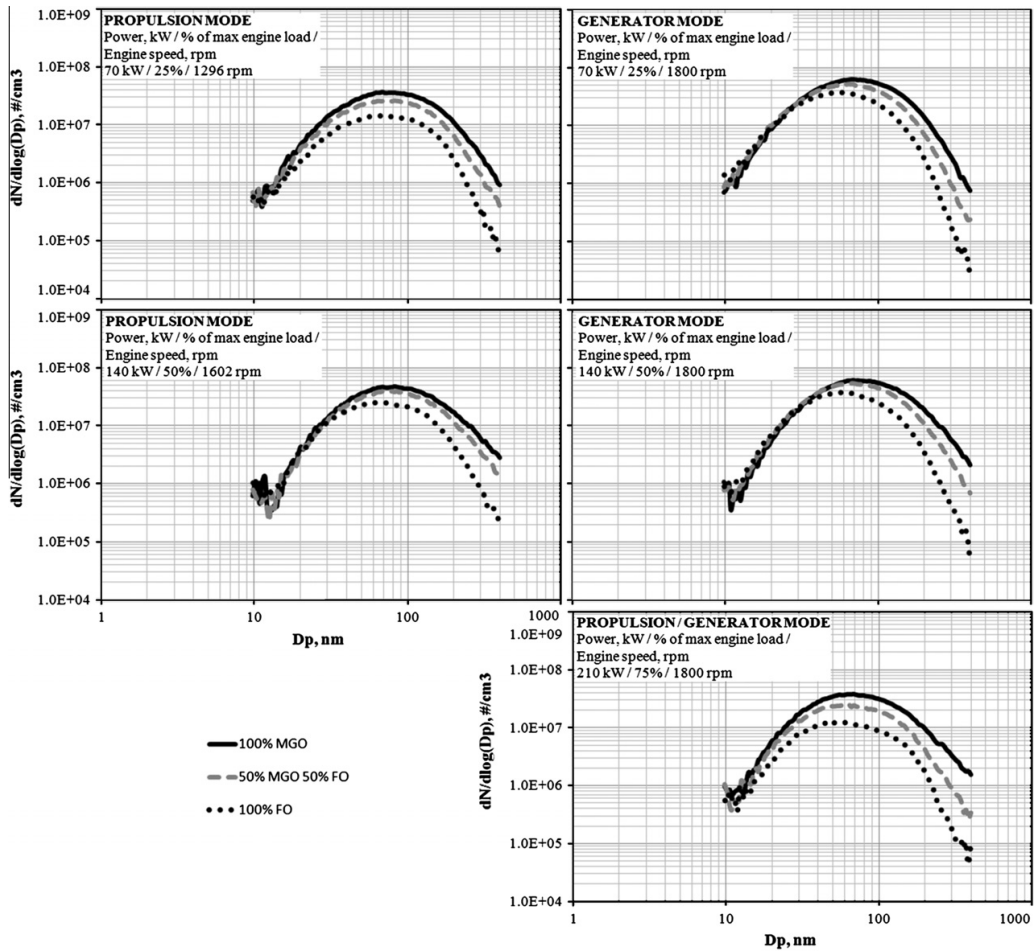
Fig. 7. Particle size distributions from SMPS measurements. Size distributions measured with FO, MGO and their 50% v/v blend at 25%, 50%, and 75% loads under modes of propulsion and generator operation.

affected. The total particle concentration decreased by up to 36% for FO–MGO blend and by up to 67% when fish oil was used alone and is reflected in Fig. 8. This effect was dictated mainly by reduction of biggest particles, which led to increased percentage of registered nanoparticle for FO and FO–MGO blend and shift of mean

CMD values to smaller diameters as seen from Figs. 9 and 10 respectively. The total PM mass, calculated from ELPI size distributions, showed a considerable decrease when FO was introduced, with the reduction being up to 56% and 79% for FO–MGO blend and pure FO correspondingly (see Fig. 11). This PM-suppressing
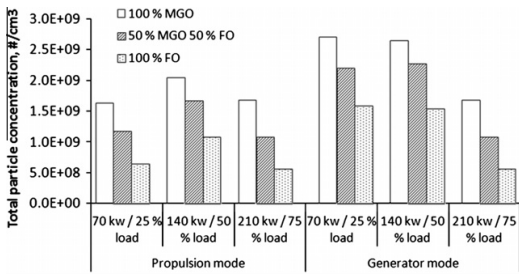
Fig. 8. Total particle concentration (10 nm < D_p < 400 nm) for FO, MGO and FO–MGO blend.
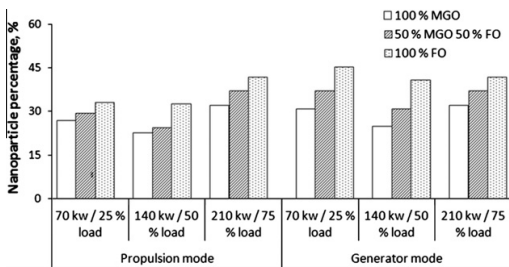
Fig. 9. Percentage of nanoparticles (<50 nm) from measured total particle concentration. Shown at various operating conditions for MGO, FO fuels and their 50% v/v blend.
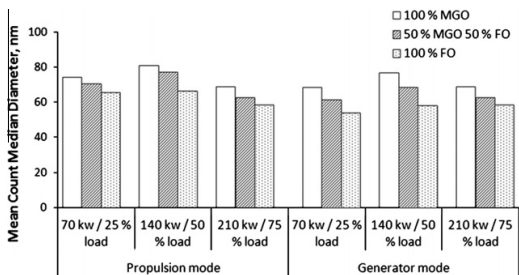
Fig. 10. Particle mean count median diameter (CMD) as a function of engine load.
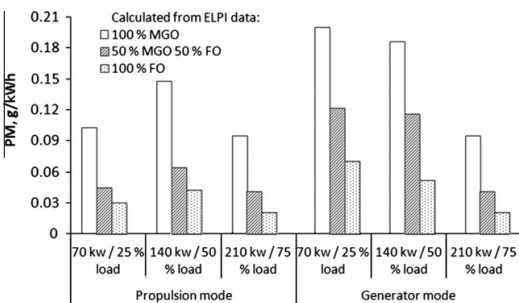
Fig. 11. PM mass concentrations calculated from ELPI number size distributions.

effect of fish oil should be attributed to its oxygen content and lack of aromatic hydrocarbons and is reported in number of studies related to similar biofuels [17,18,20,50]. At the same time, certain

studies [52,67] indicated the presence of strong nucleation mode for biofuels, which was not observed in current study either due to different dilution system used [25] or because of PM size range below 10 nm, where nucleation mode is often observed [63], was not covered. Additional beauty of fish oil as fuel is that it is almost free of sulfur (less than 10 ppm) and hence its SO_x emissions should be negligible and its contribution to PM sulfate fraction should be also minimal.

It should be also mentioned here that effect of fuel type is likely coupled with the effect of engine load and speed (mode type) as from Fig. 7 it is seen that effect of fish oil on particulate matter is more pronounced under propulsion mode. It is probably due to the fact that smaller amount of air entering cylinder at lower speeds is compensated by presence of fuel-bounded oxygen, while increasing time available for the combustion process promotes more efficient combustion [53].

During the experiments no additional deposits, clogging or excessive engine wear were observed when running on fish oil. Moreover, it exhibited good mixing properties when blended with conventional MGO and showed no phase separation at all for a period of many days. The further work is planned to performed similar experiments using medium-speed marine diesel engine and also to test rheological, cold temperature properties and oxidation stability of FO which are often of high concern [2,9] and requires further analysis.

4. Conclusions

In present paper the impact of FO, as alternative to diesel fuel, on combustion performance and emission characteristics was analyzed. The tests were performed for neat FO, MGO and their 50% blend under propulsion and generator mode marine engine cycles and were carried out on heavy-duty high-speed diesel engine. And the main conclusions of the investigation can be summarized as follows:

1. Almost identical specific fuel consumption and shaft efficiency was found when difference in density and lower heating index are taken into account. An increase in specific fuel consumption for FO–MGO blend and pure fish oil fuel was observed for all load settings and is explained by lower heating value of applied biofuel.
2. Analysis of combustion process shows that fish oil has almost the same or even better ignition and combustion properties in comparison to the reference diesel fuel (MGO).
3. The FO showed strong improvement in CO, THC and smoke (soot) emissions, while for NO_x and CO_2 only slight difference (<6%) was registered. Overall, maximum reductions in case of neat fish oil use were up to 56% of CO, 70% of THC and 90% of smoke respectively. Considerable reduction of SO_x is expected as FO is virtually free of sulfur (<10 ppm). Pollutant emissions were also decreased when FO–MGO blend was used, although reduction was somewhat lower.
4. The registered particle number size distributions were fairly unimodal at all operating conditions for all test fuels and exhibited typical accumulation (soot) mode. Hence, as for smoke, fish oil fuel also considerably improved engine PM characteristic resulting in up to 67% and 79% reduction of total particle concentration and overall PM mass respectively.
5. The reported CO, THC and especially smoke and PM emission reduction is believed to result mainly from fish oil fuel properties. The high oxygen content in fuel improves the mixing process (especially in locally rich zones) that, together with lack of aromatics, leads to easier and more complete fuel oxidation process.

6. Overall, fish oil has demonstrated good combustion and excellent emission characteristics and potentially can be regarded as alternative to MGO. Although, despite the fact that no deposits, clogging or addition engine wear problems were noticed during the study, the more detailed tests of fish oil rheological, cold temperature properties and its oxidation stability are required.

Acknowledgements

References

[1] Monyem A, van Gerpen JH. The effect of biodiesel oxidation on engine performance and emissions. Biomass Bioenerg 2001;20:317–25.
[2] Dwivedi G, Jain S, Sharma MP. Impact analysis of biodiesel on engine performance – a review. Renew Sust Energy Rev 2011;15:4633–41.
[3] Tormos B, Novella R, Garcia A, Garger K. CMT-Motores Termicos, comprehensive study of biodiesel fuel for HSDI engines in conventional and low temperature combustion conditions. Renew Energy 2010;35:368–78.
[4] Karl TR, Trenberth KE. Modern global climate change. Science 2003;302:1719–23.
[5] Bozell J, Moens L, Peterson E, Tyson KS, Wallace R. Biomass oil analysis: research needs and recommendations. NREL technical report; 2004.
[6] Balat M, Demirbas MF. Recent advances on the production and utilization trends of biofuels: a global perspective. Energy Convers Manage 2006;47:2371–81.
[7] Boyd M, Murray-Hill A, Schaddelee K. Biodiesel in British Columbia – feasibility study report. WISE Energy Co-op/Eco-Literacy Canada; 2004.
[8] Demirbas A. Use of algae as biofuel sources. Energy Convers Manage 2010;51:2738–49.
[9] Jayasinghe P, Hawboldt K. A review of bio-oil from waste biomass: focus on fish processing waste. Renew Sust Energy Rev 2012;16:798–821.
[10] Shonnard DR, Marker T, Kalnes T. Green diesel: a second generation biofuel. Int J Chem React Eng 2007;5:A48.
[11] Balat M. Potential alternatives to edible oil for biodiesel production – a review of current work. Energy Convers Manage 2011;52:1479–92.
[12] Demirbas A. Biodiesel from waste cooking oil via base-catalytic and supercritical methanol transesterification. Energy Convers Manage 2009;50:923–7.
[13] Demirbas MF, Balat M, Balat H. Biowastes-to-biofuels. Energy Convers Manage 2011;52:1815–28.
[14] Archer M, Watson, R, Denton JW. Fish waste production in the United Kingdom – the quantities produced and opportunities for better utilization. Seafish report no. SR537. Seafish Technology, Sea fish Industry Authority; 2001.
[15] Sathivel S, Prinyawiwatkul W, Grimm CC, King JM, Lloyd S. Fatty acid composition of crude oil recovered from Catfish Viscera. J Am Oil Chem Soc 2002;79(10).
[16] El-Mashad HM, Zhang R. Bio-diesel and bio-gas production from seafood processing by-products. In: Maximizing the value of marine by-products. Wood Head Publishing in Food Science, Technology and Nutrition; 2007. p. 460–85.
[17] Blythe NX. Fish oil as an alternative fuel for internal combustion engines. In: 1996 Spring technical conference, vol. 3; ASME; 1996. p. 85–92.
[18] Steigers JA. Demonstrating the use of fish oil in a large stationary diesel engine. Steigers Corporation; 2003.
[19] Mrad N, Varuvel EG, Tazerout M, Aloui F. Effects of biofuel from fish oil industrial residue – diesel blends in a diesel engine. Energy 2012;44:955–63.
[20] Lapuerta M, Rodriguez-Fernandez J, Agudelo JR. Diesel particulate emissions from used cooking oil biodiesel. Bioresour Technol 2008;99:731–40.
[21] Kannan D, Pachamuthu S, Nabi MN, Hustad JE, Løvås T. Theoretical and experimental investigation of diesel engine performance, combustion and emissions analysis fuelled with the blends of ethanol, diesel and jatropha methyl ester. Energy Convers Manage 2012;53:322–31.
[22] AVL. Smoke value measurement with the filter-paper method. Revision 02. AVL List GmbH, Graz, Austria; 2005.
[23] Kittelson DB, Arnold M, Watts WF. Review of diesel particulate matter sampling methods. Final report. Minneapolis, MN: University of Minnesota; 1999.
[24] Auvinen A, Lehtinen KEJ, Enriquez J, Jokiniemi JK, Zilliacus R. Vaporization rates of CsOH and CsI in conditions simulating a severe nuclear accident. J Aerosol Sci 2000;31(9):1029–43.
[25] Lyyränen J, Jokiniemi J, Kauppinen EI, Backman U, Vesala H. Comparison of different dilution methods for measuring diesel particle emissions. Aerosol Sci Technol 2004;38:12–23.

[26] Ntziachristos L, Giechaskiel B, Pistikopoulos P, Samaras Z, Mathis U, Mohr M, et al. Performance evaluation of a novel sampling and measurement system for exhaust particle characterization. SAE paper no. 2004-01-1439; 2004.
[27] Mathis U, Ristimaki J, Mohr M, Keskinen J, Ntziachristos L, Samaras Z, et al. Sampling conditions for the measurement of nucleation mode particles in the exhaust of a diesel vehicle. Aerosol Sci Technol 2004;38:1149–60.
[28] Koch W, Lödding H, Mölter W, Munzinger F. Dilution system for the measurement of highly concentrated aerosols with optical particle counters. Staub 1988;48:341–4 [in German].
[29] De Filippo A, Maricq MM. Diesel nucleation mode particles: semivolatile or solid? Environ Sci Technol 2008;42:7957–62.
[30] Abdul-Khalek IS, Kittelson DB, Brear F. Diesel trap performance. particle size measurements and trends. SAE paper no. 982599; 1998.
[31] Maricq MM, Chase RE, Podsiadlik DH, Vogt R. Vehicle exhaust particle size distributions: a comparison of tailpipe and dilution tunnel measurements. SAE paper no. 1999-01-1461; 1999.
[32] Khalek IA, Kittelson DB, Brear F. Nanoparticle growth during dilution and cooling of diesel exhaust: experimental investigation and theoretical assessment. SAE paper no. 2000-01-0515; 2000.
[33] Wang SC, Flagan RC. Scanning electrical mobility spectrometer. Aerosol Sci Technol 1990;13(2):230–40.
[34] Knudson EO, Whitby KT. Aerosol classification by electric mobility: apparatus, theory, and application. J Aerosol Sci 1975;6:443–51.
[35] Keskinen J, Pietarinen K, Lehtimäki M. Electrical low pressure impactor. J Aerosol Sci 1992;23:353–60.
[36] Amann CA, Siegla DC. Diesel particulates: what they are and why. Aerosol Sci Technol 1982;1:73–101.
[37] Kittelson DB, Reinertsen J, Michalski J. Further studies of electrostatic collection and agglomeration of diesel particles. SAE paper no. 910329; 1991.
[38] Maricq MM, Podsiadlik DH, Chase RE. Size distributions of motor vehicle exhaust PM: a comparison between ELPI and SMPS measurements. Aerosol Sci Technol 2000;33:239–60.
[39] Tsolakis A. Effects on particle size distribution from the diesel engine operating on RME-biodiesel with EGR. Energy Fuels 2006;20:1418–24.
[40] Yamane K, Ueta A, Shimamoto Y. Influence of physical and chemical properties of biodiesel fuels on injection, combustion and exhaust emission characteristics in a direct injection compression ignition engine. In: The fifth international symposium on diagnostics and modeling of combustion in internal combustion engines (COMODIA 2001), Nagoya, Japan; 2001.
[41] Lee CS, Park SW, Kwon S. An experimental study on the atomization and combustion characteristics of biodiesel-blended fuels. Energy Fuels 2005;19:2201–8.
[42] Usta N, Öztürk E, Can Ö, Conkur ES, Nas S, Con AH, et al. Combustion of biodiesel fuel produced from hazelnut soapstock/waste sunflower oil mixture in a diesel engine. Energy Convers Manage 2005;46:741–55.
[43] McCormick R, Graboski M, Alleman T, Herring A. Impact of biodiesel source material and chemical structure on emissions of criteria pollutants from a heavy-duty engine. Environ Sci Technol 2001;35:1742–7.
[44] Heikkilä J, Virtanen A, Rönkkö T, Keskinen J, Aakko-Saksa P, Murtonen T. Nanoparticle emissions from a heavy-duty engine running on alternative diesel fuels. Environ Sci Technol 2009;43:9501–6.
[45] Cheng AS, Upatnieks A, Mueller CJ. Invstigation of the impact of biodiesel fueling on NOₓ emissions using an optical direct injection diesel engine. Int J Engine Res 2006;7:297–319.
[46] Godinagur S, Murthy CS, Reddy RP. Performance and emission characteristics of a Kirloskar HA394 diesel engine operated on fish oil methyl esters. Renew Energy 2010;35:355–9.
[47] Keskin A, Yasar A, Gürü M, Altiparmak D. Usage of methyl ester of tall fatty acids and resinic acids as alternative diesel fuel. Energy Convers Manage 2010;51:2863–8.
[48] Lin CY, Huang JC. An oxygenating additive for improving the performance and emission characteristics of marine Diesel engines. Ocean Eng 2003;30:1699–715.
[49] Beatrice C, Di Iorio S, Guido C, Mancaruso E, Vaglieco BM, Vassalo A. Alternative diesel fuels effects on combustion and emissions of an euro4 automotive diesel engine. SAE paper no. 2009-24-0088; 2009.
[50] Mancaruso E, Vaglieco BM. Premixed combustion of GTL and RME fuels in a single cylinder research engine. Appl Energy 2012;91:385–94.
[51] Arcoumanis C, Bae C, Crookes R, Kinoshita E. The potential of di-methyl ether (DME) as an alternative fuel for compression–ignition engines: a review. Fuel 2007;87:1014–30.
[52] Xinling L, Zhen H. Emission reduction potential of using gas-to-liquid and dimethyl ether fuels on a turbocharged diesel engine. Sci Total Environ 2009;407:2234–44.
[53] Sarvi A, Fogelholm C-J, Zevenhoven R. Emissions from large-scale medium-speed diesel engines: 2. Influence of fuel type and operating mode. Fuel Process Technol 2008;89:520–7.
[54] Ristimaki J, Hellen G, Lappi M. Chemical and physical characterization of exhaust particulate matter from a marine medium speed diesel engine. Paper 73. CIMAC congress 2010, Bergen, Norway; 2010.
[55] Miyamoto H, Ogawa H, Arima T, Miyakawa K. Improvement of diesel combustion and emissions with various oxygenated fuel additives. SAE paper no. 962115; 1996.
[56] Tree DR, Svensson KI. Soot processes in compression ignition engines. Prog Energy Combust 2007;33:272–309.

[57] Chang DY, van Gerpen JH. Fuel properties and engine performance for biodiesel prepared from modified feedstocks. SAE paper no. 971684; 1997.
[58] Swanson J, Kittelson DB. Factors influencing mass collected during 2007 diesel PM filter sampling. SAE paper no. 2009-01-1517; 2009.
[59] Bagley ST, Baumgard KJ, Gratz LD, Johnson JJ, Leddy DG. Characterization of fuel and aftertreatment devices on diesel emissions. HEI research report no. 88. Boston, MA: Health Effects Institute; 1996.
[60] Shi JP, Harrison RM. Investigation of ultrafine particle formation during diesel exhaust dilution. Environ Sci Technol 1999;33:3730–6.
[61] Sakurai H, Tobias HJ, Park K, Zarling D, Docherty KS, Kittelson DB, et al. On-line measurements of diesel nanoparticle composition, volatility, and hygroscopicity. Atmos Environ 2003;37:1199–210.
[62] Rönkkö T, Virtanen A, Vaaraslahti K, Keskinen J, Pirjola L, Lappi M. Effect of dilution conditions and driving parameters on nucleation mode particles in diesel exhaust. Atmos Environ 2006;40:2893–901.
[63] Lähde T, Rönkkö T, Virtanen A, Solla A, Kytö M, Söderström C. Dependence between nonvolatile nucleation mode particle and soot number concentrations in an EGR equipped heavy-duty diesel engine exhaust. Environ Sci Technol 2010;44:3175–80.
[64] Kittelson DB. Engines and nanoparticles: a review. J Aerosol Sci 1998;29:575–88.
[65] Abdul-Khalek IS, Kittelson DB, Brear F. The influence of dilution conditions on diesel exhaust particle size distribution measurements. SAE paper no. 1999-01-1142; 1999.
[66] Armas O, Ballesteros R, Gomez A. The effect of diesel engine operating conditions on exhaust particle size distributions. Proc Mech Eng, Part D: J Autom Eng 2008;222:1513–25.
[67] Tsolakis A, Megaritis A, Wyszynskia ML, Theinnoia K. Engine performance and emissions of a diesel engine operating on diesel-RME (rapeseed methyl ester) blends with EGR (exhaust gas recirculation). Energy 2007;32:2072–80.

Paper VI

Emission characteristics of GTL fuel as an alternative to conventional marine gas oil

Sergey Ushakov, Nadine G. Halvorsen, Harald Valland, Dag H. Williksen, Vilmar Æsøy

Emission characteristics of GTL fuel as an alternative to conventional marine gas oil

Sergey Ushakov[1]*, Nadine G.M. Halvorsen[1], Harald Valland[1], Dag H. Williksen[2] and Vilmar Æsøy[3]

[1] *Norwegian University of Science and Technology, Department of Marine Technology, Otto Nielsens vei 10, NO-7491 Trondheim, Norway*
[2] *Approval Centre Ship and Offshore, Machinery Newbuilding, Det Norske Veritas AS, Veritasveien 1, NO-1363, Høvik, Norway*
[3] *Department of Product Development and Machinery Systems Design, Ålesund University College (AaUC), Larsgårdsvegen 2, NO-6009 Ålesund, Norway*

Abstract
The study examine the gaseous, smoke and particulate matter emission characteristics of a turbocharged heavy-duty diesel engine operated on conventional marine gas oil and gas-to-liquid Fischer-Tropsch fuel under modes of propulsion and generator operation. The gas-to-liquid showed average reductions up to 19% in nitrogen oxides, 25% in carbon monoxide, 4% in carbon dioxide and 30% in smoke with slight increase in unburned hydrocarbon emissions. Particulate number concentrations for gas-to-liquid were up to 21% higher, whereas particulates mass showed a 16% decrease at medium and high loads, while increasing by 12 to 15% under lower load conditions. Very low aromatic content of gas-to-liquid fuel and nearly zero sulfur level are responsible for particulate reduction.

Keywords: marine diesel engine; gas-to-liquid; particulate matter; Fischer-Tropsch fuel.

1. Introduction
Engine manufacturers are constantly challenged to meet emission regulations for permitted NO_x and PM levels, so biofuels and synthetics like Fischer-Tropsch (F-T) diesel fuels may become the most attractive and feasible short-term solutions. Interest in alternative fuels has grown increasingly mainly due to concerns about the limited future fossil fuel resources and requirements of CO_2 reduction and ultra-clean, high cetane number fuels derived from an F-T process is a very promising alternative. The basic technology known as Fischer-Tropsch process and the raw material can either be natural gas (the final liquid being GTL), residual biomass (BTL) or coal (CTL) with the resulting synthetic straight-chain HC having good compression ignitability and being applicable as automotive diesel fuel neat and in blends with conventional diesel fuels. F-T process can be designed in such way that synthesized fuel has a high cetane number, low aromatics, thus low C/H ratio and fairly low specific gravity. In addition, if derived from natural gas F-T fuel it is free of sulfur, hence is especially attractive for use together with after-treatment catalytic technologies.

The GTL fuel was extensively tested as alternative to conventional diesel fuel for light- and heavy-duty diesel engines, but little has been done considering expand its use to other fields, for example in maritime sector.

2. Experimental methods

---

* Corresponding author e-mail: sergey.ushakov@ntnu.no

A four-stroke, turbocharged, intercooled, direct injection heavy-duty diesel engine fully complied with Euro 2 emission tier was used (Table 1). A low-sulfur MGO and GTL fuels were used for the experiments with their detailed specification provided in Table 1. Gas-to-liquid fuel has higher H/C ratio, a somewhat lower viscosity, contains a very low amount of aromatics and is free of sulfur. A 4-mode steady E2 cycle simulating constant-speed main propulsion application and E3 cycle for propeller-law-operated engines were adopted. Due to engine brake limitations, there was no possibility exceed a 75% load, which determined the maximum load point for both test cycles. Mode 2, 3, 4 were 75%, 50% and 25% loads with engine speeds of 1800, 1602 and 1296 rpm under propulsion mode, while under generator mode the engine had a constant speed of 1800 rpm.

Gaseous emissions were measured in accordance to ISO 8178 (ISO, 2006) with gas samples being extracted from the tailpipe through a separate port located 3 m after the engine turbocharger. Nitrogen oxides, CO, and CO_2 were measured simultaneously by Horiba PG-250 portable multi-gas analyzer. Unburned hydrocarbon (THC) concentration was determined with a J.U.M. (model 3-200) portable heated flame ionization analyzer. An AVL 415S smoke meter was applied to measure smoke opacity. Soot emissions were estimated from FSN through the recommended correlations (AVL, 2005) as:

$$C(soot), mg/m^3 = 12.222 \cdot FSN \cdot exp(0.38 \cdot FSN) \tag{1}$$

Sampling gas was drawn from the exhaust manifold by means of J-shaped open-ended probe and was transported to dilution unit by a flexible heated sampling line. This sampling line was electrically heated and insulated to prevent thermophoretic deposition of solid PM and condensation of volatile material on the walls (Ushakov et al., 2012).

In order to dilute and cool down the exhaust sample for measurement by particle instruments a two-stage dilution unit (from Dekati Ltd., Finland), consisting of primary porous tube and secondary ejector diluters, was used.

Dilution air temperature, used for both primary and secondary diluter, was 30 °C and its relative humidity was maintained below 5%. Primary dilution ratio slightly varied with load and was around 6-7, while secondary dilution ratio was maintained ten during whole experiment, hence resulting in overall dilution ratio of approximately 60 to 70 which was determined as ratio of NO_x concentration in raw exhaust to that in diluted gas sample.

Particle size distributions were measured using a scanning mobility particle sizer (SMPS, model 3934 from TSI Inc) and electrical low-pressure impactor (ELPI) from Dekati Ltd., operating simultaneously. The measurement particle size range for SMPS was 10-400 nm, while ELPI equipped with filter stage was able to measure real-time size distributions in size range of 7 nm to 10 μm.

The PM mass concentrations were calculated from ELPI particle number distributions assuming spherical particles with unit density. Only the lowest seven stages of ELPI were taken into consideration to prevent the coarse mode artifact reported by Maricq et al. (2000). The particle concentrations and count median diameter values of the distributions were calculated by integrating over the considered particle diameter size range of 10-400 nm.

3. Results

Gaseous emissions

Engine-out and tailpipe gaseous emissions are depicted on Figure 1. It can be seen that average reduction of NO_x emissions by 15-19% can be achieved when changing from MGO to GTL fuel. It is believed that combustion of GTL results in lower in-cylinder pressure, lower maximum rate of pressure rise and lower maximum rate of heat release than MGO fuel combustion. For mechanically-injected system, GTL retards the start of injection due to its lower density and higher bulk modulus of compressibility than diesel fuel (Abu-Jrai et al., 2009). Much higher cetane number shortens ignition delay (Abu-Jrai et al., 2006) and as a result both effects balance, resulting in less pronounced pre-mixed combustion. This gives a lower combustion temperature and hence lower NO_x formation rates for GTL fuel. In addition, lack of aromatic compounds in GTL fuel also contributes to lower adiabatic flame temperature, which was reported to be lower for paraffinic compounds than for aromatic ones (Glaude et al., 2010).

Emissions of CO showed a pronounced decrease of around 17-25% for GTL in comparison to MGO at certain load points with this reduction being likely related to high cetane number and very low aromatic content of GTL (Wu et al., 2007). For turbocharged DI diesel engines CO emissions are normally low which is explained by rather high combustion temperatures and high oxygen content in the spray combustion.

Emitted CO_2 concentrations from GTL were lower than that of diesel fuel with average decrease of around 4% and can be explained by pronouncedly increased H/C ratio of GTL (Gill et al., 2011). At the same time, one should keep in mind that the density of F-T fuel was approximately 8% lower (comparing to MGO) while lower heating values were very similar, so GTL's volumetric fuel consumption had to be increased by 7.5% to provide the equal energy input required to maintain same power and torque levels.

GTL fuel showed an average 10% increase in THC emissions in comparison to conventional MGO. The flow rate of GTL was increased to compensate for lower fuel density (lower volumetric energy content), hence a higher incidence of wall-wetting is possible, which can contribute to higher HC emissions (Schaberg et al., 2002). It also should be mentioned that HC emission formation is very sensitive to fuel injection nozzle design (number of holes, hole diameter, etc.), while all experiments were performed with the same nozzle better suited for MGO fuel.

Smoke and PM emission characteristics

The results of smoke measurements with corresponding calculated soot concentrations are given in Figure 2. One can see that at low load smoke (soot) emissions either slightly increase or remain unchanged when changing from MGO to GTL, while at medium and high loads they are considerably decreased. The most pronounced smoke reduction of above 30% was achieved under generator mode operation where soot oxidation is promoted by higher amount of air passing through the engine due to higher engine speed. However, the time available for combustion process and allowing unburned and partially burned fuel molecules find extremely lean pockets and mix with them is decreasing. The latter factor is compensated by ultra low aromatic content in GTL fuel resulting in easier and more complete fuel oxidation (Ntziachristos et al., 2000; Xinling and Zhen, 2009). At low loads, the injection pressure is rather low which can result in formation of very large

fuel droplets that may impinge on combustion chamber walls and increase soot and HC emissions (Sarvi et al., 2008).

Results of PM mass concentrations calculated from ELPI size distributions are shown on Figure 3. At low load conditions PM mass is increased by 12-15% for GTL fuel in comparison to MGO, while it is decreased at both medium and high loads with maximum reduction of around 16%. PM results exhibited behavior very similar to that of smoke as particulate matter is composed mainly of soot with certain contribution of unburned and partially burned fuel and oil and sulfates, hence all findings for smoke can be also applicable to PM. Additionally, the burn fraction for GTL fuel is always less than that of conventional diesel for the same injection advance (Cowart et al., 2008) indicating that GTL has a shorter premixed combustion phase, which is consistent with a shorter ignition delay due to the higher cetane number. Low soot and hence PM levels are typically associated with a large premixed combustion phase and a comparably lower diffusion phase (Gill et al., 2011). GTL produces more soot than diesel fuel at low loads but this was improved as load increased, which is in consistence with Cowart et al. (2008). This effect is likely due to shortened premixed combustion phase with corresponding reduced levels of fueling, since higher cetane number of GTL makes ignition occur sooner before much mixing with air has occurred. At the same time, its negligible aromatic and sulfur content is known to enhance PM reduction (Xinling and Zhen, 2009).

Particle number size distributions from both tested fuels exhibited only unimodal structure with corresponding accumulation mode (Figure 4) in contrast to some Li et al., (2007) who reported bimodal particle size distributions (nucleation and accumulation modes) from conventional diesel and GTL fuels. Nucleation mode is typically composed of homogeneously nucleated HC and sulfur compounds and is formed during dilution process (Abdul-Khalek et al., 1999). The porous tube diluter, used as a primary diluter, is known to have conditions not favourable for nucleation, mainly due to rather low turbulence level (Lyyränen et al., 2004). Moreover, the presence of sufficient amount of soot enhances the adsorption of existing volatile material on the carbon particle surfaces (Armas et al., 2008), so is promoting heterogeneous nucleation/condensation, which is believed to be dominating mechanism. So accumulation mode reported here is assumed to compose of soot agglomerates with a thin layer of condensed HC and sulphur compounds upon them.

When changing from MGO to GTL the registered PM number concentration increased in average by 21% which was mainly attributed to 22-28% increase in number of nanoparticles as seen on Figure 5a. This is likely due to higher contribution of HC fraction to PM (Sarvi et al., 2008) and is caused by increased spray penetration (assuming similar vaporization properties) of GTL fuel that causes fuel impingement on the chamber walls, and so flame quenching. Spray penetration increases as flow rate of GTL had to be increased to compensate for its lower volumetric energy content. At the same time, a reduction in number of accumulation mode particles with diameter over 150 nm with corresponding shift to smaller median sizes was observed for GTL fuel (Figure 4 and 5b) and can be explained by its lack of aromatic compounds leading to more efficient combustion, hence suppressing formation of big carbonaceous particles (Ntziachristos et al., 2000). PM-suppressing effect of GTL due to lower fuel aromatic content is dominating over the higher level of emitted organic PM fraction due to possible fuel impingement on cylinder walls at medium and high loads, while opposite trend is

observed at low load conditions. This is because low loads PM mass is dominated by organic (HC) fraction (Ristimaki et al., 2010) due to small amount of fuel burned and high vapour- and solid-phase HC emissions associated with rather low injection pressureset.

4. Conclusions

When changing from MGO to GTL fuel the emissions of NO_x were on average 15-19% lower which is explained by much higher cetane number of GTL that shortens ignition delay and results in less pronounced pre-mixed combustion. CO concentrations at certain loads decreased by 17-25% and are attributed to higher cetane number and very low aromatic content of GTL, while reduction in CO_2 emissions was around 4% and can be explained by its higher H/C ratio. At the same time, GTL showed an average 10% increase in THC emissions which can be associated to possible higher incidence of wall-wetting as its flow rates should be increased to compensate for lower GTL volumetric energy content.

The measured smoke concentrations remained almost unchanged at low loads; while up to 30% reduction was achieved at medium and high loads when fuel was changed from MGO to GTL. PM exhibited a very similar behaviour, as is known to compose mainly of soot, and showed an average 16% decrease at medium and high loads, while increased by 12-15% at low load conditions. GTL negligible fuel aromatic hydrocarbon and sulfur content is responsible for PM reduction, while at low loads these effects are diminished by higher level of organic PM emitted by tested F-T fuel due to possible fuel impingement on cylinder walls. This may also explain an average 21% and 22-28% increase in and nanoparticle concentration that was observed at GTL firing. The corresponding decrease in particle count median diameter was also registered and was more pronounced under generator mode operation. At all fuels and operating conditions measured particle size distributions appeared to be unimodal with only pronounced accumulation mode. No visible signs of nucleation mode presence in the measured size range were observed and can be likely explained by a dilution system arrangement and dilution settings used.

References

Abdul-Khalek, I.S., Kittelson, D.B., Brear, F., 1999. The influence of dilution conditions on diesel exhaust particle size distribution measurements. SAE Technical Paper Series, 1999-01-1142. Society of Automotive Engineers.

Abu-Jrai, A., Tsolakis, A., Theinnoi, K., Cracknell, R., Megaritis, A., Wyszynski, M.L., Golunski, S.E., 2006. Effect of gas-to-liquid diesel fuels on combustion characteristics, engine emissions, and exhaust gas fuel reforming. Comparative study. Energy and Fuels 20, 2377-2384.

Abu-Jrai, A., Rodriguez-Fernandez, J., Tsolakis, A., Megaritis, A., Theinnoi, K., Cracknell, R.F., Clark, R.H., 2009. Performance, combustion and emissions of a diesel engine operated with reformed EGR. Comparison of diesel and GTL fuelling. Fuel 88, 1031-1041.

Armas, O., Ballesteros, R., Gomez, A., 2008. The effect of diesel engine operating conditions on exhaust particle size distributions. Proceedings of the Institution of Mechanical Engineers, Part D – Journal of Automobile Engineering 222, 1513-1525.

AVL, 2005. Smoke value measurement with the filter-paper method. Revision 02. AVL List GmbH, Graz.

Cowart, J.S., Sink, E.M., Slye, P.G., Caton, P.A., Hamilton, L.J., 2008. Performance, efficiency and emissions comparison of diesel fuel and a Fischer-Tropsch synthetic fuel in a CFR single cylinder diesel engine during high load operation. SAE Technical Paper Series, 2008-01-2382 Society of Automotive Engineers.

Gill, S.S., Tsolakis, A., Dearn, K.D., Rodriguez-Fernandez, J., 2011. Combustion characteristics and emissions of Fischer-Tropsch diesel fuels in IC engines. Progress in Energy and Combustion Science 37, 503-523.

Glaude, P.-A., Fournet, R., Bounaceur, R., Moliere, M., 2010. Adiabatic flame temperature from biofuels and fossil fuels and derived effect on NOx emissions. Fuel Processing Technology 91, 229-235.

ISO, 2006. International Standard 8178, Reciprocating internal combustion engines – Exhaust emission measurement. Second edition.

Keskinen, J., Pietarinen, K., Lehtimäki, M., 1992. Electrical low pressure impactor. Journal of Aerosol Science 23, 353-360.

Li, X., Huang, Z., Wang, J., Zhang, W., 2007. Particle size distribution from a GTL engine. Science of the Total Environment 382, 2234-2244.

Lyyränen, J., Jokiniemi, J., Kauppinen, E.I., Backman, U., Vesala, H., 2004. Comparison of different dilution methods for measuring diesel particle emissions. Aerosol Science and Technology 38, 12-23.

Maricq, M.M., Podsiadlik, D.H., Chase, R.E., 2000. Size distributions of motor vehicle exhaust PM: A comparison between ELPI and SMPS measurements. Aerosol Science and Technology 33, 239-260.

Ntziachristos, L., Samaras, Z., Pistikopoulos, P., Kyriakis, N., 2000. Statistical Analysis of Diesel Fuel Effects on Particle Number and Mass Emissions. Environmental Science and Technology 34, 5106-5114.

Ristimaki, J., Hellen, G., Lappi, M., 2010. Chemical and physical characterization of exhaust particulate matter from a marine medium speed diesel engine. Paper 73. CIMAC Congress 2010, Bergen, Norway.

Sarvi, A., Fogelholm, C.-J., Zevenhoven, R., 2008. Emissions from large-scale medium-speed diesel engines: 2. Influence of fuel type and operating mode. Fuel Process Technology 89, 520-527.

Schaberg, P., Botha, J., Schnell, M., Hermann, H.O., Pelz, N., Maly, R., 2002. Emissions performance of GTL diesel fuel and blends with optimized engine calibrations. SAE Technical Paper Series, 2002-01-2727. Society of Automotive Engineers.

SAE Technical Paper Series, 2005-01-2187. Society of Automotive Engineers.

Ushakov, S., Valland, H., Nielsen, J.B., Hennie, E., 2012. Effects of Dilution Conditions on Diesel Particle Size Distribution and Filter Mass Measurements in Case of Marine Fuels. Mimeo.

Wu, T., Huang, Z., Zhang, W.G., Fang, J.H., Yin, Q., 2007. Physical and chemical properties Of GTL-diesel fuel blends and their effects on performance and emissions of a multi-cylinder DI compression ignition engine. Energy and Fuels 21: 1908-1914.

Xinling, L., Zhen, H., 2009. Emission reduction potential of using gas-to-liquid and dimethyl ether fuels on a turbocharged diesel engine. Science of the Total Environment 407: 2234-2244.

Table 1 Properties of test fuels.

Fuel properties	MGO	GTL
Density, g/cm^3	0.849[a]	0.779[a]
Kinematic viscosity, cSt	3.16[b]	2.33[b]
Cetane number, -	51.9	76.6
Lower heating value, MJ/kg	43.10	43.5
C, wt. %	86.32	84.78
H, wt. %	13.63	14.95
O, wt. %	0	0.27
S, ppm	500	<5
H/C ratio (molar), -	1.88	2.10
Stoichiometric air/fuel ratio, -	14.59[c]	14.85[c]
Flash point, °C	62	69
Pour point, °C	-33	-27

[a] Measured at 20 °C; [b] Measured at 40 °C; [c] Calculated from fuel composition.
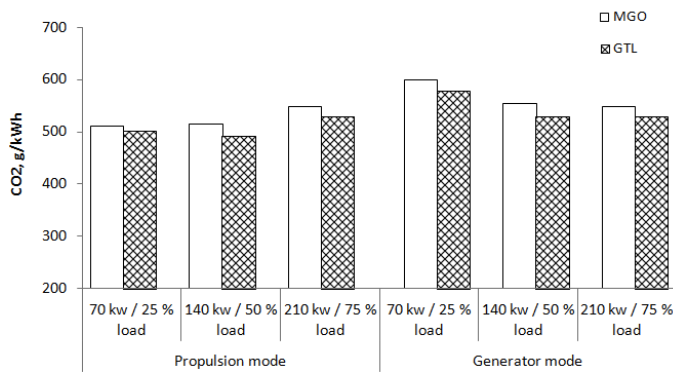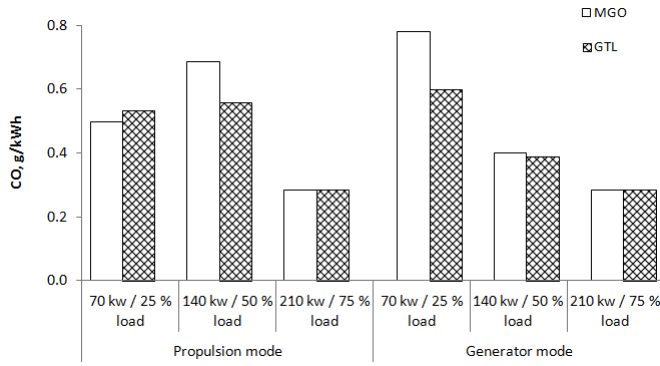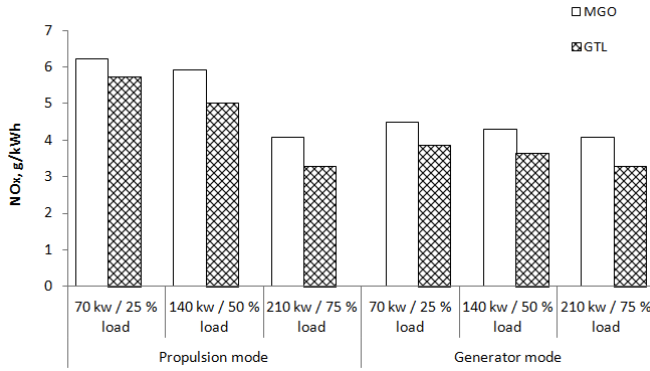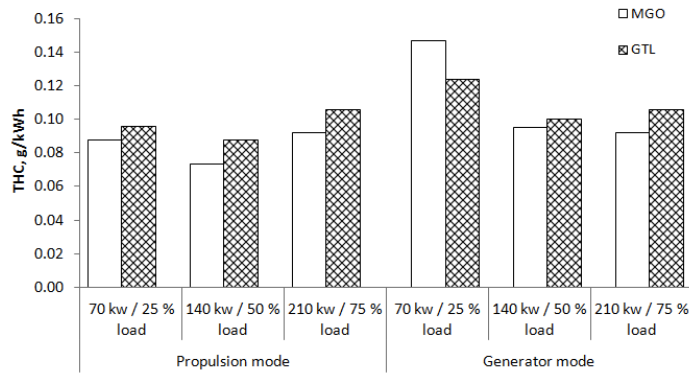
Figure 1. NO$_x$, CO, CO$_2$ and THC emissions for engine operating on MGO and GTL neat fuels under propulsion and generator modes.
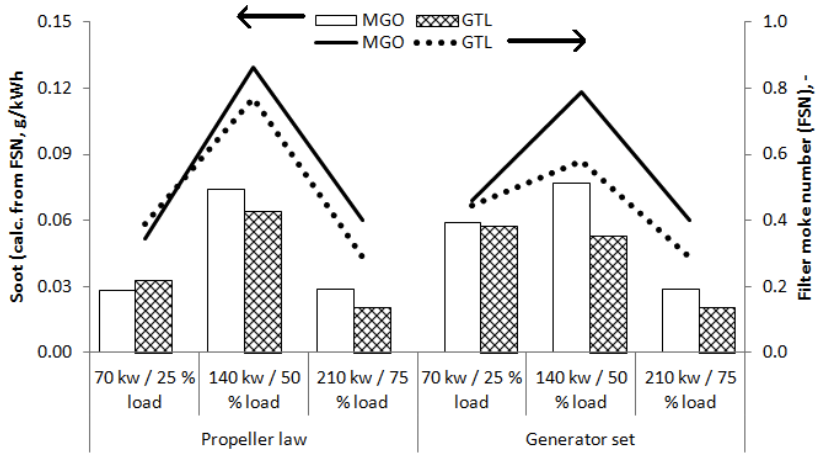
Figure 2. Filter smoke number and corresponding soot concentration calculated from FSN.
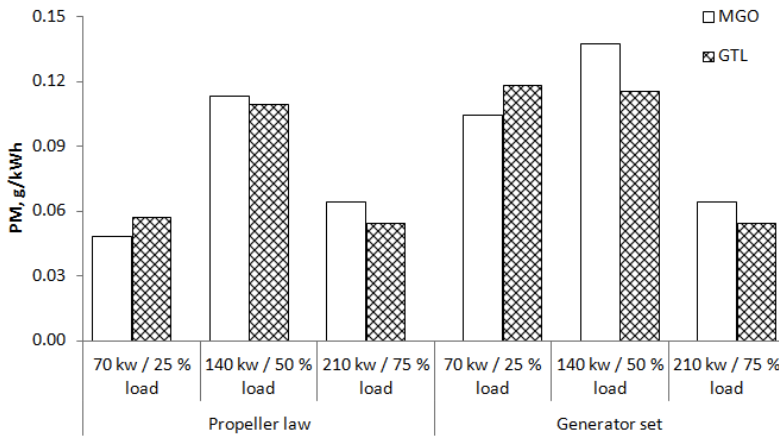
Figure 3. Particulate matter mass concentration.
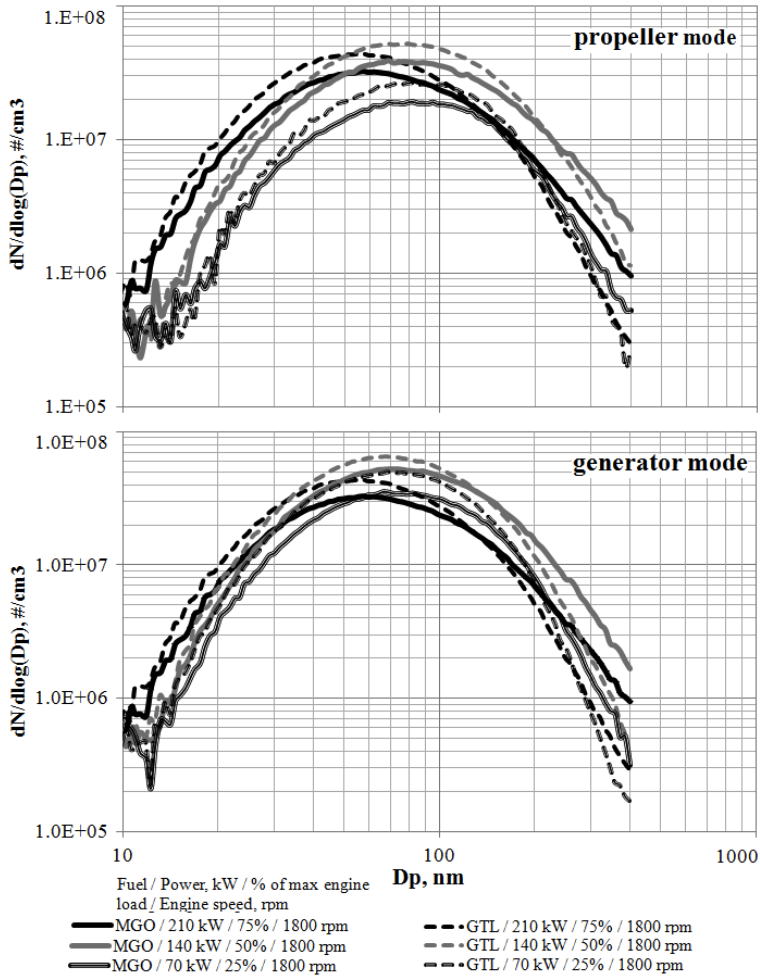
Figure 4. Particulate number size distributions for MGO and GTL fuels under propulsion and generator modes.
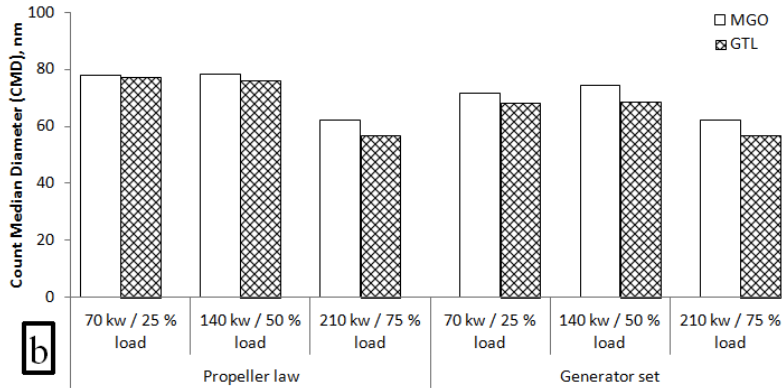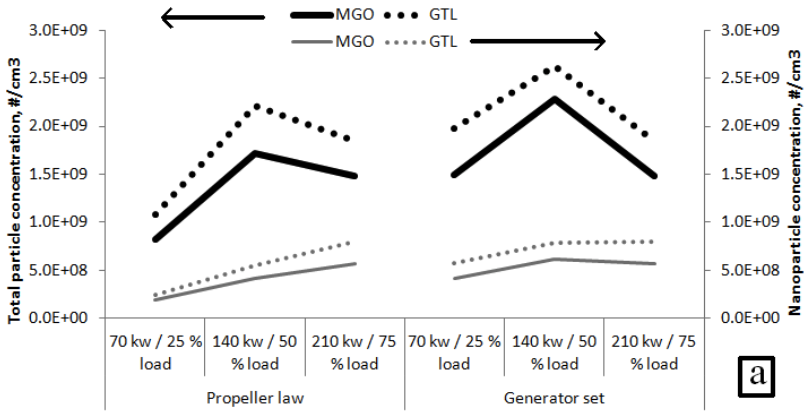
Figure 5. Exhaust particle number (a) (10 nm<D_p<400 nm) and nanoparticle (b) (D_p<50 nm) concentrations (a) and count median diameter values (b).

Appendix B: Assessment of particle losses during sampling process and exhaust sample transport

Normally, aerosol measurement requires that an aerosol sample is conveyed to a measurement device. This conveyance is accomplished by withdrawing a sample from its environment, which is in current case is exhaust system with the flowing gas stream inside, and transporting it through sample lines to the measuring device. It should be underlined here that diesel exhaust particles are formed in combustion chamber, and hence should also pass through some parts of exhaust piping until they reach the point where they are extracted. It is desirable that the sample is representative of the aerosol in its original environment and not affected by the sampling process, because such characteristics as particle mass and number concentration and size distribution should remain unchanged between the point of sampling and measurement device: this is representative sampling (Baron and Willeke, 2005). But, unfortunately, such 'ideal' scenario is only a wish, and is not feasible in real, and the sampling process is always accompanied by some degree of particle losses. Particles due to their inertia do not always enter sampling inlet representatively. Some of them can be lost from the flow, for example, by contact with wall surfaces. Inertial, diffusional, and gravitational forces are some of the affecting mechanisms that are moving particles towards a wall. So to have possibility for the correction of measurement data, all the losses should be assessed quantitatively, and at the same time sampling practices, that could introduce uncharacterized changes, should be avoided (Brockmann, 2001).

Many of the mechanisms that inhibit representative sampling depend on the aerosol particle size so that a given sampling system may exhibit representative sampling over some certain range of particle size, but not for particles larger or smaller than that range. Because larger particles are more strongly influenced by inertial and gravitational forces, and, therefore, are more difficult for representative sampling. At the same time, PM of the smaller size is more easily lost to the wall surfaces due to diffusion. If the sampled particles are charged, they can interact with electric fields near and inside the inlet. Use of conductive inlets and sampling lines can often minimize the effects of

electrical charge on particles (Brockmann, 2001). Hence, the main strategy of sampling is to minimize the losses, and trying to make sampling process close to fully representative.

Many different mechanisms are known to affect aerosol behaviour during sampling and measurement procedures. The detailed description of those mechanisms can be obtained in number of aerosol textbooks (e.g. Hinds, 1999; Baron and Willeke, 2005; Vincent, 2007), which provided the main information (basis) for current section. In general PM losses can be sub-divided into two distinct groups: 1) wall interactions with the aerosol; 2) particle dynamics and transformation during sampling (Kittelson et al., 1998). The following Table 3 summarizes the impact of various particle-wall interactions and gives recommendations how to minimize their impact, while Table 4 summarizes various losses mechanisms of PM due to different process related to particle dynamics and transformations occurring during sampling and measurement processes. Both these tables are based on the data from the works by Professor David B. Kittelson and co-workers from the University of Minnesota, USA.

Table 3:   Particle-wall interactions (Kittelson and Johnson, 1991)

Mechanism	Impact	Recommendations
Inertial impaction	Removes small number of the largest particles (represents a larger fraction of the total particulate mass) Introduces variability through unpredictable re-entrainment of deposited mass Inertial and gravitational losses are quite small for particles in 0.1-1.0 μm range	Avoid sharp changes in sample line diameter or direction Isokinetic sampling not as important for submicron particles
Electrostatic deposition	Electric charge build-up on sample lines attracts charged diesel particulate matter, causing it to deposit on line walls	Use metal sample lines to avoid electrostatic build-up Avoid Teflon sample lines, prone to large build-up of electrostatic charge

Mechanism	Impact	Recommendations
Thermophoretic deposition	Large temperature differences between exhaust gas and sample lines causes thermal driving force depositing particles on line walls Most significant losses occur during transient duty cycles	Insulate / heat sample lines to avoid large differences in temperature between lines and exhaust gas
Diffusional deposition	Diffusion for particles in the size range that represents the majority of the mass is negligible (> 0.1 μm) Diffusion for particles (< 0.03 μm) in the size range that represents the majority of number is also small, but should be considered for the smallest size ranges measured	Difficult to eliminate diffusional deposition Use short sampling lines
Gravitational deposition	Minimal impact on diesel particulate losses May introduce variability through unpredictable re-entrainment of small deposited mass	Avoid unnecessarily long horizontal sections of sample lines where large particles may settle

Table 4:   Particle dynamics and transformations (Kittelson et al., 1999)

Process	Impact
Particle coagulation	Dependent on particle size and concentration Does not affect total particle mass Causes decrease in particle number concentration and increase in particle size Increase in particle size may affect loss mechanisms May affect diesel aerosols if dilution is delayed, not critical after typical diesel exhaust dilutions Typical time constant, $t = 1/kN_0 \sim 10^9/N_0$ (s) for diesel size particles, N_0 = initial particle concentration (1/cm3) (Fuchs, 1964)
Adsorption/ Desorption	Adsorption / desorption of volatile components will affect size and mass of measured particulate matter Availability of particulate surface will affect degree of adsorption / desorption Driven by saturation ratio
Nucleation	Homogeneous nucleation may create large numbers of new particles Nucleation rates are highly nonlinear functions of saturation ratio Heterogeneous nucleation leads to the growth of existing particles

Process	Impact
Condensation/ Evaporation	Condensation / evaporation of volatile constituents will affect size and mass of measured particulate matter Affected by saturation ratio, testing conditions such as: temperature, pressure, humidity Particles formed by nucleation may grow by condensation

Particle dynamics and transformations also impact aerosol measurement, but so far they are well understood only qualitatively (Kittelson et al., 1998). Each of the mechanisms listed in Table 4 is very complicated and in current study they are not considered when correction of number (and hence, a mass) distribution is applied. At the same time, losses associated with every particle-wall interaction mechanism described in Table 3, are calculated and obtained results are used for PM data correction. Algorithm created for various losses assessment is mainly based on equations from several textbooks (Baron and Willeke, 2005; Hinds, 1999), which themselves represent a good summary of special articles overviewing each (or some combination) of the loss mechanisms individually. It should be noted that losses are calculated separately for sampling probe inlet, sampling tubes and exhaust piping (if necessary) and since losses of PM in sampling tubes and exhaust pipe system normally are affected by the same particle-wall interaction mechanisms, the losses computation algorithm only for sampling system is presented.

Losses in sampling probe inlet

In current study a thin-walled nozzle was used for sample extraction with sampling being performed isoaxially. The inlet efficiency of such nozzle is a product of the aspiration efficiency and transmission efficiency. In ideal sampling configuration, that is isoaxial isokinetic case, the particles of all sizes are sampled with efficiency close to 100%. Departure from this ideal case towards anisokinetic and anisoaxial sampling results in reduction of aspiration efficiency for larger particles so that the larger the particles, the greater the losses. Transmission losses in isokinetic, isoaxial sampling is mainly due to gravitational settling in horizontal flow and the effects of free-stream turbulence. If flow is upward or downward with respect to gravity, the transmission losses from settling will be negligible. However, the sampling velocity needs to be large compared to the particle settling velocity (Baron and Willeke, 2005). In case of

anisokinetic and anisoaxial sampling inertial deposition effects could occur; the flow can change direction in the course of entering the inlet, and hence large particles will not follow the streamlines and can deposit on the sampling inlet walls.

For the case of isoaxial sampling, which was actually utilized in this study, where exhaust gas stream velocity is U_0 and the sampling velocity is U, there is a well-known correlation for aspiration efficiency, η_{asp} (Belyaev and Levin, 1972, 1974), which showed a rather satisfactory accuracy of around 10% and a good agreement with experimental data (Stevens, 1986; Jayasekera and Davies, 1980; Davies and Subari, 1982):

$$\eta_{asp} = 1 + \left[\frac{U_0}{U} - 1\right]\left[1 - \frac{1}{1 + kStk}\right] \tag{B1}$$

for $0.18 \leq Stk \leq 2.03$ and $0.17 \leq U_0/U \leq 5.6$, where:

$$Stk = \frac{\tau U_0}{d} \tag{B2}$$

$$k = 2 + 0.617\left[\frac{U_0}{U}\right]^{-1} \tag{B3}$$

There are several works (e.g. Liu et al., 1989; Hangal and Willike, 1990) that examined inertial losses in sampling inlet. And in case of sub-isokinetic sampling, i.e. where $U_0/U > 1$, some particles, which velocity vectors directed towards the walls, will be deposited on wall surfaces and inertial transmission efficiency, $\eta_{trans.inert}$, will be less than 1, and could be defined using following formula (Liu et al., 1989):

$$\eta_{trans.inert} = \frac{1 + \left[\frac{U_0}{U} - 1\right]\Big/\left[1 + \frac{2.66}{Stk^{2/3}}\right]}{1 + \left[\frac{U_0}{U} - 1\right]\Big/\left[1 + \frac{0.418}{Stk}\right]} \tag{B4}$$

for $0.01 \le Stk \le 100$ and $1 \le U_0/U \le 10$. At the same time, some authors (e.g. Hangal and Willeke, 1990) assume no inertial transmission losses for the case of sub-isokinetic isoaxial sampling.

For the case of super-isokinetic sampling, i.e. when $U_0/U < 1$, particles are not deposited since vectors of particles velocities are not directed to the walls (Liu et al., 1989), and inertial transmission efficiency for this case is:

$$\eta_{trans.inert} = 1.0 \qquad \text{(B5)}$$

for $0.01 \le Stk \le 100$ and $0.01 \le U_0/U \le 1$. There is other opinion (Hangal and Willike, 1990) that in super-isokinetic sampling a vena contracta is formed in nozzle inlet and that turbulence in the vena contracta will deposit those particles that are contained in it.

A good overview and the procedure for the assessment of losses due to gravitational settling could be found in reference literature (e.g. Okazaki et al., 1987 a, b). It is assumed there that a particle which penetrated into the boundary layer, formed in the entrance region of the sampling system inlet, will be deposited on inside walls due to gravitational settling effects. It is well-known that the boundary layer thickness can be described by Reynolds number, $\text{Re} = Ud/\nu$ (Schlichting, 1968). At the same time, the Stokes number, based on exhaust gas velocity, $Stk = \tau U_0/d$, can be used as a characteristic parameter to assess the fraction of PM that penetrate into the boundary layer. Finally, the gravitational-settling transmission efficiency, $\eta_{trans.grav}$, for horizontal isoaxial sampling could be found (Okazaki et al., 1987 a, b):

$$\eta_{trans.grav} = \exp\left[-4.7K^{0.75}\right] \qquad \text{(B6)}$$

$$K = Z^{1/2} Stk^{1/2} \, \text{Re}^{-1/4} \qquad \text{(B7)}$$

where the gravitational deposition in the boundary layer of the inlet is characterized by the gravitational deposition parameter, Z, which is actually the ratio of particle-settling distance during the transport process in the inlet region, LV_{ts}/U, to the inlet diameter of the sampling probe, d, i.e.:

$$Z = \frac{L}{d}\frac{V_{ts}}{U} \tag{B8}$$

where L is length of the probe's inlet region.

For the case of inclined nozzle inlet, with inclination angle, θ, the equation (B6) should be slightly modified to account for the probe orientation, and transmission efficiency for gravitational settling, $\eta_{trans.grav}$, can be defined as:

$$\eta_{trans.grav} = \exp\left[-4.7K_\theta^{0.75}\right] \tag{B9}$$

$$K_\theta = Z^{1/2}Stk^{1/2}\,\mathrm{Re}^{-1/4}\cos\theta = K\cos\theta \tag{B10}$$

Hence, inlet efficiency for PM sampling is the product of aspiration efficiency, η_{asp}, inertial transmission efficiency, $\eta_{trans.inert}$, and gravitational-settling transmission efficiency, $\eta_{trans.grav}$ (which is represented by equation (B6) for horizontal tube case or by (B9) for the case of inclined sampling tube inlet), i.e.:

$$\eta_{inlet} = \eta_{asp}\eta_{trans.inert}\eta_{trans.grav} \tag{B11}$$

To summarize the aforesaid, it should be noted that overall inlet efficiency for the case of sampling with thin-walled nozzle depends on the Stokes number based on exhaust gas stream velocity and nozzle inlet diameter, the ratio of gas velocity in exhaust pipe system to the sampling gas velocity, and the sampling angle. To obtain representative sample, the sampling should be performed isoaxially and isokinetically (with iso-mean-velocity) and the Stokes number should be kept small (Brockmann, 2001).

Particle losses in sampling lines

Even with efficient entry of particles into sampling probe, some particles can be lost in the tubing and fittings between the inlet and the measuring device. Deposition in sampling tubes, i.e. the losses of sampled particles, is a result of particle-wall interactions, based on several mechanisms that are described in Table 3. Each of these mechanisms could be important, although for the case when the hot gas is sampled through the cooler tubing, the thermophoretic mechanism is becoming dominant. Taking all this into account, the sample transport system should be designed to minimize the particle losses; this is often can be accomplished by minimizing the distance and the transit time between the inlet and the destination point, so in simple wording, the transport path should be as short and straight as possible.

Gravitational settling and hence the deposition of particles on the lower wall of non-vertical line within the sampling system occurs due to gravitational force acting on PM. Correlation for gravitational settling are available in literature (e.g. Brockmann, 2001) but have different form under various tube orientations and flow regimes.

For the case of laminar flow in a horizontal straight circular tube the transport efficiency for gravitational deposition, $\eta_{tube.grav}$, can be defined using following formula (Thomas, 1958; Fuchs, 1964):

$$\eta_{tube.grav} = 1 - \frac{2}{\pi}\left[2\varepsilon\sqrt{1-\varepsilon^{2/3}} - \varepsilon^{1/3}\sqrt{1-\varepsilon^{2/3}} + \arcsin\left(\varepsilon^{1/3}\right) \right] \tag{B12}$$

$$\varepsilon = \frac{3}{4}Z = \frac{3}{4}\frac{L}{d}\frac{V_{ts}}{U} \tag{B13}$$

where Z is gravitational deposition parameter; L is length of the tube and d is inner diameter of the sampling tube.

In case of inclined tube that has an angle of inclination, θ, comparing to the horizontal tube case, the component of sedimentation velocity of particle that is perpendicular to the wall, is $V_{ts} \cos \theta$. So for gravitational deposition in a circular tube for laminar flow regime, the transport efficiency, $\eta_{tube.grav}$, can be calculated using other equation (Heyder and Gebhart, 1977), although in special case of inclined tube with $\theta = 0°$, i.e. for horizontal tube case, the following equation (B14) reduces to (B12):

$$\eta_{tube.grav} = 1 - \frac{2}{\pi} \left[2\kappa\sqrt{1-\kappa^{2/3}} - \kappa^{1/3}\sqrt{1-\kappa^{2/3}} + \arcsin\left(\kappa^{1/3}\right) \right] \tag{B14}$$

$$\kappa = \varepsilon \cos \theta = \frac{3}{4} \frac{L}{d} \frac{V_{ts}}{U} \cos \theta \tag{B15}$$

for

$$\frac{V_{ts} \sin \theta}{U} << 1 \tag{B16}$$

The losses of particles associated with gravitational settling in case of horizontal tube for turbulent flow regime originates due to a well-mixed volume through the boundary layer, and could be quantified by transport efficiency, $\eta_{tube.grav}$ (Schwendiman et al., 1975) as follows:

$$\eta_{tube.grav} = \exp\left[-\frac{4Z}{\pi}\right] = \exp\left[-\frac{dLV_{ts}}{Q}\right] \tag{B17}$$

where Q is volumetric flow rate of the gas sampled through the tube.

Similarly to laminar flow case, for inclined or vertical tube with the sampled gas under turbulent regime, the desired transport efficiency for gravitational deposition, $\eta_{tube.grav}$, can be calculated using next expression:

$$\eta_{tube.grav} = \exp\left[-\frac{4Z\cos\theta}{\pi}\right] = \exp\left[-\frac{dLV_{ts}\cos\theta}{Q}\right] \tag{B18}$$

For simplicity, the logic of choosing the appropriate equation for the correction of losses due to gravitational settling is highlighted in Table 5 below, where any particular sampling case linked to the corresponding equation for the PM transport efficiency assessment.

Table 5: Corresponding equations to assess the transport efficiency with gravitational deposition at various gas flow regimes and sampling tube orientations

	Laminar flow	**Turbulent flow**
Horizontal tube	Eq. (B12)	Eq. (B17)
Inclined (or horizontal) tube	Eq. (B14)	Eq. (B18)

The smallest particles undergoing Brownian motion have tendency for diffusion from regions with high PM concentration to ones with low concentration. The wall concentration of particles can be assumed a zero, and will act as a sink for PM, so that particles will diffuse towards the wall surfaces and be deposited on them, with diffusional transport efficiency, $\eta_{tube.diff}$, that in general can be assessed with following formula:

$$\eta_{tube.diff} = \exp\left[-\frac{\pi d L V_{diff}}{Q}\right] = \exp\left[-\xi Sh\right] \tag{B19}$$

where V_{diff} is deposition velocity for particle diffusion losses to wall surfaces, sometimes is also called mass transfer coefficient, and can be determined from the available heat and mass transfer correlations; Sh is Sherwood number ($Sh = V_{diff} d / D$), a dimensionless mass transfer coefficient, which is similar to more known Nusselt

number for heat-transfer problems (Kays et al., 2005). Sherwood number correlates well with Reynolds number ($\mathrm{Re}_{fl} = \rho_{fl} U d / \eta$) and Schmidt number ($Sc = \eta / [\rho_{fl} D]$) for both laminar and turbulent flow regimes. And then for laminar flow case (Holman, 1972):

$$Sh = 3.66 + \frac{0.0668 \dfrac{d}{L} \mathrm{Re}_{fl} \, Sc}{1 + 0.04 \left[\dfrac{d}{L} \mathrm{Re}_{fl} \, Sc \right]^{2/3}} = 3.66 + \frac{0.2672}{\xi + 0.10079 \xi^{1/3}} \tag{B20}$$

$$\xi = \frac{\pi D L}{Q} \tag{B21}$$

where L is tube length, Q is volumetric flow rate through the sampling tube, D is particle diffusion coefficient, defined as:

$$D = kTB \tag{B22}$$

In equation (B22) k is Boltzmann constant (1.38×10^{-23} N·m/K or 1.38×10^{-16} dyne·cm/K), T is absolute temperature of sampled gas; B is particle dynamic mobility, which by itself can be calculated by following equation (Baron and Willeke, 2005):

$$B = \frac{C_C}{3 \pi \eta d_p} \tag{B23}$$

With C_C as Cunningham slip correction factor used to account for non-continuum effects when calculating the drag on small particles. Several empirical formulas exist to define this parameter (e.g. Rader, 1990; Hinds, 1999; Baron and Willeke, 2005) and there is some variation between the values that could be obtained from the mentioned sources. But here a well-recognized empirical formula from a well-known textbook (Hinds, 1999) is applied, so eventually:

$$C_C = 1 + \frac{1}{pd}\Big[15.60 + 7.00\exp\big(-0.059\,pd_p\big)\Big] \tag{B24}$$

where p is the absolute pressure and d_p is particle diameter respectevely.

The equation to calculate Sherwood number for turbulent flow can be also obtained from literature (Friedlander, 1977):

$$Sh = 0.0118\,\mathrm{Re}_{fl}^{7/8}\,Sc^{1/3} \tag{B25}$$

Hence, the diffusional transport efficiency, $\eta_{tube.diff}$, for sampling tubes can be assessed using equation (B19), for which Sherwood number, Sh, for laminar flow case is computed with expression (B20) and for turbulent flow case with equation (B25) respectively.

In accordance to some sources (e.g. Guha, 1997), there are three regimes of depositions observed in turbulent tube flow. The first one is turbulent diffusion regime where turbulence influences central mixing, and Brownian diffusion is the mechanism whereby particles are transported through the laminar sublayer to the wall surface. As one might notice, this regime was already described above. The second is turbulent diffusion-eddy impaction regime and is applied to larger particles and in which particle inertia plays a role, and here the amount of particles deposited on walls increases with increasing particle size. In third regime particles are so large that their trajectories are less affected by turbulence, and turbulent deposition actually decreases slightly with the particle size increasing (Baron and Willeke, 2005). From the aforesaid, one might guess that the second two regimes are essentially referred to as turbulent inertial deposition. There were a lot experimental studies directed to investigate the enhanced particulate deposition in turbulent flow (e.g. Friedlander and Johnstone, 1957; Liu and Agarwal, 1974; Lee and Gieseke, 1994) and up to now several models of PM inertial deposition exist, which are perfectly overviewed in literature (e.g. Reynolds, 1999; Chen and Ahmadi, 1996; Ziskind et al., 1998; Guna, 1997). In current work, the transport

efficiency for the circular tube with turbulent inertial deposition, $\eta_{tube.turb.inert}$, of particles using the turbulent deposition velocity, V_t , is calculated by following formula:

$$\eta_{tube.turb.inert} = \exp\left[-\frac{\pi dL V_t}{Q}\right]$$
(B26)

Several parameters, like dimensionless turbulent deposition velocity, V_+ , and dimensionless particle relaxation time, τ_+ , are actually needed to calculate the desired efficiency for particle transport. The approach used here is taken from literature sources (Liu and Agarwal, 1974) with some later modifications (Lee and Gieseke, 1994) to account for turbulent inertial deposition, but not Brownian diffusion (Brockmann, 2001):

$$V_+ = 6 \cdot 10^{-4} \tau_+^2$$
(B27)

where

$$V_+ = 5.03 \frac{V_t}{U} \mathrm{Re}_{fl}^{1/8}$$
(B28)

$$\tau_+ = 0.0395 Stk \, \mathrm{Re}_{fl}^{3/4}$$
(B29)

Some experimental results (Liu and Agarwal, 1974) also show that dimensionless deposition velocity, V_+ , for τ_+ larger than 12.9, can be regarded as constant. So, is:

$$V_+ = 0.1 \qquad \text{for} \qquad \tau_+ > 12.9$$
(B30)

In presence of bend in sampling line system, the aerosol particles can deviate from the gas flow due to inertia and deposit on wall surface of the bend. For the flow case of laminar flow, secondary recirculation zones exist in bended sector of tube and it pushes the axial flow core to the outside of the bend and is responsible for particle deposition both on inside and outside of the bend (Baron and Willeke, 2005). In this case the characteristic parameters defining the deposition in bend are the curvature ratio, R_0 ,

determined as the radius of the bend divided by the radius of the tube, flow Reynolds number, $Re_{fl} = \rho dU/\eta$, and Stokes number formulated for the tube diameter and mean exhaust gas velocity, $Stk = \tau U/d$.

For laminar flow and an angle of tube bend (in radians), φ, the transport efficiency, $\eta_{bend.inert}$, of particles through this bend can be estimated by the following correlation based on approximation of experimental data (Crane and Evans, 1977):

$$\eta_{bend.inert} = 1 - Stk\varphi \qquad\qquad (B31)$$

For turbulent flow case the deposition in a bend can be expressed independently of the Reynolds number (Pui et al., 1987), and particles are actually deposited through the boundary layer are forming a well-mixed core at a constant rate. Hence transport efficiency, $\eta_{bend.inert}$, in this case can be estimated (with particle deposition proportional to the angle of sampling tube bend):

$$\eta_{bend.inert} = \exp\left[-2.823 Stk\varphi\right] \qquad\qquad (B32)$$

Although, it should be pointed here that for turbulent flow there are other correlations to determine the transport efficiency of aerosol particles in tube bend and two next equations correspondingly summarize the results obtained by two research groups found during literature study, i.e. equation (B33) - (Pui et al., 1987) and equation (B34) from (McFarland et al., 1997). Some variation in results is noticed, but mainly for supermicron particles. The presented formulas below are only optional (for reference) and are not used in current study:

$$\eta_{bend.inert} = 10^{-0.963 Stk} \qquad\qquad (B33)$$

$$\eta_{bend.inert} = \exp\left[\frac{4.61 + a\varphi Stk}{1 + b\varphi Stk + c\varphi Stk^2 + d\varphi^2 Stk}\right] \qquad\qquad (B34)$$

where coefficients from (B34) can be determined as:

$$a = -0.95 - 0.05686R_0 \qquad\qquad b = \frac{-0.297 - 0.0174R_0}{1 - 0.07R_0 + 0.017R_0^2}$$

$$c = -0.306 + \frac{1.895}{\sqrt{R_0}} - \frac{2.0}{R_0} \qquad\qquad d = \frac{0.131 - 0.132R_0 + 0.000383R_0^2}{1 - 0.129R_0 + 0.0136R_0^2}$$

It should be obvious to anyone that any flow constriction in sampling lines should be avoided where possible, since they cause PM losses and are also difficult to characterize. For instance, flow can be constricted by passing through valves, in-line orifices, abrupt changes in flow direction (like a tee or a cross), and changes from a large to small tube diameter (like in abrupt contraction or in case of converging tube). In case the proposed sampling system should have several of the mentioned above features, particle transport should be characterized experimentally over a range of applicable operating conditions. All the listed flow constrictions should be avoided (as well as sudden expansions, which can cause the appearance of eddies, from which the deposition is extremely difficult to characterize) and there were none of them actually in current study, but for reference purposes, the particle transport efficiency through the pipe abrupt contraction can be determined as follows (Muyshondt et al., 1996):

$$\eta_{cont.inert} = 1 - \frac{1}{1 + \left(\dfrac{2Stk\left[1 - \left(\dfrac{d_0}{d_i}\right)^2\right]}{3.14\exp\left(-0.0185\theta\right)} \right)} \qquad\qquad (B35)$$

where Stk is Stokes number based on the small diameter tube and the mean exhaust gas velocity ($Stk = \tau U / d_0$), θ is the contraction angle in degrees, and (d_0 / d_i) is the tube diameter ratio.

The formula (B35) fits the experimental data well and is mathematically simpler than other correlations found in literature (e.g. Ye and Pui, 1990; Chen and Pui, 1996), so it is advised to used in appropriate cases (Baron and Willeke, 2005).

Electrostatic forces can also cause losses of particles during sampling. Even in neutral (on average) aerosol, some particles are charged, because of the diffusion of ions to the particles. Particles can be also charged by the mechanism that produces them. Static charge in sampling lines or an externally imposed electrical field in the line can produce particle deposition. So these effects should be avoided, and in metal or electrically conductive lines set up normally obviate this problem. In current work stainless steel tubes have been mainly used; additionally some sections made of Tygon were also applied where steel pipe set up was not possible. It should be known that Tygon is an acceptable substitute of steel (Liu et al., 1985).

If temperature gradient is established in gas, an aerosol particle in that gas experiences a force in the direction of decreasing temperature. The movement of the particle that results from that force is called thermophoresis (Hinds, 1999). The magnitude of this force depends on number of parameters like particle properties and temperature gradient. Particles can be deposited on wall surfaces due to the thermophoresis when a cold surface is proximate to a hot (or warm) gas. The thermophoretic velocity, V_{th}, of particles is the velocity that is achieved by setting the balance between the thermophoretic force and drag force. And it is independent of particle size for particles much larger than the gas molecule mean free path (continuum-regime particle), i.e. $d_p \gg \lambda$, and for particles much smaller than the gas molecule mean free path (free-molecule regime), i.e. $d_p \ll \lambda$, and is defined correspondingly by following equations (Friedlander, 1977):

$$V_{th} = \frac{2\left(\dfrac{k_g}{k_p}\right)k_g \nabla T}{5p\left[1 + 2\dfrac{k_g}{k_p}\right]} \qquad \text{in continuum regime} \qquad (B36)$$

$$V_{th} = \frac{3\nu \nabla T}{4\left[1 + \pi \frac{0.9}{8}\right] T} \qquad \text{in free-molecule regime} \qquad (B37)$$

where V_{th} is thermophoretic velocity, k_g and k_p are thermal conductivity of the gas and the particle respectevely, p is pressure in sampling lines, T is temperature of sampled exhaust gas, ν is kinematic viscosity of the gas, and finally ∇T is temperature gradient in sampling tubes.

There is other expression for thermophoretic velocity, V_{th}, which covers all particle sizes, i.e. can be used for both continuum and free-molecule regimes. It can be found in literature (Talbot et al., 1980), but has not been applied in current thesis:

$$V_{th} = \frac{2C_S \nu \left[\frac{k_g}{k_p} + C_t Kn\right] C\left(Kn\right)}{\left(1 + 3C_m Kn\right)\left[1 + 2\frac{k_g}{k_p} + 2C_t Kn\right]} \frac{\nabla T}{T} \qquad (B38)$$

where coefficients: $C_s = 1.13$, $C_t = 2.63$, $C_m = 1.14$; Kn is particle Knudsen number ($Kn = 2\lambda / d_p$), and $C\left(Kn\right)$ is slip correction factor.

Hence, the transport efficiency in turbulent flow case in tube with thermophoretic deposition, $\eta_{tube.th}$, can be assessed with following equation utilizing the quantity of thermophoretic velocity defined by (B36) and (B37):

$$\eta_{tube.th} = \exp\left[-\frac{\pi dL V_{th}}{Q}\right] \qquad (B39)$$

For laminar flow case at the same time, the flow and temperature gradient conditions become more involved, and no expression exists for particle transport efficiency.

Estimation of losses related to thermophoresis is not a straightforward operation, since it might be that particle thermal conductivity is not exactly known and also it is not so obvious to determine the correct value of temperature gradient (Baron and Willeke, 2005). Therefore, it is advised to heat the sampling lines to the gas temperature or cool the gas to the line temperature by diluting it to avoid losses due to the thermophoresis effects. In current study, as it was already described in previous sections, the sampling lines were heated to exhaust gas temperature or even higher, and one of the reason for this was the minimization of thermophoretic forces acting on aerosol particles under consideration.

For calculation of the overall transport efficiency, $\eta_{transport}$, of aerosol particles through the sampling system, it is needed to take the product (in other words, to multiply) of the transport efficiencies in each flow element for each mechanism. Hence, number of flow elements in sampling system should be minimized and for each element, the transport efficiency can be assessed as:

$$\eta_{transport} = \eta_{tube.grav}\eta_{tube.diff}\eta_{tube.turb.inert}\eta_{bend.inert}\eta_{cont.inert}\eta_{tube.th} \tag{B40}$$

where $\eta_{tube.grav}$ is transport efficiency for gravitational deposition, $\eta_{tube.diff}$ is diffusional transport efficiency, $\eta_{tube.turb.inert}$ is transport efficiency for a tube with turbulent inertial deposition, $\eta_{bend.inert}$ is the transport efficiency of particles through the bend, $\eta_{cont.inert}$ is transport efficiency for particles undergoing inertial deposition in a contraction, and finally $\eta_{tube.th}$ is thermophoretic deposition. All these efficiencies can be calculated using the corresponding formulas described above, but for the appropriate conditions.

In the sampling system used in current study, the number of bends was minimized, and the radiuses of these bends were rather big to neglect losses associated with inertial deposition in bends, so $\eta_{bend.inert} = 1$, as well there were no contractions in sampling tubes and they were also heated to temperature higher than gas temperature, so it can be

assumed that $\eta_{cont.inert} = 1$ and $\eta_{tube.th} = 1$ respectively. So for this work equation (B40) can be reduced to:

$$\eta_{transport} = \eta_{tube.grav}\eta_{tube.diff}\eta_{tube.turb.inert} \tag{B41}$$

It should be also mentioned here that the same approach can be also applied if one wants to calculate the particle losses during transport of aerosol in exhaust pipe (for example, from combustion chamber till the sampling point location). In that case the transport efficiency throughout the exhaust system will be a product of overall efficiencies in all flow elements comprising tailpipe system, and basically this transport efficiency for any element can be assessed with general equation (B40). Following this logic, the amount of particles produced inside the cylinder of ICE can be computed from the measured number size distribution, applying correction for particle losses in exhaust pipe system, sampling inlet and sampling tubes.

References for Appendix B

Baron, P.A. and Willeke, K. (2005). *Aerosol measurement: Principles, techniques, and applications, 2nd edition*. New Jersey: John Wiley & Sons Inc., 1131 pp.

Belyaev, S.P. and Levin, L.M. (1972). Investigation of aerosol aspiration by photographing particle tracks under flash illumination. *Journal of Aerosol Science*, 3, 127-140.

Belyaev, S.P. and Levin, L.M. (1974). Techniques for sollection of representative aerosol samples. *Journal of Aerosol Science*, 5, 325-338.

Brockmann, J.E. (2001). Sampling and transport of aerosols. In *Aerosol Measurement: Principles, Techniques, and Applications, 2nd Edition*. Baron, P.A., Willeke, K. (editors). Wiley-InterScience Inc., pp. 143-195.

Chen, D.-R. and Pui, D.Y.H. (1995). Numerical and experimental studies of particle deposition in a tube with local contraction – Laminar flow regime. *Journal of Aerosol Science*, 26(4), 563-574.

Chen, Q. and Ahmadi, G. (1997). Deposition of particles in turbulent pipe flow. *Journal of Aerosol Science*, 28, 789-796.

Crane, R.L. and Evans, R.L. (1977). Inertial deposition of particles in a bent pipe. *Journal of Aerosol Science*, 8, 161-170.

Davies, C.N. and Subari, M. (1982). Aspiration above wind velocity of aerosols with thin-walled nozzles facing and at right angles to the wind direction. *Journal of Aerosol Science*, 13, 59-71.

Friedlander, S.K. (1977). *Smoke, dust, and haze*. New York: John Wiley & Sons Inc. 317 pp.

Friedlander, S.K. and Johnstone, H.F. (1957). Deposition of suspended particles from turbulent gas stream. *Industrial and Engineering Chemistry Research*, 49, 1151-1156.

Fuchs, N.A. (1964). *The mechanics of aerosols*. Oxford: Pergamon. 408 pp.

Guha, A. (1997). A unified Eulerian theory of turbulent deposition to smooth and rough surfaces. *Journal of Aerosol Science*, 28, 1517-1537.

Hangal, S. and Willeke, K. (1990). Aspiration efficiency: Unified model for all forward sampling angles. *Environmental Science and Technology*, 24, 688-691.

Heyder, J. and Gebhart, J. (1977). Gravitational deposition of particles from laminar aerosol flow through inclined circular tubes. *Journal of Aerosol Science*, 8, 289-295.

Hinds, W.C. (1999). *Aerosol technology: Properties, behavior, and measurement of airborne particles, 2nd edition*. Canada: John Wiley & Sons Inc. 483 pp

Holman, J.P. (1972). *Heat transfer*. New York: McGraw-Hill. 462 pp.

Jayasekera, P.N. and Davies, C.N. (1980). Aspiration below wind velocity of aerosols with sharp edged nozzles facing the wind. *Journal of Aerosol Science*, 11, 535-547.

Kays, W.M., Crawford, M.E., Weigand, B. (2005). *Convective heat and mass transfer, 4th edition*. McGraw-Hill Education (Asia), 546 pp.

Kittelson, D.B. and Johnson, J.H. (1991). Variability in particle emission measurements in the heavy duty transient test. . *SAE Technical Paper* 910738.

Kittelson, D.B., Watts, W.F., Arnold, M. (1998). *Review of diesel particulate matter sampling methods*. Supplemental report #2: Aerosol dynamics, laboratory and on-road studies. Minneapolis, MN, USA: University of Minnesota. 59 pp.

Kittelson, D.B., Watts, W.F., Arnold, M. (1999). *Review of diesel particulate matter sampling methods*. Final report. Minneapolis, MN, USA: University of Minnesota. 64 pp.

Lee, K.W. and Gieseke, J.A. (1994). Deposition of particles in turbulent pipe flows. *Journal of Aerosol Science,* 25, 699-709.

Liu, B.Y.H. and Agarwal, J.K. (1974). Experimental observation of aerosol deposition in turbulent flow. *Journal of Aerosol Science,* 5, 145-155.

Liu, B.Y.H. Zhang, Z.Q., Kuehn, T.H. (1989). A numerical study of inertial errors in anisokinetic sampling. *Journal of Aerosol Science,* 20, 367-380.

Liu, B.Y.H., Pui, D.Y.H., Rubow, K.L., Szymanski, W.W. (1985). Electrostatic effects in aerosol sampling and filtration. *Annals of Occupational Hygiene*, 29, 251-269.

McFarland, A.R., Gong, H., Muyshondt, A., Wente, W.B., Anand, N.K. (1997). Aerosol deposition in bends with turbulent flow. *Environmental Science and Technology*, 31, 3371-3377.

Muyshondt, A., McFarland, A.R., Anand, N.K. (1996). Deposition of aerosol particles in contraction fittings. *Aerosol Science and Technology*, 24, 205-216.

Okazaki, K., Wiener, R.W., Willeke, K. (1987a). The combined effect of aspiration and transmission on aerosol sampling accuracy for horizontal isoaxial sampling. *Atmospheric Environment*, 21, 1181-1185.

Okazaki, K., Wiener, R.W., Willeke, K. (1987b). Isoaxial aerosol sampling: Nondimensional representation of overall sampling efficiency. *Environmental Science and Technology*, 21, 178-182.

Pui, D.Y.H., Romay-Novas, F., Liu, B.Y.H. (1987). Experimental study of particle deposition in bends of circular cross section. *Aerosol Science and Technology*, 7, 301-305.

Rader, D.J. (1990). Momentum slip correction factor for small particles in nine common gases. *Journal of Aerosol Science*, 21, 161-168.

Reynolds, A.M. (1999). Lagrangian stochastic model for heavy particle deposition. *Journal of Colloid and Interface Science*, 215, 85-91.

Schlichting, H. (1968). *Boundary layer theory, 6th edition*. New York: McGraw-Hill Inc.

Schwendiman, L.C., Stegen, G.E., Glissmeyer, J.A. (1975). Report BNWL-SA-5138. Richland, WA: Batelle Pacific Northwest Laboratory.

Stevens, D.C. (1986). Review of aspiration coefficients of thin-walled sampling nozzle. *Journal of Aerosol Science,* 17, 729-743.

Talbot, L., Cheng, R.K., Schefer, R.W., Willis, D.R. (1980). Thermophoresis of particles in a heated boundary layer. *Journal of Fluid Mechanics*, 101, 737-758.

Thomas, J.W. (1958). Gravity settling of particles in a horizontal tube. *Journal of the Air Pollution Control Association,* 8, 32–34.

Vincent, J.H. (2007). *Aerosol sampling: Science, standards, instrumentation and applications*. Chichester, England: John Wiley & Sons Ltd., 616 pp.

Ye, Y. and Pui, D.Y.H. (1990). Particle deposition in a tube with abrupt contraction. *Journal of Aerosol Science,* 21, 29-40.

Ziskind, G., Fichman, M., Gutfinger, C. (1998). Effects of shear on particle motion near a surface – Application to resuspension. *Journal of Aerosol Science,* 29, 323-338.

Appendix C: Previous PhD thesises at Marine Technology Department of NTNU

Report No.	Author	Title
	Kavlie, Dag	Optimization of Plane Elastic Grillages, 1967
	Hansen, Hans R.	Man-Machine Communication and Data-Storage Methods in Ship Structural Design, 1971
	Gisvold, Kaare M.	A Method for non-linear mixed -integer programming and its Application to Design Problems, 1971
	Lund, Sverre	Tanker Frame Optimalization by means of SUMT-Transformation and Behaviour Models, 1971
	Vinje, Tor	On Vibration of Spherical Shells Interacting with Fluid, 1972
	Lorentz, Jan D.	Tank Arrangement for Crude Oil Carriers in Accordance with the new Anti-Pollution Regulations, 1975
	Carlsen, Carl A.	Computer-Aided Design of Tanker Structures, 1975
	Larsen, Carl M.	Static and Dynamic Analysis of Offshore Pipelines during Installation, 1976
UR-79-01	Brigt Hatlestad, MK	The finite element method used in a fatigue evaluation of fixed offshore platforms. (Dr.Ing. Thesis)
UR-79-02	Erik Pettersen, MK	Analysis and design of cellular structures. (Dr.Ing. Thesis)
UR-79-03	Sverre Valsgård, MK	Finite difference and finite element methods applied to nonlinear analysis of plated structures. (Dr.Ing. Thesis)
UR-79-04	Nils T. Nordsve, MK	Finite element collapse analysis of structural members considering imperfections and stresses due to fabrication. (Dr.Ing. Thesis)
UR-79-05	Ivar J. Fylling, MK	Analysis of towline forces in ocean towing systems. (Dr.Ing. Thesis)
UR-80-06	Nils Sandsmark, MM	Analysis of Stationary and Transient Heat Conduction by the Use of the Finite Element Method. (Dr.Ing. Thesis)
UR-80-09	Sverre Haver, MK	Analysis of uncertainties related to the stochastic modeling of ocean waves. (Dr.Ing. Thesis)
UR-81-15	Odland, Jonas	On the Strength of welded Ring stiffened cylindrical Shells primarily subjected to axial Compression
UR-82-17	Engesvik, Knut	Analysis of Uncertainties in the fatigue Capacity of Welded Joints
UR-82-18	Rye, Henrik	Ocean wave groups
UR-83-30	Eide, Oddvar Inge	On Cumulative Fatigue Damage in Steel Welded Joints
UR-83-33	Mo, Olav	Stochastic Time Domain Analysis of Slender Offshore Structures
UR-83-34	Amdahl, Jørgen	Energy absorption in Ship-platform impacts
UR-84-37	Mørch, Morten	Motions and mooring forces of semi submersibles as determined by full-scale measurements and theoretical analysis
UR-84-38	Soares, C. Guedes	Probabilistic models for load effects in ship structures
UR-84-39	Aarsnes, Jan V.	Current forces on ships
UR-84-40	Czujko, Jerzy	Collapse Analysis of Plates subjected to Biaxial Compression and Lateral Load
UR-85-46	Alf G. Engseth, MK	Finite element collapse analysis of tubular steel offshore structures. (Dr.Ing. Thesis)
UR-86-47	Dengody Sheshappa, MP	A Computer Design Model for Optimizing Fishing Vessel Designs Based on Techno-Economic Analysis. (Dr.Ing. Thesis)
UR-86-48	Vidar Aanesland, MH	A Theoretical and Numerical Study of Ship Wave Resistance. (Dr.Ing. Thesis)

UR-86-49	Heinz-Joachim Wessel, MK	Fracture Mechanics Analysis of Crack Growth in Plate Girders. (Dr.Ing. Thesis)
UR-86-50	Jon Taby, MK	Ultimate and Post-ultimate Strength of Dented Tubular Members. (Dr.Ing. Thesis)
UR-86-51	Walter Lian, MH	A Numerical Study of Two-Dimensional Separated Flow Past Bluff Bodies at Moderate KC-Numbers. (Dr.Ing. Thesis)
UR-86-52	Bjørn Sortland, MH	Force Measurements in Oscillating Flow on Ship Sections and Circular Cylinders in a U-Tube Water Tank. (Dr.Ing. Thesis)
UR-86-53	Kurt Strand, MM	A System Dynamic Approach to One-dimensional Fluid Flow. (Dr.Ing. Thesis)
UR-86-54	Arne Edvin Løken, MH	Three Dimensional Second Order Hydrodynamic Effects on Ocean Structures in Waves. (Dr.Ing. Thesis)
UR-86-55	Sigurd Falch, MH	A Numerical Study of Slamming of Two-Dimensional Bodies. (Dr.Ing. Thesis)
UR-87-56	Arne Braathen, MH	Application of a Vortex Tracking Method to the Prediction of Roll Damping of a Two-Dimension Floating Body. (Dr.Ing. Thesis)
UR-87-57	Bernt Leira, MK	Gaussian Vector Processes for Reliability Analysis involving Wave-Induced Load Effects. (Dr.Ing. Thesis)
UR-87-58	Magnus Småvik, MM	Thermal Load and Process Characteristics in a Two-Stroke Diesel Engine with Thermal Barriers (in Norwegian). (Dr.Ing. Thesis)
MTA-88-59	Bernt Arild Bremdal, MP	An Investigation of Marine Installation Processes – A Knowledge - Based Planning Approach. (Dr.Ing. Thesis)
MTA-88-60	Xu Jun, MK	Non-linear Dynamic Analysis of Space-framed Offshore Structures. (Dr.Ing. Thesis)
MTA-89-61	Gang Miao, MH	Hydrodynamic Forces and Dynamic Responses of Circular Cylinders in Wave Zones. (Dr.Ing. Thesis)
MTA-89-62	Martin Greenhow, MH	Linear and Non-Linear Studies of Waves and Floating Bodies. Part I and Part II. (Dr.Techn. Thesis)
MTA-89-63	Chang Li, MH	Force Coefficients of Spheres and Cubes in Oscillatory Flow with and without Current. (Dr.Ing. Thesis
MTA-89-64	Hu Ying, MP	A Study of Marketing and Design in Development of Marine Transport Systems. (Dr.Ing. Thesis)
MTA-89-65	Arild Jæger, MH	Seakeeping, Dynamic Stability and Performance of a Wedge Shaped Planing Hull. (Dr.Ing. Thesis)
MTA-89-66	Chan Siu Hung, MM	The dynamic characteristics of tilting-pad bearings
MTA-89-67	Kim Wikstrøm, MP	Analysis av projekteringen for ett offshore projekt. (Licenciat-avhandling)
MTA-89-68	Jiao Guoyang, MK	Reliability Analysis of Crack Growth under Random Loading, considering Model Updating. (Dr.Ing. Thesis)
MTA-89-69	Arnt Olufsen, MK	Uncertainty and Reliability Analysis of Fixed Offshore Structures. (Dr.Ing. Thesis)
MTA-89-70	Wu Yu-Lin, MR	System Reliability Analyses of Offshore Structures using improved Truss and Beam Models. (Dr.Ing. Thesis)
MTA-90-71	Jan Roger Hoff, MH	Three-dimensional Green function of a vessel with forward speed in waves. (Dr.Ing. Thesis)
MTA-90-72	Rong Zhao, MH	Slow-Drift Motions of a Moored Two-Dimensional Body in Irregular Waves. (Dr.Ing. Thesis)
MTA-90-73	Atle Minsaas, MP	Economical Risk Analysis. (Dr.Ing. Thesis)
MTA-90-74	Knut-Aril Farnes, MK	Long-term Statistics of Response in Non-linear Marine Structures. (Dr.Ing. Thesis)
MTA-90-75	Torbjørn Sotberg, MK	Application of Reliability Methods for Safety Assessment of Submarine Pipelines. (Dr.Ing. Thesis)
MTA-90-76	Zeuthen, Steffen, MP	SEAMAID. A computational model of the design process in a constraint-based

		logic programming environment. An example from the offshore domain. (Dr.Ing. Thesis)
MTA-91-77	Haagensen, Sven, MM	Fuel Dependant Cyclic Variability in a Spark Ignition Engine - An Optical Approach. (Dr.Ing. Thesis)
MTA-91-78	Løland, Geir, MH	Current forces on and flow through fish farms. (Dr.Ing. Thesis)
MTA-91-79	Hoen, Christopher, MK	System Identification of Structures Excited by Stochastic Load Processes. (Dr.Ing. Thesis)
MTA-91-80	Haugen, Stein, MK	Probabilistic Evaluation of Frequency of Collision between Ships and Offshore Platforms. (Dr.Ing. Thesis)
MTA-91-81	Sødahl, Nils, MK	Methods for Design and Analysis of Flexible Risers. (Dr.Ing. Thesis)
MTA-91-82	Ormberg, Harald, MK	Non-linear Response Analysis of Floating Fish Farm Systems. (Dr.Ing. Thesis)
MTA-91-83	Marley, Mark J., MK	Time Variant Reliability under Fatigue Degradation. (Dr.Ing. Thesis)
MTA-91-84	Krokstad, Jørgen R., MH	Second-order Loads in Multidirectional Seas. (Dr.Ing. Thesis)
MTA-91-85	Molteberg, Gunnar A., MM	The Application of System Identification Techniques to Performance Monitoring of Four Stroke Turbocharged Diesel Engines. (Dr.Ing. Thesis)
MTA-92-86	Mørch, Hans Jørgen Bjelke, MH	Aspects of Hydrofoil Design: with Emphasis on Hydrofoil Interaction in Calm Water. (Dr.Ing. Thesis)
MTA-92-87	Chan Siu Hung, MM	Nonlinear Analysis of Rotordynamic Instabilities in Highspeed Turbomachinery. (Dr.Ing. Thesis)
MTA-92-88	Bessason, Bjarni, MK	Assessment of Earthquake Loading and Response of Seismically Isolated Bridges. (Dr.Ing. Thesis)
MTA-92-89	Langli, Geir, MP	Improving Operational Safety through exploitation of Design Knowledge - an investigation of offshore platform safety. (Dr.Ing. Thesis)
MTA-92-90	Sævik, Svein, MK	On Stresses and Fatigue in Flexible Pipes. (Dr.Ing. Thesis)
MTA-92-91	Ask, Tor Ø., MM	Ignition and Flame Growth in Lean Gas-Air Mixtures. An Experimental Study with a Schlieren System. (Dr.Ing. Thesis)
MTA-86-92	Hessen, Gunnar, MK	Fracture Mechanics Analysis of Stiffened Tubular Members. (Dr.Ing. Thesis)
MTA-93-93	Steinebach, Christian, MM	Knowledge Based Systems for Diagnosis of Rotating Machinery. (Dr.Ing. Thesis)
MTA-93-94	Dalane, Jan Inge, MK	System Reliability in Design and Maintenance of Fixed Offshore Structures. (Dr.Ing. Thesis)
MTA-93-95	Steen, Sverre, MH	Cobblestone Effect on SES. (Dr.Ing. Thesis)
MTA-93-96	Karunakaran, Daniel, MK	Nonlinear Dynamic Response and Reliability Analysis of Drag-dominated Offshore Platforms. (Dr.Ing. Thesis)
MTA-93-97	Hagen, Arnulf, MP	The Framework of a Design Process Language. (Dr.Ing. Thesis)
MTA-93-98	Nordrik, Rune, MM	Investigation of Spark Ignition and Autoignition in Methane and Air Using Computational Fluid Dynamics and Chemical Reaction Kinetics. A Numerical Study of Ignition Processes in Internal Combustion Engines. (Dr.Ing. Thesis)
MTA-94-99	Passano, Elizabeth, MK	Efficient Analysis of Nonlinear Slender Marine Structures. (Dr.Ing. Thesis)
MTA-94-100	Kvålsvold, Jan, MH	Hydroelastic Modelling of Wetdeck Slamming on Multihull Vessels. (Dr.Ing. Thesis)
MTA-94-102	Bech, Sidsel M., MK	Experimental and Numerical Determination of Stiffness and Strength of GRP/PVC Sandwich Structures. (Dr.Ing. Thesis)
MTA-95-103	Paulsen, Hallvard, MM	A Study of Transient Jet and Spray using a Schlieren Method and Digital Image Processing. (Dr.Ing. Thesis)
MTA-95-104	Hovde, Geir Olav, MK	Fatigue and Overload Reliability of Offshore Structural Systems, Considering the Effect of Inspection and Repair. (Dr.Ing. Thesis)
MTA-95-105	Wang, Xiaozhi, MK	Reliability Analysis of Production Ships with Emphasis on Load Combination and Ultimate Strength. (Dr.Ing. Thesis)

MTA-95-106	Ulstein, Tore, MH	Nonlinear Effects of a Flexible Stern Seal Bag on Cobblestone Oscillations of an SES. (Dr.Ing. Thesis)
MTA-95-107	Solaas, Frøydis, MH	Analytical and Numerical Studies of Sloshing in Tanks. (Dr.Ing. Thesis)
MTA-95-108	Hellan, Øyvind, MK	Nonlinear Pushover and Cyclic Analyses in Ultimate Limit State Design and Reassessment of Tubular Steel Offshore Structures. (Dr.Ing. Thesis)
MTA-95-109	Hermundstad, Ole A., MK	Theoretical and Experimental Hydroelastic Analysis of High Speed Vessels. (Dr.Ing. Thesis)
MTA-96-110	Bratland, Anne K., MH	Wave-Current Interaction Effects on Large-Volume Bodies in Water of Finite Depth. (Dr.Ing. Thesis)
MTA-96-111	Herfjord, Kjell, MH	A Study of Two-dimensional Separated Flow by a Combination of the Finite Element Method and Navier-Stokes Equations. (Dr.Ing. Thesis)
MTA-96-112	Æsøy, Vilmar, MM	Hot Surface Assisted Compression Ignition in a Direct Injection Natural Gas Engine. (Dr.Ing. Thesis)
MTA-96-113	Eknes, Monika L., MK	Escalation Scenarios Initiated by Gas Explosions on Offshore Installations. (Dr.Ing. Thesis)
MTA-96-114	Erikstad, Stein O., MP	A Decision Support Model for Preliminary Ship Design. (Dr.Ing. Thesis)
MTA-96-115	Pedersen, Egil, MH	A Nautical Study of Towed Marine Seismic Streamer Cable Configurations. (Dr.Ing. Thesis)
MTA-97-116	Moksnes, Paul O., MM	Modelling Two-Phase Thermo-Fluid Systems Using Bond Graphs. (Dr.Ing. Thesis)
MTA-97-117	Halse, Karl H., MK	On Vortex Shedding and Prediction of Vortex-Induced Vibrations of Circular Cylinders. (Dr.Ing. Thesis)
MTA-97-118	Igland, Ragnar T., MK	Reliability Analysis of Pipelines during Laying, considering Ultimate Strength under Combined Loads. (Dr.Ing. Thesis)
MTA-97-119	Pedersen, Hans-P., MP	Levendefiskteknologi for fiskefartøy. (Dr.Ing. Thesis)
MTA-98-120	Vikestad, Kyrre, MK	Multi-Frequency Response of a Cylinder Subjected to Vortex Shedding and Support Motions. (Dr.Ing. Thesis)
MTA-98-121	Azadi, Mohammad R. E., MK	Analysis of Static and Dynamic Pile-Soil-Jacket Behaviour. (Dr.Ing. Thesis)
MTA-98-122	Ulltang, Terje, MP	A Communication Model for Product Information. (Dr.Ing. Thesis)
MTA-98-123	Torbergsen, Erik, MM	Impeller/Diffuser Interaction Forces in Centrifugal Pumps. (Dr.Ing. Thesis)
MTA-98-124	Hansen, Edmond, MH	A Discrete Element Model to Study Marginal Ice Zone Dynamics and the Behaviour of Vessels Moored in Broken Ice. (Dr.Ing. Thesis)
MTA-98-125	Videiro, Paulo M., MK	Reliability Based Design of Marine Structures. (Dr.Ing. Thesis)
MTA-99-126	Mainçon, Philippe, MK	Fatigue Reliability of Long Welds Application to Titanium Risers. (Dr.Ing. Thesis)
MTA-99-127	Haugen, Elin M., MH	Hydroelastic Analysis of Slamming on Stiffened Plates with Application to Catamaran Wetdecks. (Dr.Ing. Thesis)
MTA-99-128	Langhelle, Nina K., MK	Experimental Validation and Calibration of Nonlinear Finite Element Models for Use in Design of Aluminium Structures Exposed to Fire. (Dr.Ing. Thesis)
MTA-99-129	Berstad, Are J., MK	Calculation of Fatigue Damage in Ship Structures. (Dr.Ing. Thesis)
MTA-99-130	Andersen, Trond M., MM	Short Term Maintenance Planning. (Dr.Ing. Thesis)
MTA-99-131	Tveiten, Bård Wathne, MK	Fatigue Assessment of Welded Aluminium Ship Details. (Dr.Ing. Thesis)
MTA-99-132	Søreide, Fredrik, MP	Applications of underwater technology in deep water archaeology. Principles and practice. (Dr.Ing. Thesis)
MTA-99-133	Tønnessen, Rune, MH	A Finite Element Method Applied to Unsteady Viscous Flow Around 2D Blunt Bodies With Sharp Corners. (Dr.Ing. Thesis)

MTA-99-134	Elvekrok, Dag R., MP	Engineering Integration in Field Development Projects in the Norwegian Oil and Gas Industry. The Supplier Management of Norne. (Dr.Ing. Thesis)
MTA-99-135	Fagerholt, Kjetil, MP	Optimeringsbaserte Metoder for Ruteplanlegging innen skipsfart. (Dr.Ing. Thesis)
MTA-99-136	Bysveen, Marie, MM	Visualization in Two Directions on a Dynamic Combustion Rig for Studies of Fuel Quality. (Dr.Ing. Thesis)
MTA-2000-137	Storteig, Eskild, MM	Dynamic characteristics and leakage performance of liquid annular seals in centrifugal pumps. (Dr.Ing. Thesis)
MTA-2000-138	Sagli, Gro, MK	Model uncertainty and simplified estimates of long term extremes of hull girder loads in ships. (Dr.Ing. Thesis)
MTA-2000-139	Tronstad, Harald, MK	Nonlinear analysis and design of cable net structures like fishing gear based on the finite element method. (Dr.Ing. Thesis)
MTA-2000-140	Kroneberg, André, MP	Innovation in shipping by using scenarios. (Dr.Ing. Thesis)
MTA-2000-141	Haslum, Herbjørn Alf, MH	Simplified methods applied to nonlinear motion of spar platforms. (Dr.Ing. Thesis)
MTA-2001-142	Samdal, Ole Johan, MM	Modelling of Degradation Mechanisms and Stressor Interaction on Static Mechanical Equipment Residual Lifetime. (Dr.Ing. Thesis)
MTA-2001-143	Baarholm, Rolf Jarle, MH	Theoretical and experimental studies of wave impact underneath decks of offshore platforms. (Dr.Ing. Thesis)
MTA-2001-144	Wang, Lihua, MK	Probabilistic Analysis of Nonlinear Wave-induced Loads on Ships. (Dr.Ing. Thesis)
MTA-2001-145	Kristensen, Odd H. Holt, MK	Ultimate Capacity of Aluminium Plates under Multiple Loads, Considering HAZ Properties. (Dr.Ing. Thesis)
MTA-2001-146	Greco, Marilena, MH	A Two-Dimensional Study of Green-Water Loading. (Dr.Ing. Thesis)
MTA-2001-147	Heggelund, Svein E., MK	Calculation of Global Design Loads and Load Effects in Large High Speed Catamarans. (Dr.Ing. Thesis)
MTA-2001-148	Babalola, Olusegun T., MK	Fatigue Strength of Titanium Risers – Defect Sensitivity. (Dr.Ing. Thesis)
MTA-2001-149	Mohammed, Abuu K., MK	Nonlinear Shell Finite Elements for Ultimate Strength and Collapse Analysis of Ship Structures. (Dr.Ing. Thesis)
MTA-2002-150	Holmedal, Lars E., MH	Wave-current interactions in the vicinity of the sea bed. (Dr.Ing. Thesis)
MTA-2002-151	Rognebakke, Olav F., MH	Sloshing in rectangular tanks and interaction with ship motions. (Dr.Ing. Thesis)
MTA-2002-152	Lader, Pål Furset, MH	Geometry and Kinematics of Breaking Waves. (Dr.Ing. Thesis)
MTA-2002-153	Yang, Qinzheng, MH	Wash and wave resistance of ships in finite water depth. (Dr.Ing. Thesis)
MTA-2002-154	Melhus, Øyvin, MM	Utilization of VOC in Diesel Engines. Ignition and combustion of VOC released by crude oil tankers. (Dr.Ing. Thesis)
MTA-2002-155	Ronæss, Marit, MH	Wave Induced Motions of Two Ships Advancing on Parallel Course. (Dr.Ing. Thesis)
MTA-2002-156	Økland, Ole D., MK	Numerical and experimental investigation of whipping in twin hull vessels exposed to severe wet deck slamming. (Dr.Ing. Thesis)
MTA-2002-157	Ge, Chunhua, MK	Global Hydroelastic Response of Catamarans due to Wet Deck Slamming. (Dr.Ing. Thesis)
MTA-2002-158	Byklum, Eirik, MK	Nonlinear Shell Finite Elements for Ultimate Strength and Collapse Analysis of Ship Structures. (Dr.Ing. Thesis)
IMT-2003-1	Chen, Haibo, MK	Probabilistic Evaluation of FPSO-Tanker Collision in Tandem Offloading Operation. (Dr.Ing. Thesis)
IMT-2003-2	Skaugset, Kjetil Bjørn, MK	On the Suppression of Vortex Induced Vibrations of Circular Cylinders by Radial Water Jets. (Dr.Ing. Thesis)
IMT-2003-3	Chezhian, Muthu	Three-Dimensional Analysis of Slamming. (Dr.Ing. Thesis)

IMT-2003-4	Buhaug, Øyvind	Deposit Formation on Cylinder Liner Surfaces in Medium Speed Engines. (Dr.Ing. Thesis)
IMT-2003-5	Tregde, Vidar	Aspects of Ship Design: Optimization of Aft Hull with Inverse Geometry Design. (Dr.Ing. Thesis)
IMT-2003-6	Wist, Hanne Therese	Statistical Properties of Successive Ocean Wave Parameters. (Dr.Ing. Thesis)
IMT-2004-7	Ransau, Samuel	Numerical Methods for Flows with Evolving Interfaces. (Dr.Ing. Thesis)
IMT-2004-8	Soma, Torkel	Blue-Chip or Sub-Standard. A data interrogation approach of identity safety characteristics of shipping organization. (Dr.Ing. Thesis)
IMT-2004-9	Ersdal, Svein	An experimental study of hydrodynamic forces on cylinders and cables in near axial flow. (Dr.Ing. Thesis)
IMT-2005-10	Brodtkorb, Per Andreas	The Probability of Occurrence of Dangerous Wave Situations at Sea. (Dr.Ing. Thesis)
IMT-2005-11	Yttervik, Rune	Ocean current variability in relation to offshore engineering. (Dr.Ing. Thesis)
IMT-2005-12	Fredheim, Arne	Current Forces on Net-Structures. (Dr.Ing. Thesis)
IMT-2005-13	Heggernes, Kjetil	Flow around marine structures. (Dr.Ing. Thesis
IMT-2005-14	Fouques, Sebastien	Lagrangian Modelling of Ocean Surface Waves and Synthetic Aperture Radar Wave Measurements. (Dr.Ing. Thesis)
IMT-2006-15	Holm, Håvard	Numerical calculation of viscous free surface flow around marine structures. (Dr.Ing. Thesis)
IMT-2006-16	Bjørheim, Lars G.	Failure Assessment of Long Through Thickness Fatigue Cracks in Ship Hulls. (Dr.Ing. Thesis)
IMT-2006-17	Hansson, Lisbeth	Safety Management for Prevention of Occupational Accidents. (Dr.Ing. Thesis)
IMT-2006-18	Zhu, Xinying	Application of the CIP Method to Strongly Nonlinear Wave-Body Interaction Problems. (Dr.Ing. Thesis)
IMT-2006-19	Reite, Karl Johan	Modelling and Control of Trawl Systems. (Dr.Ing. Thesis)
IMT-2006-20	Smogeli, Øyvind Notland	Control of Marine Propellers. From Normal to Extreme Conditions. (Dr.Ing. Thesis)
IMT-2007-21	Storhaug, Gaute	Experimental Investigation of Wave Induced Vibrations and Their Effect on the Fatigue Loading of Ships. (Dr.Ing. Thesis)
IMT-2007-22	Sun, Hui	A Boundary Element Method Applied to Strongly Nonlinear Wave-Body Interaction Problems. (PhD Thesis, CeSOS)
IMT-2007-23	Rustad, Anne Marthine	Modelling and Control of Top Tensioned Risers. (PhD Thesis, CeSOS)
IMT-2007-24	Johansen, Vegar	Modelling flexible slender system for real-time simulations and control applications
IMT-2007-25	Wroldsen, Anders Sunde	Modelling and control of tensegrity structures. (PhD Thesis, CeSOS)
IMT-2007-26	Aronsen, Kristoffer Høye	An experimental investigation of in-line and combined inline and cross flow vortex induced vibrations. (Dr. avhandling, IMT)
IMT-2007-27	Gao, Zhen	Stochastic Response Analysis of Mooring Systems with Emphasis on Frequency-domain Analysis of Fatigue due to Wide-band Response Processes (PhD Thesis, CeSOS)
IMT-2007-28	Thorstensen, Tom Anders	Lifetime Profit Modelling of Ageing Systems Utilizing Information about Technical Condition. (Dr.ing. thesis, IMT)
IMT-2008-29	Berntsen, Per Ivar B.	Structural Reliability Based Position Mooring. (PhD-Thesis, IMT)
IMT-2008-30	Ye, Naiquan	Fatigue Assessment of Aluminium Welded Box-stiffener Joints in Ships (Dr.ing. thesis, IMT)
IMT-2008-31	Radan, Damir	Integrated Control of Marine Electrical Power Systems. (PhD-Thesis, IMT)

IMT-2008-32	Thomassen, Paul	Methods for Dynamic Response Analysis and Fatigue Life Estimation of Floating Fish Cages. (Dr.ing. thesis, IMT)
IMT-2008-33	Pákozdi, Csaba	A Smoothed Particle Hydrodynamics Study of Two-dimensional Nonlinear Sloshing in Rectangular Tanks. (Dr.ing.thesis, IMT)
IMT-2007-34	Grytøyr, Guttorm	A Higher-Order Boundary Element Method and Applications to Marine Hydrodynamics. (Dr.ing.thesis, IMT)
IMT-2008-35	Drummen, Ingo	Experimental and Numerical Investigation of Nonlinear Wave-Induced Load Effects in Containerships considering Hydroelasticity. (PhD thesis, CeSOS)
IMT-2008-36	Skejic, Renato	Maneuvering and Seakeeping of a Singel Ship and of Two Ships in Interaction. (PhD-Thesis, CeSOS)
IMT-2008-37	Harlem, Alf	An Age-Based Replacement Model for Repairable Systems with Attention to High-Speed Marine Diesel Engines. (PhD-Thesis, IMT)
IMT-2008-38	Alsos, Hagbart S.	Ship Grounding. Analysis of Ductile Fracture, Bottom Damage and Hull Girder Response. (PhD-thesis, IMT)
IMT-2008-39	Graczyk, Mateusz	Experimental Investigation of Sloshing Loading and Load Effects in Membrane LNG Tanks Subjected to Random Excitation. (PhD-thesis, CeSOS)
IMT-2008-40	Taghipour, Reza	Efficient Prediction of Dynamic Response for Flexible amd Multi-body Marine Structures. (PhD-thesis, CeSOS)
IMT-2008-41	Ruth, Eivind	Propulsion control and thrust allocation on marine vessels. (PhD thesis, CeSOS)
IMT-2008-42	Nystad, Bent Helge	Technical Condition Indexes and Remaining Useful Life of Aggregated Systems. PhD thesis, IMT
IMT-2008-43	Soni, Prashant Kumar	Hydrodynamic Coefficients for Vortex Induced Vibrations of Flexible Beams, PhD thesis, CeSOS
IMT-2009-43	Amlashi, Hadi K.K.	Ultimate Strength and Reliability-based Design of Ship Hulls with Emphasis on Combined Global and Local Loads. PhD Thesis, IMT
IMT-2009-44	Pedersen, Tom Arne	Bond Graph Modelling of Marine Power Systems. PhD Thesis, IMT
IMT-2009-45	Kristiansen, Trygve	Two-Dimensional Numerical and Experimental Studies of Piston-Mode Resonance. PhD-Thesis, CeSOS
IMT-2009-46	Ong, Muk Chen	Applications of a Standard High Reynolds Number Model and a Stochastic Scour Prediction Model for Marine Structures. PhD-thesis, IMT
IMT-2009-47	Hong, Lin	Simplified Analysis and Design of Ships subjected to Collision and Grounding. PhD-thesis, IMT
IMT-2009-48	Koushan, Kamran	Vortex Induced Vibrations of Free Span Pipelines, PhD thesis, IMT
IMT-2009-49	Korsvik, Jarl Eirik	Heuristic Methods for Ship Routing and Scheduling. PhD-thesis, IMT
IMT-2009-50	Lee, Jihoon	Experimental Investigation and Numerical in Analyzing the Ocean Current Displacement of Longlines. Ph.d.-Thesis, IMT.
IMT-2009-51	Vestbøstad, Tone Gran	A Numerical Study of Wave-in-Deck Impact usin a Two-Dimensional Constrained Interpolation Profile Method, Ph.d.thesis, CeSOS.
IMT-2009-52	Bruun, Kristine	Bond Graph Modelling of Fuel Cells for Marine Power Plants. Ph.d.-thesis, IMT
IMT 2009-53	Holstad, Anders	Numerical Investigation of Turbulence in a Sekwed Three-Dimensional Channel Flow, Ph.d.-thesis, IMT.
IMT 2009-54	Ayala-Uraga, Efren	Reliability-Based Assessment of Deteriorating Ship-shaped Offshore Structures, Ph.d.-thesis, IMT
IMT 2009-55	Kong, Xiangjun	A Numerical Study of a Damaged Ship in Beam Sea Waves. Ph.d.-thesis, IMT/CeSOS.
IMT 2010-56	Kristiansen, David	Wave Induced Effects on Floaters of Aquaculture Plants, Ph.d.-thesis, IMT/CeSOS.
IMT 2010-57	Ludvigsen, Martin	An ROV-Toolbox for Optical and Acoustic Scientific Seabed Investigation. Ph.d.-thesis IMT.

IMT 2010-58	Hals, Jørgen	Modelling and Phase Control of Wave-Energy Converters. Ph.d.thesis, CeSOS.
IMT 2010- 59	Shu, Zhi	Uncertainty Assessment of Wave Loads and Ultimate Strength of Tankers and Bulk Carriers in a Reliability Framework. Ph.d. Thesis, IMT.
IMT 2010-60	Shao, Yanlin	Numerical Potential-Flow Studies on Weakly-Nonlinear Wave-Body Interactions with/without Small Forward Speed, Ph.d.thesis, IMT.
IMT 2010-61	Califano, Andrea	Dynamic Loads on Marine Propellers due to Intermittent Ventilation. Ph.d.thesis, IMT.
IMT 2010-62	El Khoury, George	Numerical Simulations of Massively Separated Turbulent Flows, Ph.d.-thesis, IMT
IMT 2010-63	Seim, Knut Sponheim	Mixing Process in Dense Overflows with Emphasis on the Faroe Bank Channel Overflow. Ph.d.thesis, IMT
IMT 2010-64	Jia, Huirong	Structural Analysis of Intect and Damaged Ships in a Collission Risk Analysis Perspective. Ph.d.thesis CeSoS.
IMT 2010-65	Jiao, Linlin	Wave-Induced Effects on a Pontoon-type Very Large Floating Structures (VLFS). Ph.D.-thesis, CeSOS.
IMT 2010-66	Abrahamsen, Bjørn Christian	Sloshing Induced Tank Roof with Entrapped Air Pocket. Ph.d.thesis, CeSOS.
IMT 2011-67	Karimirad, Madjid	Stochastic Dynamic Response Analysis of Spar-Type Wind Turbines with Catenary or Taut Mooring Systems. Ph.d.-thesis, CeSOS.
IMT -2011-68	Erlend Meland	Condition Monitoring of Safety Critical Valves. Ph.d.-thesis, IMT.
IMT – 2011-69	Yang, Limin	Stochastic Dynamic System Analysis of Wave Energy Converter with Hydraulic Power Take-Off, with Particular Reference to Wear Damage Analysis, Ph.d. Thesis, CeSOS.
IMT – 2011-70	Visscher, Jan	Application of Particla Image Velocimetry on Turbulent Marine Flows, Ph.d.Thesis, IMT.
IMT – 2011-71	Su, Biao	Numerical Predictions of Global and Local Ice Loads on Ships. Ph.d.Thesis, CeSOS.
IMT – 2011-72	Liu, Zhenhui	Analytical and Numerical Analysis of Iceberg Collision with Ship Structures. Ph.d.Thesis, IMT.
IMT – 2011-73	Aarsæther, Karl Gunnar	Modeling and Analysis of Ship Traffic by Observation and Numerical Simulation. Ph.d.Thesis, IMT.
Imt – 2011-74	Wu, Jie	Hydrodynamic Force Identification from Stochastic Vortex Induced Vibration Experiments with Slender Beams. Ph.d.Thesis, IMT.
Imt – 2011-75	Amini, Hamid	Azimuth Propulsors in Off-design Conditions. Ph.d.Thesis, IMT.
IMT –2011-76	Nguyen, Tan-Hoi	Toward a System of Real-Time Prediction and Monitoring of Bottom Damage Conditions During Ship Grounding. Ph.d.thesis, IMT.
IMT- 2011-77	Tavakoli, Mohammad T.	Assessment of Oil Spill in Ship Collision and Grounding, Ph.d.thesis, IMT.
IMT- 2011-78	Guo, Bingjie	Numerical and Experimental Investigation of Added Resistance in Waves. Ph.d.Thesis, IMT.
IMT- 2011-79	Chen, Qiaofeng	Ultimate Strength of Aluminium Panels, considering HAZ Effects, IMT
IMT-2012-80	Kota, Ravikiran S.	Wave Loads on Decks of Offshore Structures in Random Seas. Ph.d.thesis, CeSOS.
IMT-2012-81	Sten, Ronny	Dynamic Simulation of Deep Water Drilling Risers with Heave Compensating Sysetm, IMT.
IMT-2012-82	Berle, Øyvind	Risk and resilience in global maritime supply chains, IMT.
IMT-2012-83	Fang, Shaoji	Fault Tolerant Position Mooring Control Based on Structural Reliability, IMT.

IMT-2012-84	You, Jikun	Numerical studies on wave forces and moored ship motions in intermediate and shallow water, IMT.
IMT-2012-85	Xiang, Xu	Maneuvering of two interacting ships in waves.
IMT-2012-86	Dong, Wenbin	Time-domain fatigue response and reliability analysis of offshore wind turbines with emphasis on welded tubular joints and gear components.
IMT-2012-87	Al Ryati, Nabil	Technical Condition Indexes for Auxiliary Marine Diesel Engines.
IMT-2012-88	Zhu, Suji	Investigation of Wave-Induced Nonlinear Load Effects in Open Ships considering Hull Girder Vibrations in Bending and Torsion.
IMT-2012-89	Sergey Ushakov	Particulate matter emission characteristics from diesel engines operating on conventional and alternative marine fuels.